Vol. 55 • No. 2

February 2012

# Microwave Journal

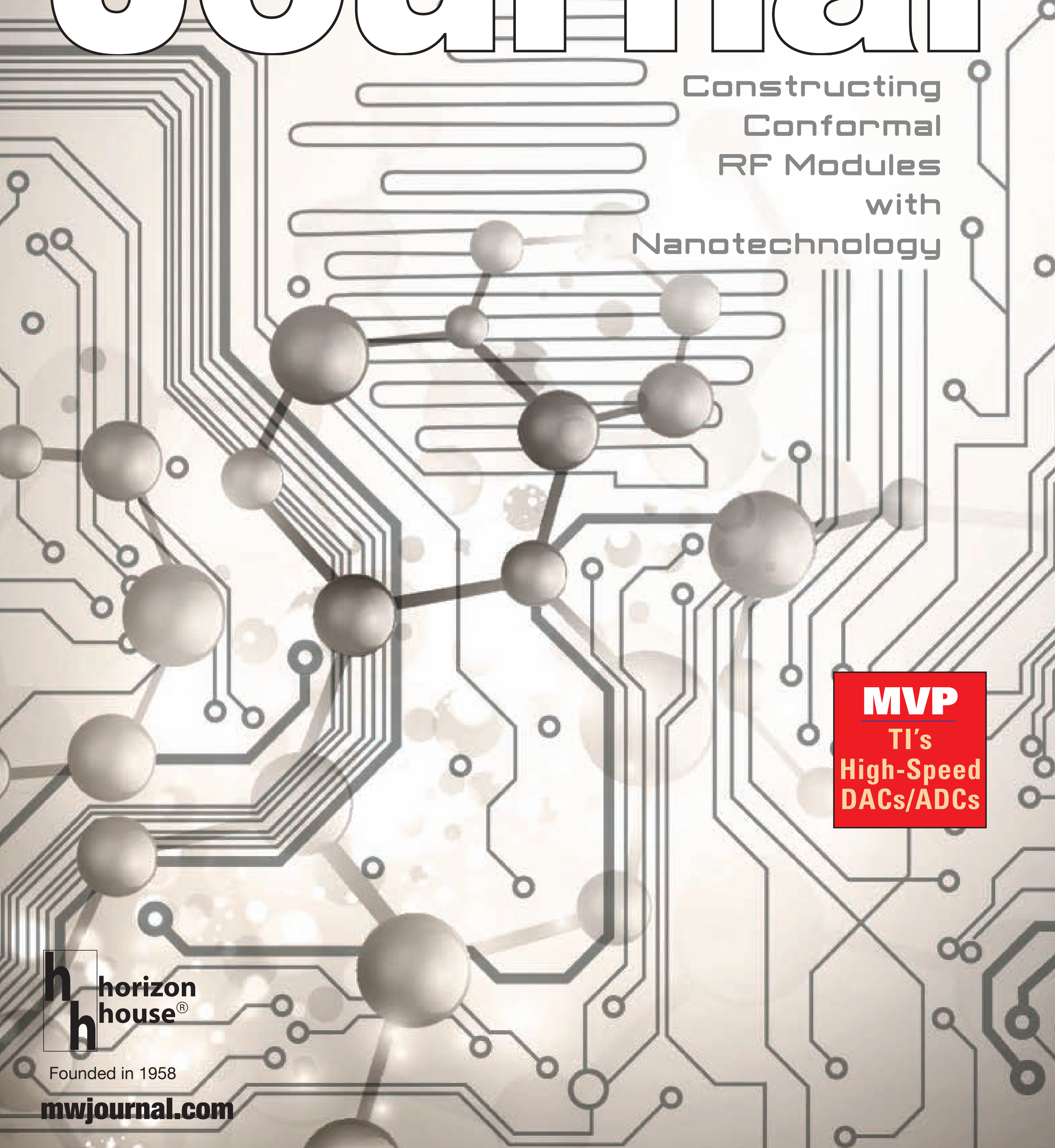

## Constructing Conformal RF Modules with Nanotechnology

**MVP**
TI's High-Speed DACs/ADCs

horizon house®
Founded in 1958
mwjournal.com

RUGGED & RELIABLE
MADE IN THE USA FOR 50 YEARS!
M*E*C*A* – MICROWAVE ELECTRONIC COMPONENTS OF AMERICA
Aviation
Earth Station
Instrumentation
L, S, C, X, and Ku Bands
Microwave Radio
Mobile Satellite
Radar
Telemetry
MOST MODELS AVAILABLE FROM STOCK - 4 WEEKS ARO
POWER DIVIDERS/ COMBINERS
2-way through 16-way in N, SMA, BNC, TNC and 7/16 DIN connector styles from 0.4 to 18.0 GHz.
ATTENUATORS
Most available in 1 dB increments from 0 - 40dB. Power ratings from 2 to 150 Watts.
RF LOADS
Power ratings from 1 to 500 watts and frequency ranges up to 18 GHz.
DIRECTIONAL & HYBRID COUPLERS
Average power handling from 50W to 1kW. Standard coupling values of 3, 6, 10, 20, 30 and 40 dB.
DC BLOCKS
Available in N, BNC, TNC, SMA & 7/16 DIN configurations. Power ratings to 500 watts (2.5 kW peak).
INTEGRATED ASSEMBLIES
Let MECA create an integrated assembly with any of our standard RF/Microwave products on 19" panels, shelves or enclosures.
BIAS TEES
Covering bands from 0.5 – 2.5 GHz and 0.7 to 2.7 GHz in 7/16 DIN, SMA, N, BNC & TNC configurations with RF power ratings to 300 watts (3 kW peak).
CIRCULATORS & ISOLATORS
In both N & SMA-Female connectors with average power ratings from 2 to 250 watts. "Popular" frequency bands between 0.7 - 18.0 GHz.
MECA ELECTRONICS, INC.
459 East Main Street Denville, NJ 07834
To learn more, please call 866-444-6322 or visit our website at www.e-MECA.com
1961-2011


MCL B 744
ADP-2-10
MCL
QBA-12

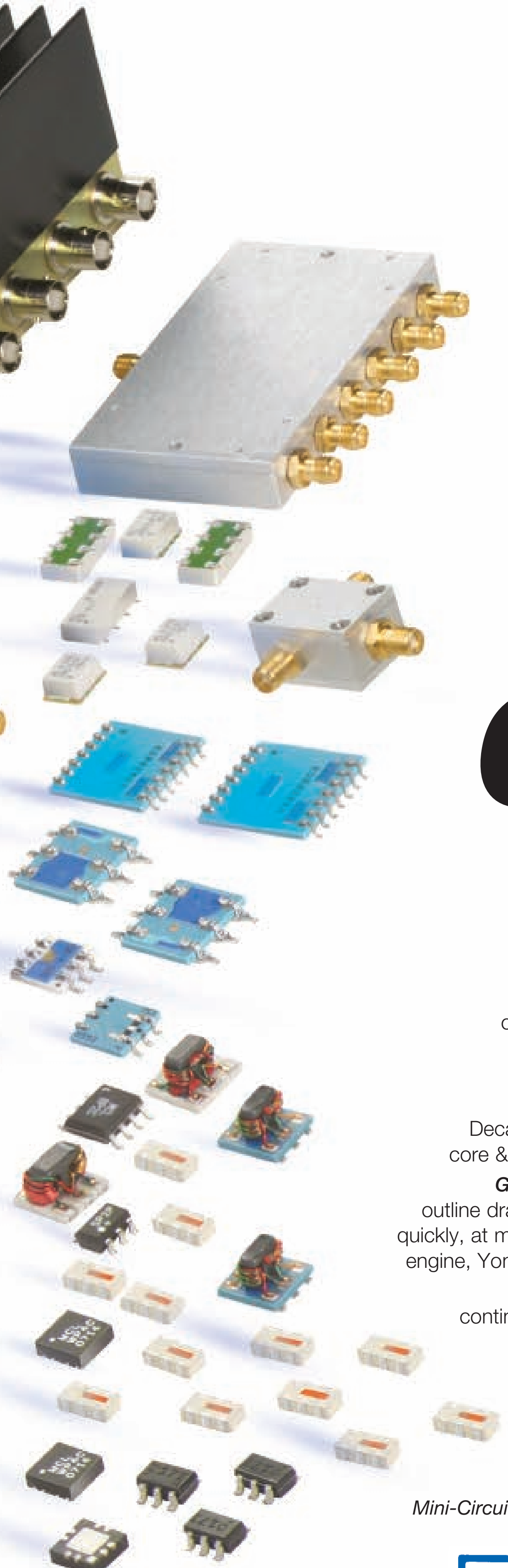

# POWER SPLITTERS/ COMBINERS

**NOW!** from **2 kHz to 18 GHz** as low as **79¢**

***The Industry's Largest Selection includes THOUSANDS*** of models, from 2 kHz to 18 GHz, at up to 300 watts power, and in coaxial, flat-pack, and surface-mount housings for 50 and 75 systems.

***From 2-way through 48-way designs, with 0°, 90°, or 180°*** phase configurations, Mini-Circuits power splitters/combiners offer outstanding performance for insertion loss, isolation, and VSWR. Decades of experience with multiple technologies make it all possible, from core & wire, microstrip, and stripline, to semiconductors and LTCC ceramics.

***Get easy-to-find, detailed data and performance curves, S-parameters,*** outline drawings, PCB layouts, and everything else you need to make a decision quickly, at minicircuits.com. Just enter your requirements, and our patented search engine, Yoni2, searches *actual test data* to find the models that meet your needs.

***All Mini-Circuits catalog models are in stock,*** continuously replenished, and backed by our 1-year guarantee. We even list *current stock quantities and real-time availability*, as well as pricing, to help our customers plan ahead and make quick decisions. So why wait? Take a look at minicircuits.com today!

***RoHS Compliant***
Product availability is listed on our website.

*Mini-Circuits...we're redefining what VALUE is all about!*

**Mini-Circuits®**
*ISO 9001 ISO 14001 AS 9100*

P.O. Box 350166, Brooklyn, New York 11235-0003 (718) 934-4500 Fax (718) 332-4661

**Yoni2®** ***The Design Engineers Search Engine*** *finds the model you need, Instantly* • For detailed performance specs & shopping online see **minicircuits.com**

U.S. Patents
7739260, 7761442

***IF/RF MICROWAVE COMPONENTS***

448 rev H

Leading Global Communications

# New 0.1μm pHEMT Technology

## WIN is the world's largest and leading 6" GaAs foundry

- 0.1μm gate length pHEMT technology
- 9V off-state breakdown voltage for power application
- Wafer thickness options of 50um (PP10-10) and 100um (PP10-11) available
- 860 mW/mm $P_{sat}$ at 29GHz with Vd=4V
- 400 mF/mm$^2$ capacitor for design flexibility

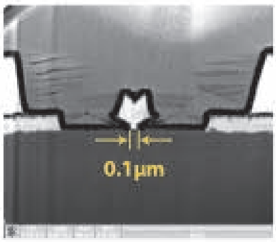


### PP10-10, 11 Tranconductance Curve

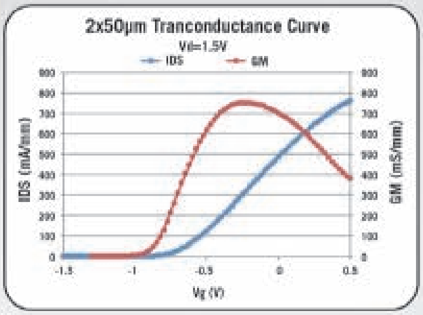


### PP10-10, 11 I-V Curves

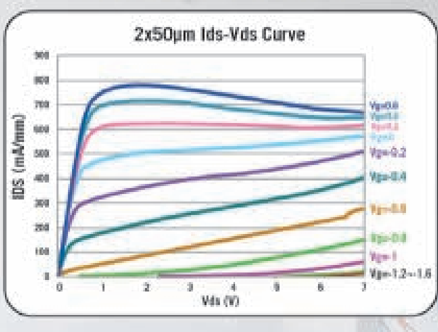


### Comparison of WIN's millimeter wave pHEMT technologies

| | PP25-21 | PP15-50/51 | PP10-10/11 |
|---|---|---|---|
| Gate length | 0.25μm | 0.15μm | 0.1μm |
| Operating Frequency | Up to 20GHz | Up to 30 GHz | Up to 90GHz |
| Max Drain Bias | 8V | 6V | 4V |
| Max Id (Vg=0.5V) | 490 mA/mm | 630 mA/mm | 760 mA/mm |
| IDSS (Vg=0V) | 340 mA/mm | 470 mA/mm | 520 mA/mm |
| Max Gm | 410 mS/mm | 460 mS/mm | 725 mS/mm |
| Vto | -1.15 V | -1.35 V | -0.95 V |
| Von (Diode turn on) | 0.8 V | 0.8 V | 0.9 V |
| BVGD | 20V (18V min) | 16V (14V min) | 9V (8V min) |
| $f_T$ | 65 GHz | 90 GHz | 130 GHz |
| $f_{max}$ | 190 GHz | 185 GHz | 180 GHz |
| Power Density (2x75μm) | 1100 mW/mm @ 8V, 10GHz | 870 mW/mm @ 6V, 29GHz | 860 mW/mm @4V, 29GHz (2x50μm) |


WIN SEMICONDUCTORS CORP. Tel:+886-3-397-5999 Fax:+886-3-397-5069 http://www.winfoundry.com

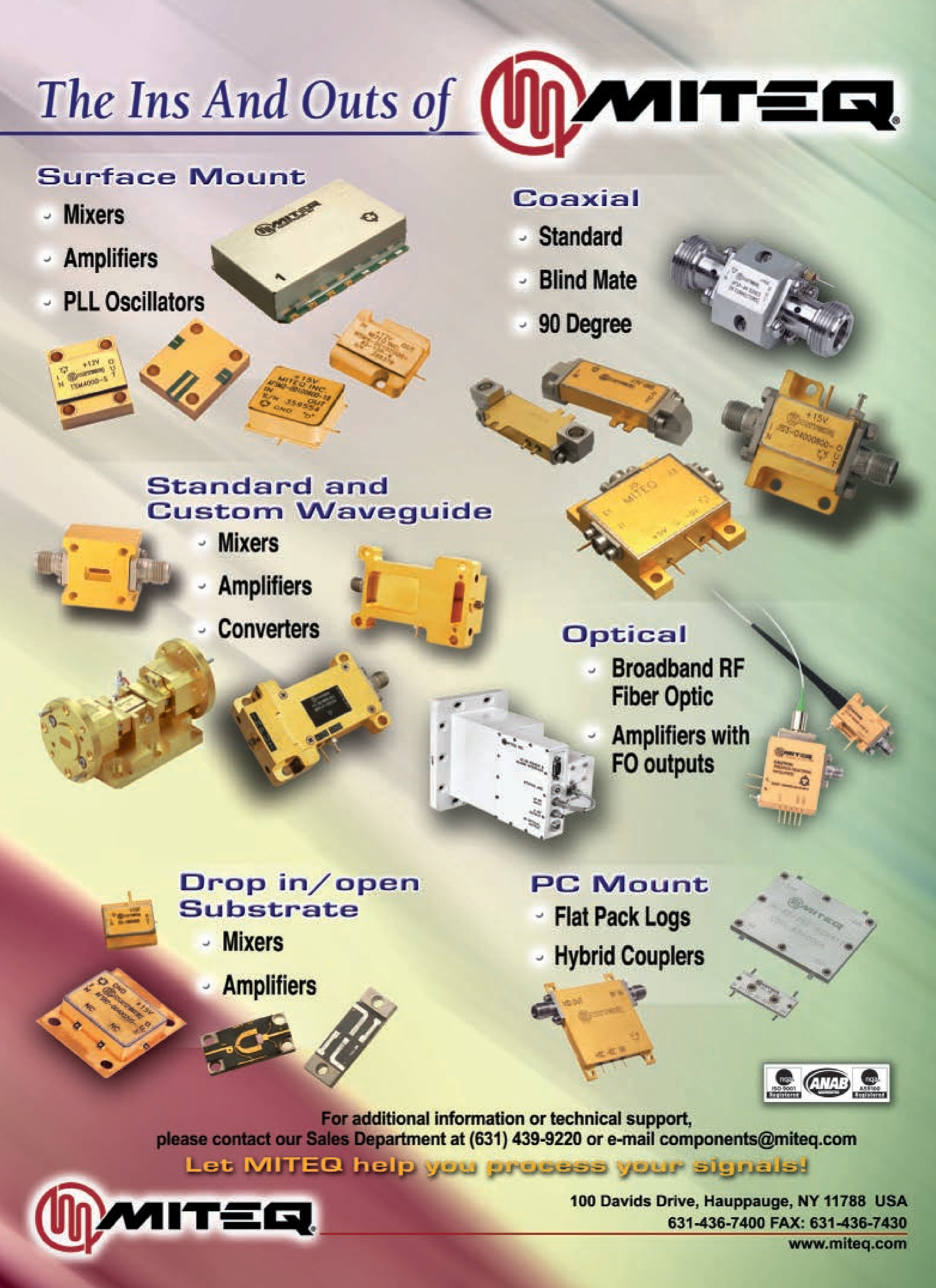

The Ins And Outs of MITEQ
Surface Mount
Mixers
Amplifiers
PLL Oscillators
Coaxial
Standard
Blind Mate
90 Degree
Standard and Custom Waveguide
Mixers
Amplifiers
Converters
Optical
Broadband RF Fiber Optic
Amplifiers with FO outputs
Drop in/open Substrate
Mixers
Amplifiers
PC Mount
Flat Pack Logs
Hybrid Couplers
For additional information or technical support,
please contact our Sales Department at (631) 439-9220 or e-mail components@miteq.com
Let MITEQ help you process your signals!
MITEQ
100 Davids Drive, Hauppauge, NY 11788 USA
631-436-7400 FAX: 631-436-7430
www.miteq.com

Microwave Journal

FEBRUARY 2012 VOL. 55 • NO. 2

## COVER FEATURE



## MVP: MOST VALUABLE PRODUCT



## PERSPECTIVE



## TECHNICAL FEATURES



55 Years of Publishing Excellence

*Microwave Journal* (USPS 396-250) (ISSN 0192-6225) is published monthly by Horizon House Publications Inc., 685 Canton St., Norwood, MA 02062. Periodicals postage paid at Norwood, MA 02062 and additional mailing offices.



POSTMASTER: Send address corrections to *Microwave Journal*, PO Box 3256, Northbrook, IL 60065-3256 or e-mail mwj@omeda.com. Subscription information: (847) 291-5216. This journal is issued without charge upon written request to qualified persons working in the RF & microwave industry. Other subscriptions are: domestic, $120.00 per year, two-year subscriptions, $185.00; foreign, $200.00 per year, two-year subscriptions, $370.00; back issues (if available) and single copies, $10.00 domestic and $20.00 foreign. Claims for missing issues must be filed within 90 days of date of issue for complimentary replacement.



Posted under Canadian international publications mail agreement #PM40612608

Microwave Journal

## SPECIAL REPORTS



## PRODUCT FEATURE



## TECH BRIEF



## Departments



## STAFF

**Publisher:** Carl Sheffres
**Editor:** David Vye
**Managing Editor:** Jennifer DiMarco
**Technical Editor:** Patrick Hindle
**Associate Technical Editor:** Dan Massé
**Staff Editor:** Kerri Germani
**Editorial Assistant:** Barbara Walsh
**Consulting Editor:** Harlan Howe, Jr.
**Consulting Editor:** Frank Bashore
**Consulting Editor:** Peter Staecker
**Consulting Editor:** Dan Swanson
**Web Editor:** Chris Stanfa
**Audience Development Manager:** Michelle Barry
**Traffic Manager:** Edward Kiessling
**Marketing and Event Coordinator:** Kristen Anderson
**Director of Production & Distribution:** Robert Bass
**Lead Designer & Production Coordinator:** Janice Levenson
**Graphic Designer:** Sachiko Stiglitz

**EUROPE**

**International Editor:** Richard Mumford
**Office Manager:** Nina Plesu

**CORPORATE STAFF**

**CEO:** William M. Bazzy
**President:** Ivar Bazzy
**Vice President:** Jared Bazzy



**Executive Editorial Office:**

685 Canton Street, Norwood, MA 02062
Tel: (781) 769-9750
FAX: (781) 769-5037
e-mail: mwj@mwjournal.com

**European Editorial Office:**

16 Sussex Street, London SW1V 4RW, England
Tel: Editorial: +44 207 596 8730 Sales: +44 207 596 8740
FAX: +44 207 596 8749

**www.mwjournal.com**

**Printed in the USA**

# You work in all kinds of conditions, so should your spectrum analyzer.

**Worst-case scenario:** You've got minutes to troubleshoot RF interference that has shut down communications on the ground, at dusk, in the desert.

**Best-case scenario:** You've got the only spectrum analyzer with benchtop performance in a lightweight MIL-PRF 28800F Class 2 compliant handheld—with secure erase to keep classified data classified.

**That's thinking ahead. That's Agilent.**

Scan the QR code or visit http://goo.gl/Rfbde to see a HSA N9344C demo guide video

## Handheld Spectrum Analyzers (HSA)

| Key Specs | N9344C | N9343C | N9342C |
|---|---|---|---|
| Frequency | 1 MHz–20 GHz | 1 MHz–13.6 GHz | 100 kHz–7 GHz |
| DANL | -155 dBm/Hz | -155 dBm/Hz | -164 dBm/Hz |
| Sweep time | < 0.9 s | < 0.7 s | < 0.4 s |
| Weight with battery | 3.6 kg (7.9 lbs) | 3.6 kg (7.9 lbs) | 3.6 kg (7.9 lbs) |

**Agilent and our Distributor Network**
*Right Instrument.*
*Right Expertise.*
*Delivered Right Now.*

Newark element14

*800-463-9275*
*www.newark.com/agilent*

**View online HSA video demos**
**Download demonstration guides**
www.newark.com/Agilent_HSA



Agilent Technologies

# Microwave Journal Online

This month on our all **new website**
**mwjournal.com**

## Free Webinars

**Innovation Series** *by Agilent Technologies*

| | |
|---|---|
| **Measurement-Based FET Modeling** | **available On Demand** |
| **HSPA+ & LTE Test Challenges** | **available On Demand** |
| **Optimal Spurious Measurements** | **2/15/12 @ 1:00 PM ET** |
| **Manufacturing Test - Wireless DUTs** | **2/23/12 @ 1:00 PM ET** |
| **Back to Basics, Signal Analysis** | **2/29/12 @ 1:00 PM ET** |
| **Understanding the LTE Radio Channel** *by Elektrobit* | **2/22/12 @ 1:00 PM ET** |

## Web Survey

How do you determine the load impedance for a power amp?

Look for our multiple choice survey online at mwjournal.com

## INDUSTRY BLOG

Measurement expert **Darren McCarthy** of Tektronix joins our stable of industry insiders sharing their insights and expertise on all aspects of high frequency matters of interest.

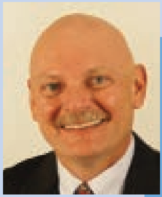

**John Hoffman**, CEO of GSMA Ltd., talks about the technology behind the headlines at Mobile World Congress 2012.

## Executive Interviews

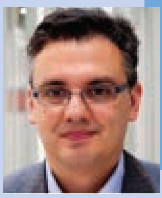

**Prof. Stan Skafidas**, University of Melbourne, talks about his research in the areas of RF CMOS, antennas and propagation, wireless communications and implantable devices.

## White Papers

LTE-Advanced Physical Layer Design and Test
*Agilent Technologies*

Measuring Leakage Current in RF Power Transistors
*Richardson RFPD*

Leveraging OFDMA Technology for HLS Apps
*Runcom Techologies*

Electronically Scanned Arrays for Fast Testing of Large Antennas
*Microwave Vision Group*

## Community Watch

LinkedIn
RF & Microwave Community

Who will be our 10,000th member?


.COM

# 88dB SFDR @ 100MHz

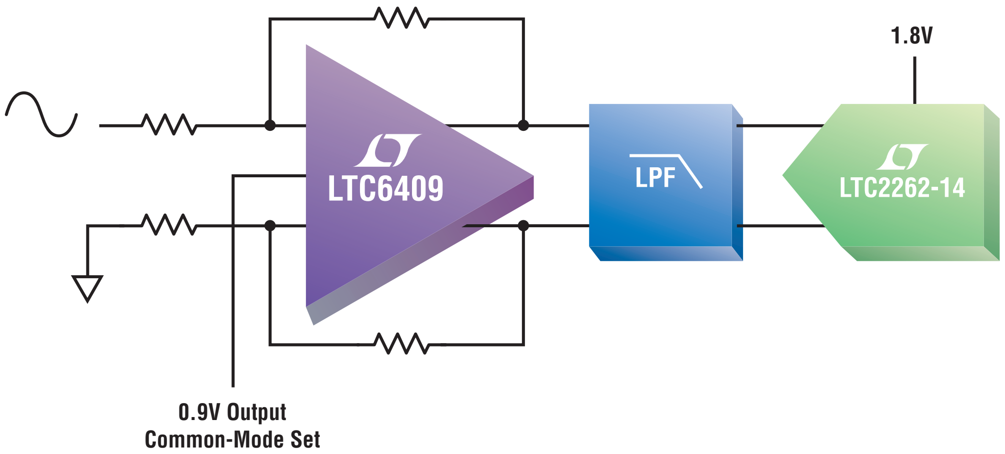


## Unleash Your High Speed ADC

With 1.1nV/√Hz input noise density and 88dB SFDR performance at 100MHz, the LTC®6409 enables your high speed ADC to achieve outstanding performance. Its input common mode range includes ground and its output common mode can be set as low as 0.5V, making the LTC6409 the perfect choice for driving AC- or DC-coupled signals into the latest 1.8V data converters. Fully specified over the –40°C to 125°C temperature range, and available in a tiny 3mm x 2mm QFN package, the LTC6409 combines excellent AC performance with flexibility, robustness and a minimal footprint.

### Features

- Unity Gain Stable
- 1.1nV/√Hz Input Noise Density
- 10GHz GBW @ 100MHz
- DC- or AC-Coupled Inputs
- 0.5V to 3.5V $V_{OCM}$
- –40°C to 125°C Fully Specified
- Tiny 3mm x 2mm QFN Package

### Differential ADC Drivers

| Part Number | 80dBc HD2/HD3 (MHz) | Input Referred Noise (nV/√Hz) | Voltage Gain |
|---|---|---|---|
| LTC6409 | 110 | 1.1 | R-set |
| LTC6406 | 30 | 1.6 | R-set |
| LTC6404-1 | 15 | 1.5 | R-set |
| LTC6400-20 | 120 | 1.9 | 20dB |
| LTC6416 | 90 | 1.8 | 0dB |

### Info & Free Samples

www.linear.com/6409

1-800-4-LINEAR

www.linear.com/ampsflyer



LINEAR TECHNOLOGY

# MARCH 2012

| SUNDAY | MONDAY | TUESDAY | WEDNESDAY | THURSDAY | FRIDAY | SATURDAY |
|---|---|---|---|---|---|---|
| 26 | 27 | 28 | 29 | 1 **Webinar:** Portable Test Equipment Sponsored by Mini-Circuits; **Webinar:** Innovations in EDA Agilent Technologies | 2 | 3 |
| 4 | 5 | 6 | 7 | 8 **Webinar:** Agilent in Wireless Communications Agilent Technologies | 9 | 10 |
| 11 | 12 ← SATELLITE 2012 Washington, DC | 13 | 14 | 15 → **Webinar:** Agilent in Aerospace/ Defense Agilent Technologies | 16 RADAR 2012 Call for Papers Deadline | 17 |
| 18 | 19 ← isQED Symposium 2012 March 19-21, 2012 TechMart Center, Santa Clara, CA, USA | 20 MWJ/Besser **Webinar:** LTE Sponsored by AWR Anritsu | 21 → | 22 **Webinar:** Agilent in LTE Agilent Technologies | 23 | 24 |
| 25 | 26 | 27 | 28 | 29 | 30 | 31 |

## Go to: www.mwjournal.com/events

# Coming Events

**CALL FOR PAPERS**

EuMW 2012
Deadline: February 17, 2012
MMS 2012
Deadline: February 29, 2012
RADAR 2012
Deadline: March 16, 2012
MILCOM 2012
Deadline: April 6, 2012

**www.mwjournal.com/events**

## FEBRUARY

**ISSCC 2012**
**IEEE International Solid-State Circuits**
*February 19–23, 2012 • San Francisco, CA*
www.isscc.org

**IWCE 2012**
**International Wireless Communications Expo**
*February 20–24, 2012 • Las Vegas, NV*
www.iwceexpo.com

**AUSA's ILW Winter Symposium and Exposition**
*February 22–24, 2012 • Ft. Lauderdale, FL*
www.ausa.org

**MWC 2012**
**Mobile World Congress**
*February 27–March 1, 2012*
*Barcelona, Spain*
www.mobileworldcongress.com

## MARCH

**SATELLITE 2012**
*March 12–15, 2012 • Washington, DC*
www.satellitetoday.com/satellite2012/

**ISQED Symposium 2012**
**13th Annual International Symposium on Quality Electronic Design**
*March 19–21, 2012 • Santa Clara, CA*
www.isqed.org

## APRIL

**ACES 2012**
**28th Annual International Review of Progress in Applied Computational Electromagnetics**
*April 10–14, 2012 • Columbus, OH*
http://aces.ee.olemiss.edu/

**WIMA NFC Monaco 2012**
**6th Global NFC Applications Products & Services Congress**
*Apriil 11–13, 2012 • Monte Carlo, Monaco*
www.wima.mc

**WAMICON 2012**
**IEEE Wireless and Microwave Technology Conference**
*April 16–17, 2012 • Cocoa Beach, FL*
www.wamicon.org

## MAY

**ICMMT 2012**
**International Conference on Microwave and Millimeter Wave Technology**

**MWIE 2012**
**Microwave Wireless Industry Exhibition in China**
*May 5–8, 2012 • Shenzhen, China*
www.mws-cie.org

**CTIA WIRELESS 2012**
*May 8–10, 2012 • New Orleans, LA*
www.ctiawireless.com

## JUNE

**RFIC 2012**
**IEEE Radio Frequency Integrated Circuits Symposium**
*June 17–19, 2012 • Montreal, Canada*
www.rfic2012.org

**IMS 2012**
**IEEE MTT-S International Microwave Symposium**
*June 17–22, 2012 • Montreal, Canada*
www.ims2012.org

**79th ARFTG Microwave Measurement Symposium**
*June 22, 2012 • Montreal, Canada*
www.arftg.org

## AUGUST

**IEEE EMC 2012**
*August 5–10, 2012 • Pittsburgh, PA*
http://2012emc.org

## SEPTEMBER

**MMS 2012**
**12th Mediterranean Microwave Symposium**
*September 2–5, 2012 • Istanbul, Turkey*
www.mms2102.org

## OCTOBER

**AMTA 2012**
**34th Annual Symposium of the Antenna Measurement Techniques Association**
*October 21–26, 2012 • Bellevue, WA*
www.amta.org

**RADAR 2012**
**International Conference on Radar**
*October 22–25, 2012 • Glasgow, UK*
www.radar2012.org

**EuMW 2012**
**European Microwave Week**
*October 28–November 2, 2012*
*Amsterdam, The Netherlands*
www.eumweek.com

**MILCOM 2012**
**Military Communications Conference**
*October 29–November 1, 2012 • Orlando, FL*
www.milcom.org


REALIZE YOUR VISION

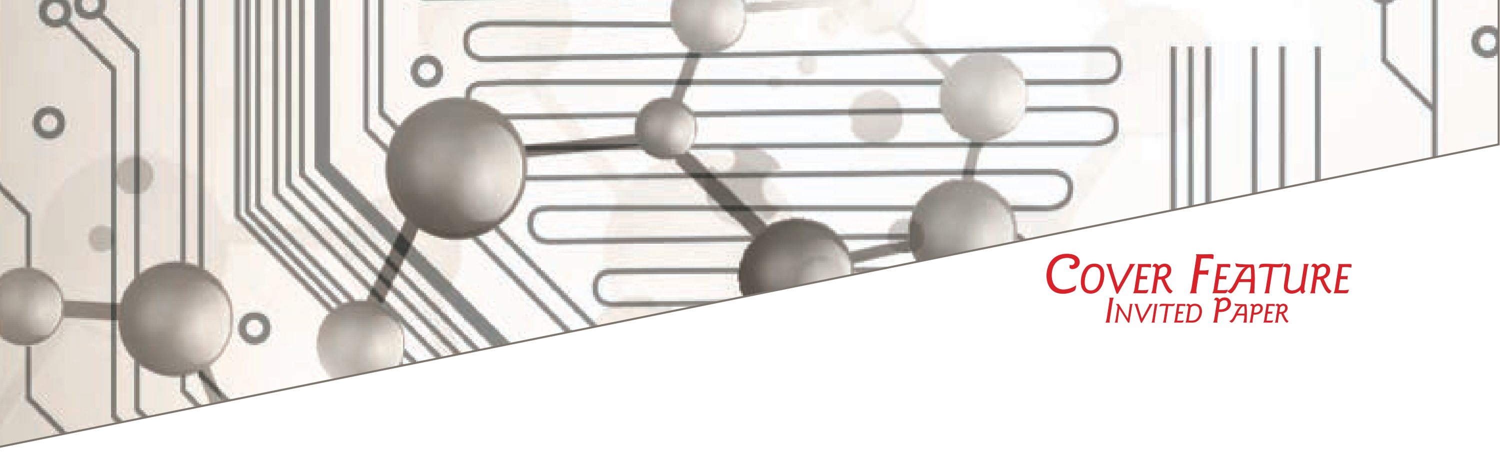

Cover Feature
Invited Paper

# Conformal 2D/3D Wireless Modules Utilizing Inkjet Printing and Nanotechnology

Inkjet-printed and nanotechnology-enabled flexible antennas, RF electronics and sensors fabricated on paper and polymer substrates (e.g. Liquid Crystal Polymer (LCP), Kapton®) are introduced as a system-level solution for ultra-low-cost mass production of communication, Radio Frequency Identification (RFID) Tags and Wireless Sensor Nodes (WSN) in an approach that could be easily extended to other microwave and wireless applications. The review will cover examples from UHF up to the millimeter-wave frequency ranges (mmID). This article will cover the state-of-the-art area of fully-integrated conformal wireless sensor modules on paper or flexible LCP, and demonstrate the first 2D/3D wireless sensor integration with an RFID tag module on paper, as well as numerous 3D multilayer paper-based and LCP-based RF/microwave structures that could potentially set the foundation for convergent wireless sensor ad-hoc networks of the future with enhanced cognitive intelligence and "rugged" packaging.

## ECO-FRIENDLY PAPER SUBSTRATE

Paper is an organic-based, inexpensive and flexible substrate. It is widely available and one of the cheapest materials for mass production in the industry.[1] Plus, it is not only environmentally friendly but also suited for reel-to-reel processing. In addition, paper can be hydrophobic and/or fire-retardant by adding certain textiles to it.[2] In addition, paper is suited for fast printing processes and direct write methodologies like inkjet printing techniques instead of the traditional metal etching techniques to maximize its cost efficiency. This is because inkjet printing directly deposits metals on the desired place while traditional metal etching techniques remove metals during etching that are not renewable. Therefore,

Manos M. Tentzeris, Rushi Vyas, Vasileios Lakafosis, Taoran Le, Amin Rida and Sangkil Kim
*School of ECE, Georgia Tech, Atlanta, GA*

# RLC Power Dividers...

## Known for high performance, innovative solutions, and cost-effective pricing.

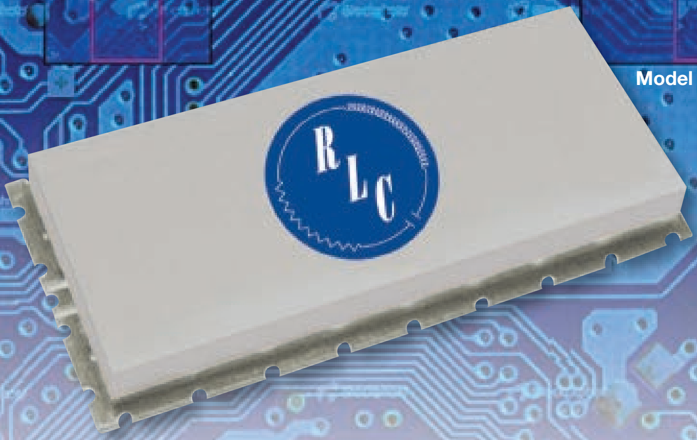

Model DSM-0520-2 shown here

RLC Electronics' Power Dividers offer superior performance in compact microstrip units with wide bandwidth and multiple outputs. These units provide low VSWR, high isolation and excellent phase characteristics between all the output ports.

Since 1959, RLC has been recognized as a leading designer and manufacturer of high quality, state-of-the-art components for the microwave & RF industry.

- Our family of Power Dividers are available in a choice of 2, 3, 4, 6, 8, 9, 12, and 16-way configurations
- Available in frequencies from DC to 40 GHz
- A wide choice of connector styles or surface mount configurations to suit any specific need
- Proven applications for instrumentation, TelCom, and SatCom

*For more detailed information, or to access **RLC's exclusive Filter Selection Software**, visit our web site.*

**RLC ELECTRONICS, INC.**

83 Radio Circle, Mount Kisco, New York 10549 • Tel: 914.241.1334 • Fax: 914.241.1753
E-mail: sales@rlcelectronics.com • www.rlcelectronics.com

***ISO 9001:2008 CERTIFIED***

VISA MasterCard

*RLC is your complete microwave & RF component resource for Switches, Filters, Power Dividers, Terminations, Attenuators, DC Blocks, Bias Tees & Detectors.*

a fast process like this can be used efficiently to print electronics on paper substrates. RF characterization of the paper substrate and conductive ink for inkjet printing is essential to build high frequency circuits and antennas using these techniques. A number of paper-based materials are available commercially at low costs with varying properties such as density, coating, thickness and weight for a wide variety of applications such as printing, photography, packaging, etc. Choosing the correct paper material for use as a substrate requires careful selection based on the paper's response to the propagating microwave fields and robustness to the fabrication process.

Paper substrates for inkjet printing purposes should be hydrophilic and heat-resistant. In addition, it is commercially available to enable mass production. The conductive ink cannot attach on the surface if it is highly hydrophobic, while it cannot form a conductive solid metal if the paper cannot withstand certain temperatures. In the previous works, commercially available photo paper fulfilling the above conditions and its electric properties are studied.[3-5]

## CONDUCTIVE INKJET PRINTING

The conventional masks for traditional etching techniques for fabrication are not necessary for inkjet printing since it is a direct-write technology, which means that designed circuit pattern is transferred to the substrate without any byproducts.[4] Therefore, dangerous chemicals, such as etchants are not needed, which make it an environmentally friendly fabrication process. The nano-silver ink used has high conductivity when it is printed and sintered since silver has the highest electrical conductivity among all of the metals. To remove the solvent in silver ink and impurities from the printing process, the sintering process is required after printing. In addition, the bond between the deposited silver ink and the substrate can be improved by the sintering process. The conductivity of the silver ink after sintering varies from 4 to about 16 μΩ-cm, which is about 2.5 to 10.1 times higher than bulk silver's resistivity, which is dependent on sintering time and temperature.[6] ***Figure 1*** shows a Scanning Electron Microscope (SEM) image of nano-silver ink before/after sintering at 180°C for 10 minutes. ***Figure 2*** shows a surface image of printed nano-silver ink from Atomic Force Microscopy (AFM), which is sintered at 120°C for four hours. The measured roughness based on the arithmetic average of absolute values ($R_a$) is 11.4 nm, root mean squared value ($R_q$) is 14.4 nm and the grain size after sintering at 120°C varies from about 20 to 200 nm. The roughness of the inkjet printed metal is very small so that the inkjet printing technique can be applied to mm-wave applications in the future.

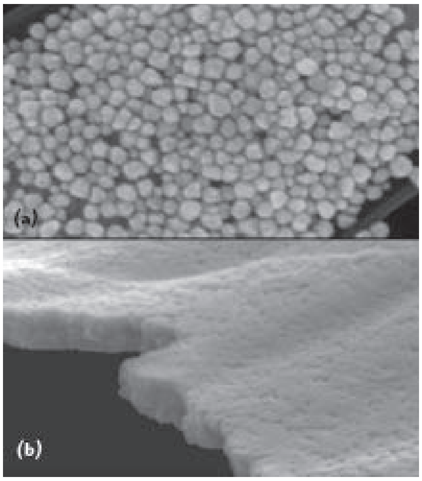


▲ *Fig. 1 Inkjet-printed nano-silver ink (a) before sintering (b) sintering at 180°C for 10 minutes.*

## INKJET PRINTED ANTENNAS

Based on previous characterization of the paper substrate and nano-silver ink, many types of devices and circuits were designed and fabricated using inkjet printing techniques and integrated into wireless sensor systems and modules. Among many applications, inkjet printing techniques are mainly applied to RFID technology due to their low cost and mass production features.

Recently, the use of the inkjet printing technology has been broadly extended in the area of integrated antennas up to the millimeter-wave (mm-wave) frequencies. For instance, the feasibility of inkjet printed antennas for various applications, such as Ultra-Wideband (UWB) and mm-wave modules on LCP and integrated power scavenging topologies have been studied.[7-10] Among the plethora of applications, one of the most recent efforts focuses on the

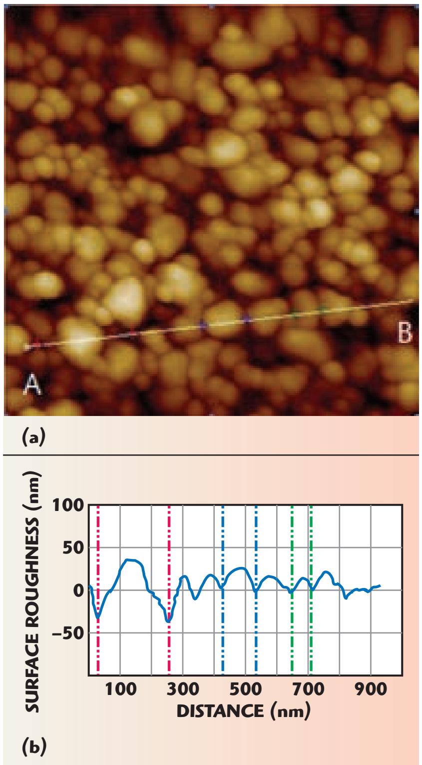


▲ *Fig. 2 (a) Surface image in the area of 1 μm by 1 μm; (b) surface profile of line AB.*

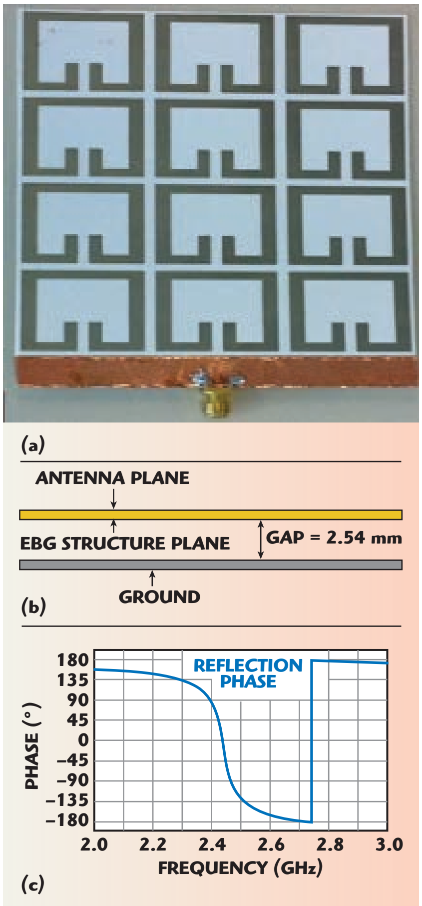


▲ *Fig. 3 (a) Inkjet-printed 4×3 EBGs, (b) integrated antenna, EBGs and ground plane and (c) phase response of reflected wave.*

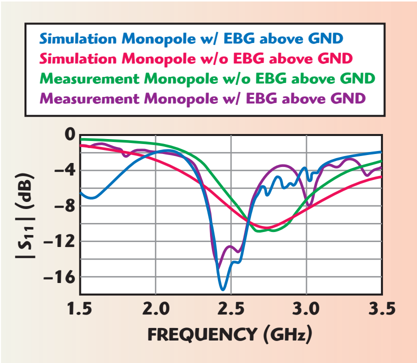


▲ *Fig. 4 $S_{11}$ of the fabricated antenna on the EBGs.*

inkjet printing of an Electromagnetic Band Gap (EBG) structure for wearable sensors. In previous efforts, a dipole antenna was placed above the inkjet printed EBGs to increase the gain for low-proximity ground planes.[11] In this case, the EBGs and ground plane form an Artificial Magnetic Conductor (AMC), and the reflected waves from the AMC constructively interfere with the radiated waves over the designated frequency band. EBGs are designed using single ring resonators instead of split ring resonators by an inkjet printing technique.[12] ***Figure 3a*** shows an inkjet-printed 4×3 resonator array. ***Figure 3b*** shows the integrated topology of an integrated monopole antenna, EBGs and ground plane. ***Figure 3c*** shows the phase response of the designed EBGs, demonstrating reflected phase values within the range within –90 to about +90 degrees verifying constructive interference. ***Figure 4*** shows the measured $S_{11}$ of the antenna. The EBG-backed antenna shows a better performance than the antenna without EBGs. The simulated and measured radiation patterns are shown in ***Figure 5***. The most notable difference is the gain of the designed antenna. The gain of the EBG-backed antenna is 0.95 dBi, while the antenna without EBGs on the ground plane is –4.6 dBi. The gain is increased by 5.5 dBi and this type of antenna can be placed on any kind of material (e.g., conductive surfaces, human body, liquid containers) since the EBGs over the ground plane virtually isolate the antenna system from the ambient environment.

As a next step, this antenna was integrated with a commercially available wireless temperature sensor in order to demonstrate its applicability to wearable wireless biosensors. The inkjet-printed EBG-backed antenna has tripled the communication range of the sensor from 29.5 to 82.8 m. This prototype verifies the capability of the inkjet printing technology to seamlessly integrate into conventional technology.

## INKJET PRINTED 2D ACTIVE WIRELESS SENSOR MODULES

To verify the module-level integration feasibility of this approach, a low-power active (battery-powered) RFID-enabled wireless temperature sensor tag was designed on paper ("System-on-Paper") to operate at 900 MHz. The power, digital and RF transmission lines/traces in the design were formed by the sintered nano-based ink that was deposited using the inkjet printing process on a paper-based substrate. The basic system comprised of a commercial microcontroller unit (MCU) that was used to sample a commercial temperature sensor and broadcast its information out by modulating a phase locked loop (PLL) module in a wireless transmitter integrated in the same



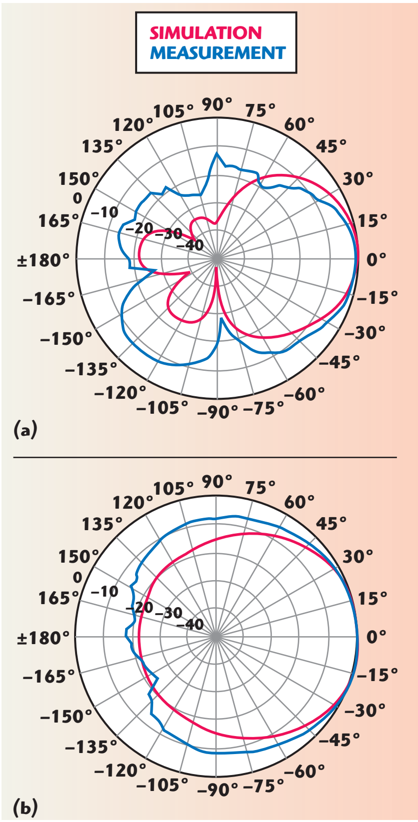


▲ *Fig. 5 Radiation patterns at 2.45 GHz (a) E-plane and (b) H-plane.*

COMSOL MULTIPHYSICS®

RF FILTERS: An evanescent-mode cavity filter is resonant at a frequency lower than its original fundamental mode frequency, and can be brought about by creating a discontinuity inside the cavity. The electric field and S-parameter analysis in this example shows that this discontinuity, the dielectric tube inside the cavity, does not significantly distort the signal.

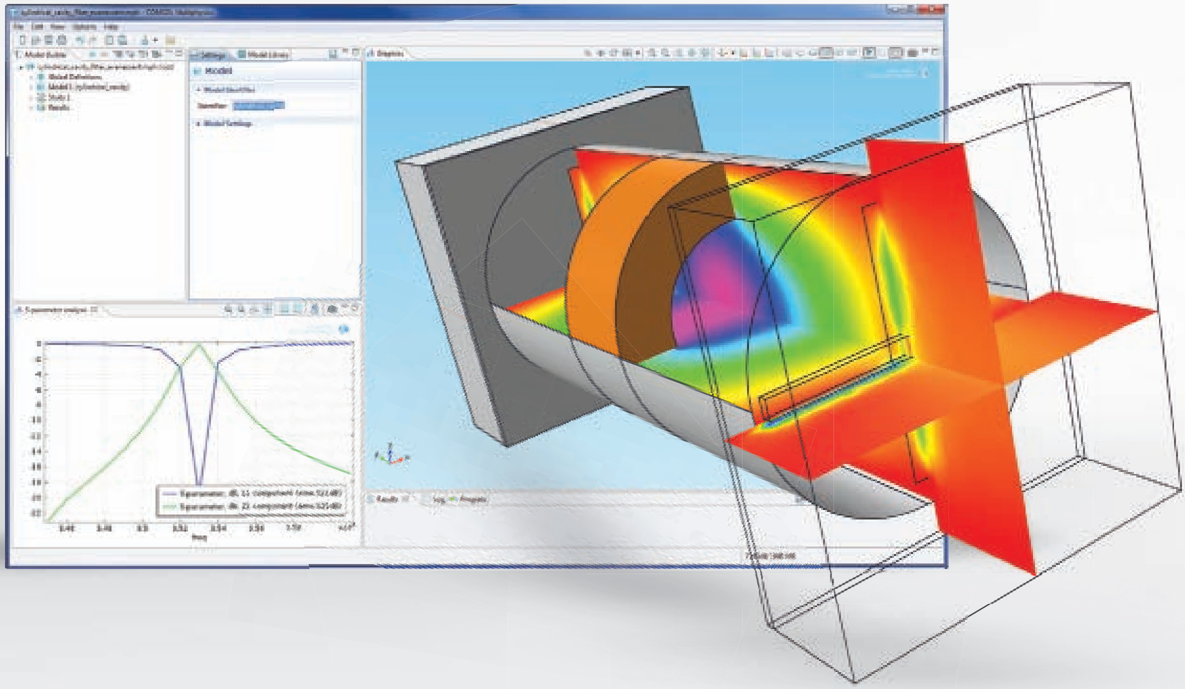

# Capture the Concept.

With COMSOL Multiphysics® you are empowered to build simulations that accurately replicate the important characteristics of your designs. The key is the ability to include all physical effects that exist in the real world. This multiphysics approach delivers results—tangible results that save precious development time and spark innovation.

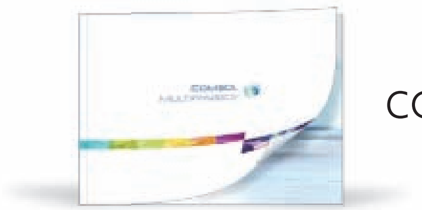

comsol.com/booklet

COMSOL

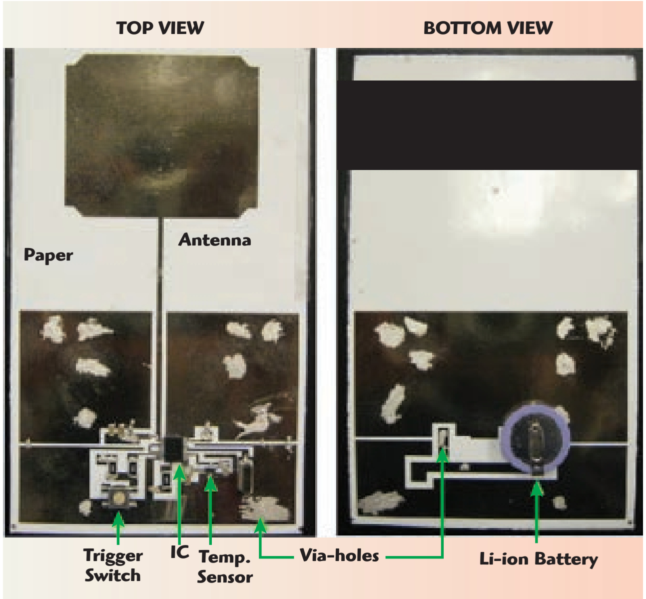


▲ *Fig. 6 Wireless sensor module prototype circuit developed on paper using inkjet printing of the silver nanoparticle-based conductor.*

chip as the microcontroller unit. The battery, temperature sensor and MCU/wireless transmitter IC were mounted on the inkjet-printed nano-particle-based traces using a conductive silver epoxy due to the low temperature tolerance of paper to the heat generated by a soldering iron.[13,14]

The signals used in the circuit included the high-speed digital signals used in the clocking of the MCU with an external crystal oscillator and the base-band signals used by the MCU to modulate the PLL in the integrated transmitter. In addition, 900 MHz amplitude-shift-keyed (ASK) and frequency-shift-keyed (FSK) signals between 860 and 925 MHz, similar to those required by the UHF Gen-2 protocol,[15] were output by the transmitter's PA into a UHF antenna also fabricated using the same conductive ink. To ensure maximum conductivity and antenna efficiency, the entire circuit was printed over with 12 layers of silver nano-particle ink resulting in a conductor thickness of 12 microns. The concentration of the silver nano-particles in the different traces was accurately controlled to achieve the optimum tradeoff between precision and conductivity for the different signals in the circuit. A higher precision inkjet cartridge spraying 1 picoliter droplets was used to print finer areas in the circuit layout, such as the digital MCU traces (~150 microns wide), and a 10 picoliter cartridge was used to print larger areas on the antenna and the RF ground planes/traces in the circuit layout to further increase conductivity. The final prototype developed can be seen in ***Figure 6***.[13]

The simulated gain of the monopole antenna printed using the silver nano-particle based ink was a maximum of 2.6 dBi, as shown in the simulated radiation pattern in ***Figure 7***. The transmitted signal as captured by a Real Time Spectrum Analyzer attached to an RFID antenna on the receiver side is shown in ***Figure 8*** verifying the operation of the wireless sensor module. From the captured power in Figure 7, the effective isotropic radiated power (PEIRP) from the wireless sensor circuit was determined to be 4.91 dBm,[13,16] which

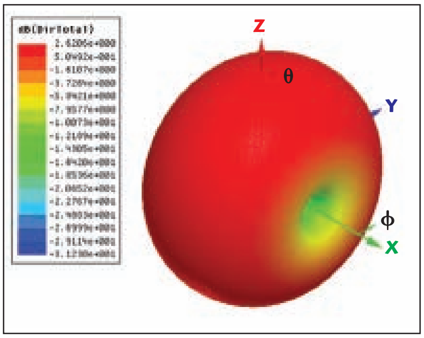


▲ *Fig. 7 Simulated radiation pattern of the monopole antenna.*

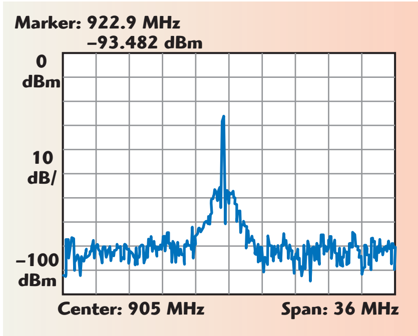


▲ *Fig. 8 Wireless sensor module prototype circuit developed on silver nanoparticle-based conductor on paper using inkjet printing.*

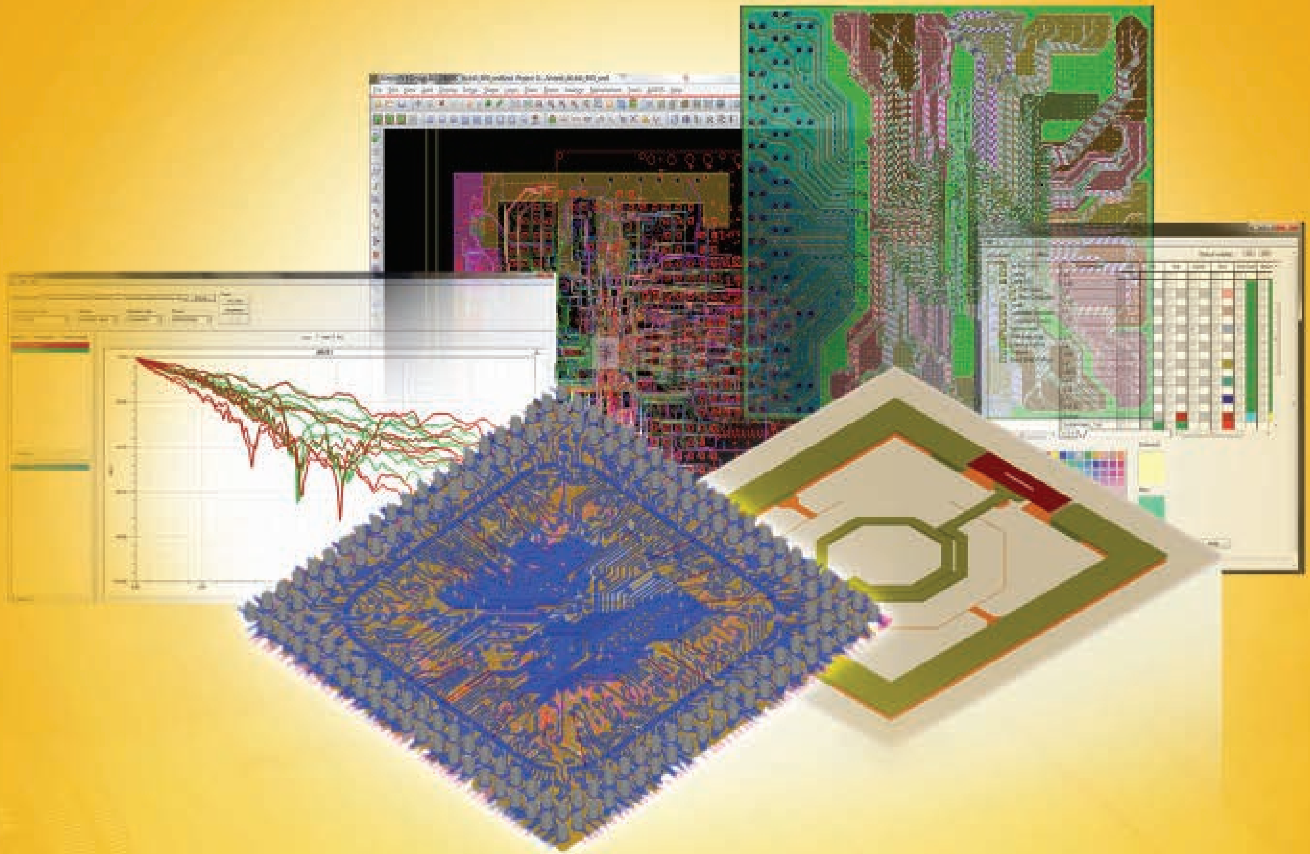

translates into a radiation efficiency of 61 percent for the silver nano-particle based antenna using Equation 1:

$$G_{ANTENNA} = P_{EIRP} - P_{PA} \quad (1)$$

$$\eta = \frac{\text{Directivity}}{G_{ANTENNA}} \quad (2)$$

where $P_{EIRP}$ = effective isotropic radiated power (4.91 dBm = 3.097 mW), $P_{PA}$ = power amplifier output fed into the antenna (4.5 dBm = 2.81 mW), $G_{ANTENNA}$ = antenna gain and Directivity = Antenna directivity (~2.6 dBi).

## BATTERY-LESS INKJET-PRINTED CARBON NANOTUBE SENSORS

Further work was done to evaluate the performance of inkjet-printed carbon nanotubes (CNT) as a zero power, battery-less, remote sensor. The idea was to use the ion-exchanging behavior of the CNTs with ambient gases as a mechanism to sense the chemical content in them. The varying electrical properties of the CNTs, due to their ability to absorb certain chemicals, present in the gases can be remotely interrogated and measured by embedding them as gas-sensitive loads of specially designed antennas. An optimized recipe that can be easily realized on various flexible substrates using inkjet printing was used. Chemical absorption produces changes in the properties of CNT embedded antenna structures, such as real and imaginary impedance, DC resistance, conductance and effective dielectric constant. These changes can be used to determine the presence of various chemical compounds by translating the material effects into measurable electrical quantities such as changes in measurable voltage, current and resonant frequency.[17] As a first step in the development of such zero power remote CNT sensors, stable carbon nanotube and graphene-based inks capable of integration in a wide range of potential devices via common inkjet printing methods have been developed.[17] Based on these inks, several devices have been produced.

## SENSOR TYPE 1: RF RESPONSIVE CNT AS A CHEMICAL SENSING ELEMENT

In order to study the RF response of the CNT to the different chemical gas concentrations, several samples of the microstrip waveguides embedded with single- and multi-walled (MWCNT) molecules were fabricated using inkjet printing technology. The sensitivity of each sample to the gases is shown in ***Figure 9***. Sensitivity is defined as the change of the CNT structure's impedance in the presence of the test gas relative to air (or other controlled environment). The CNT embedded microstrip line's response for gas concentration and the material's timing response were taken at room temperature and impedance measurements of 75-layer MWCNT samples were taken in air and in the presence of different $NH_3$ and $NO_2$ concentrations, i.e., 10, 15, 20, 30, 50, 70 and 90 ppm, across a range of frequencies from 50 MHz to 3 GHz.

Figure 9 shows the change in sensitivity as a function of concentration for both gases at the non-licensed spectrum bands of 864 MHz and 2.4 GHz. Sensitivity of 21.7 percent and 9.4 percent was achieved for 10 ppm $NO_2$ and 4 ppm $NH_3$, respectively, at 864 MHz, which is higher than that achieved in recent works[18,19] for high-

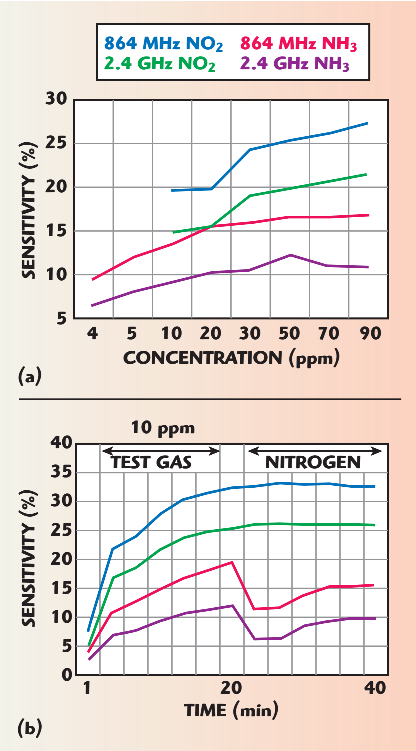


▲ *Fig. 9 (a) Response as a function of concentration taken after stabilization and (b) timing response for $NH_3$ and $NO_2$ using concentration of 10 ppm at 864 MHz and 2.4 GHz.*

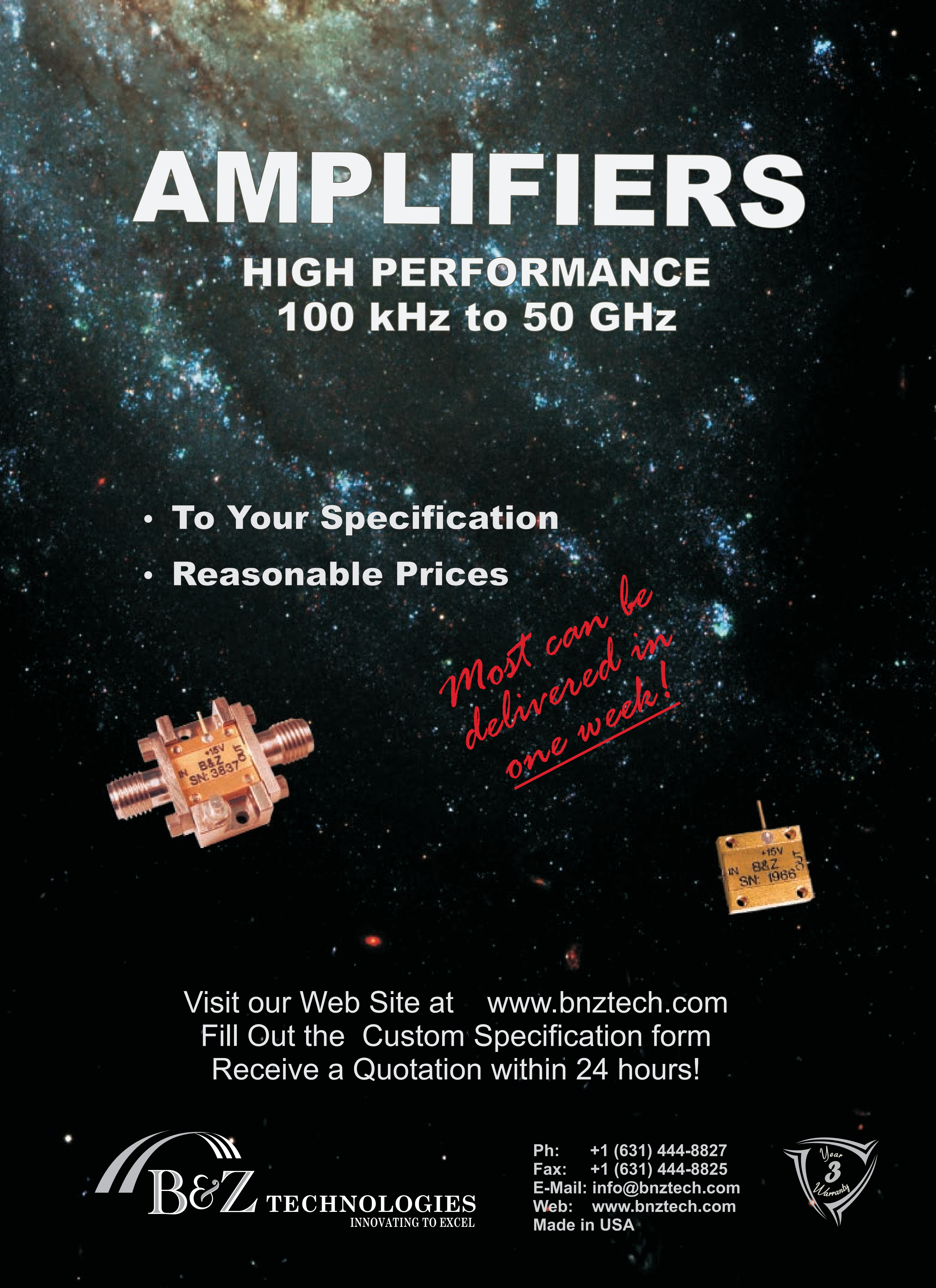
AMPLIFIERS
HIGH PERFORMANCE
100 kHz to 50 GHz
• To Your Specification
• Reasonable Prices
Most can be delivered in one week!
+15V
IN
B&Z
SN: 3837
OUT
+15V
IN
B&Z
SN: 1966
OUT
Visit our Web Site at www.bnztech.com
Fill Out the Custom Specification form
Receive a Quotation within 24 hours!
B&Z TECHNOLOGIES
INNOVATING TO EXCEL
Ph: +1 (631) 444-8827
Fax: +1 (631) 444-8825
E-Mail: info@bnztech.com
Web: www.bnztech.com
Made in USA
Year 3 Warranty

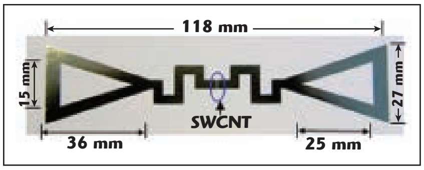


▲ *Fig. 10 Inkjet-printed CNT antenna sensor prototype embedded with SWCNT film on a flexible paper substrate.*

er concentration (100 ppm) of $NH_3$. Figure 9b provides the timing response to the same chemical gases at the chosen frequencies. For this portion of the experiment, 10 ppm was used as the concentration for both gas tests. The measurements were taken at 1, 2, 5, 10, 15 and 20 minutes. As shown in Figure 9b, the MWNT-based gas sensor demonstrates fast response to both gases (few seconds); the sensitivity achieved at 864 MHz is 24.2 percent for $NO_2$ and 12.7 percent for $NH_3$ in just two minutes. Note that after testing, the sensor exposed to $NH_3$ shows more rapid recovery, possibly due to the greater electro-negativity of one pole of the $NH_3$ molecule.

## SENSOR TYPE 2: INKJET PRINTED CNT EMBEDDED ANTENNAS AS A BATTERY-LESS REMOTE WIRELESS SENSOR

With the inkjet printed CNT structure impedance response showing a measured variability in the presence of gases, a battery-less, wirelessly interrogated RFID-enabled CNT-based antenna sensor tag was developed in which the silver electrodes connected to the CNT film, as shown in ***Figure 10***, were inkjet-printed in the form of a specially designed antenna. The operation of the CNT-based antenna sensor utilizes the same backscattering principles that are currently in use with existing RFID tags in order to communicate the data from the tag side to the reader without using a built-in power source. Unlike the digital logic-altered impedance of the antenna in a conventional RFID tag, the CNT-based antenna sensor utilizes the inkjet-printed CNTs to alter its own impedance in the presence of a chemical gas, and in the process its own radar cross section to the incident field coming at it from a wireless interrogator. The changing radar cross section of the CNT-based antenna sensor reflects back a proportional amount of the incident wireless power back to the interrogator which it measures, digitizes and displays for the end user remotely away from the gas being sensed. This proportion of reflected wireless power as a function of the response of the CNT-based antenna sensor is represented by its power reflection co-efficient ($\eta$) given by Equation 3.

$$\eta = \left| \frac{Z_{load} - Z_{ANT}^*}{Z_{load} + Z_{ANT}} \right|^2 \qquad (3)$$

where $Z_{load}$ represents the impedance of the CNT-based sensing element and $Z_{ANT}$ represents the impedance of the antenna element with $Z_{ANT}^*$ being its complex conjugate. The same mechanism can be used to realize completely inkjet-printed RFID-enabled sensor modules. The CNT film functions as a tunable resistor $Z_{load}$ with its value determined by the existence of the target gas. An interrogating reader monitors the backscattered power level. When the power level (controlled by the modification of the imaginary part of the CNT-based impedance) and/or the frequency (controlled by the modification of the real part of the CNT-based impedance) changes, it means that there is variation in the load impedance; therefore, the sensor detects the existence of the gas. Calculated from Friis free-space formula, the backscattered power in decibels received by the RFID reader is defined as Equation 4:[16]

$$P_R = P_T + 2G_T + 2G_R - 40\log_{10}\left(\frac{4\pi}{\lambda}\right) - 40\log_{10}(d) + \eta \qquad (4)$$

where $P_T$ is the power fed into the reader antenna, $G_T$ and $G_R$ is the gain of the interrogating reader antenna and CNT antenna sensor, respectively, and d is the distance between both. In Equation 4, except for the term $\eta$, all the values remain constant before and after the RFID tag meets the gas. Therefore, the variation of the backscattered power level solely depends on $\eta$, which is determined by the impedance of the SWCNT film in the CNT-based antenna sensor, as shown in ***Figure 11***.

## GRAPHENE-BASED WISP WIRELESS GAS SENSOR

In addition to CNT materials, ink-

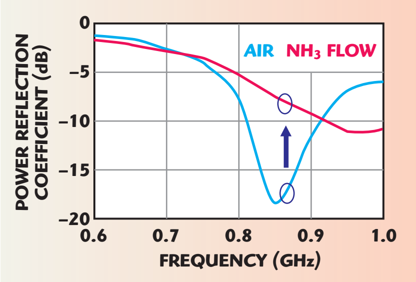


▲ *Fig. 11 The calculated power reflection coefficient (η) of the CNT-based antenna sensor with a SWCNT film before and after the gas flow.*

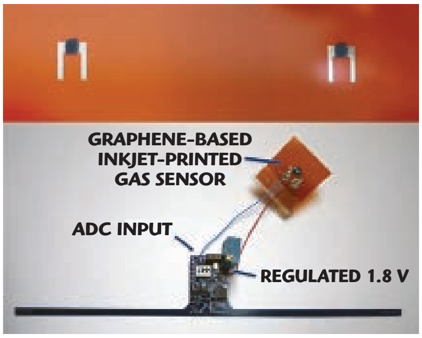


▲ *Fig. 12 (a) Thin graphene films inkjet-printed in between and overlapping silver conductive inkjet-printed trace on Kapton substrate and (b) integrated WISP device.*

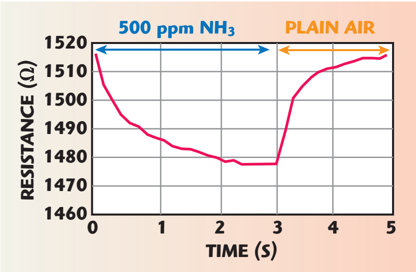


▲ *Fig. 13 DC resistance measurements of the graphene sample 1.*

jet-printed graphene has also been investigated as a potential sensor material to improve the sensor selectivity (the ability to distinguish between different types of gases), response and recovery time. The sensing structure of this device comprised of layers of graphene film inkjet selectively deposited atop silver nano-particle-based feeding lines using a special inkjet printing technique/recipe on a robust Kapton substrate due to its robust tolerance to the harsh reduction environment required for extracting graphene. ***Figure 12*** shows the final sensor that was integrated with the WISP platform to remotely sample, store and transmit the sensed information using the RFID EPC Gen 2 protocol.[15]

The response time of the graphene sensor was tested by delivering a controlled concentration of ammonia gas in a semi-closed glass chamber to direct the flow of gas onto the sensor. The results of the measured resistance for 500 ppm of ammonia/air mixture are shown in ***Figure 13***.[20]

The graphene-based sensor demonstrates a fast response time, producing a resistance change of approximately five percent in response to the ammonia gas within three minutes. More interesting is the recovery time of the material. Within the first 15 seconds, the material is recovered by over 31 percent with no heating or UV treatments. Within the first minute, the material is recovered by over 80 percent. This result is different in comparison with the literature,[21] where recovery times are generally on the order of several minutes. Additionally, the heating and UV treatments applied by some authors to achieve reported material recovery limits their usefulness in real-world environments.

## INKJET-PRINTED AMBIENT WIRELESS POWER SCAVENGING DEVICE

In addition to battery-less sensors and antennas, inkjet printing has also been successfully utilized to develop a wireless power scavenging platform that uses the ambient power currently found in the existing wireless spectrum to power up a wireless node (mote) made up of a microcontroller and a transceiver. Based on wireless spectrum measurements carried out in downtown Tokyo, a perpetual ambient source of wireless power was found in the frequency band from between 470 to 570 MHz, which is currently used for Analog (470 to 495 MHz) and Digital TV (520 to 570 MHz) broadcasts. These lower UHF bands offer superior propagation characteristics in terms of low attenuation through air and walls and also experiences lower parasitic losses through circuit components.

A review of microcontrollers and transceiver technology currently manufactured by a host of IC companies shows them to have the lowest operating voltage range of between 1.8 and 3.6 V. In order to completely eliminate the use of a battery, the wireless


**RFHIC's GaN solutions are so affordable**
**that RRHs based on RFHIC's GaN pay for themselves in a few years.**

### RFHIC's LTE Power Amps Sold

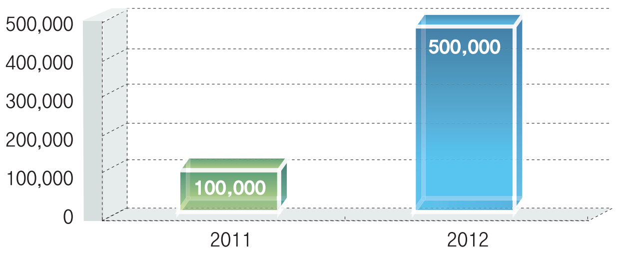


While LDMOS is the mainstay of the Telecom industry, recent price drops of GaN based amplifiers have placed it on par with LDMOS based Remote Radio Head (RRH) systems' price. GaN's technological advantage remains in its wider bandwidth coverage, allowing future application upgrades, and most importantly, its efficiency. With more than 35 million watts of GaN powered RRHS rolled out to LTE providers already in U.S. and Asia, GaN technology is just starting to take hold of the market. Thanks to these efficient GaN power amplifiers, these carriers will not only save billions of dollars of operating costs over the lifespan of the RRH systems but also be greener by reducing significant amounts of carbon dioxide. Again, analyst estimates that wireless carriers in U.S. alone can save over $2 billion per year on operating costs, primarily from energy savings on their wireless infrastructures by simply switching to GaN power amplifiers from LDMOS.

Moreover, GaN's efficiency enables RRH designers to make systems smaller by reducing the heat sink size and power supply requirement. This directly translates to lower installation and RRH space rental expenses for carriers. Additionally, overall reliability also affects the carriers' bottom lines by producing more reliable LTE services to end users, and also by reducing expected maintenance expenses. Furthermore, carriers can save on future upgrades as GaN based RRH can support multi-band, multi-mode, and multi-carrier technology.

RFHIC is a leading manufacturer of GaN power amplification solutions worldwide, having produced solutions for Sprint, LG Telecom, SK Telecom, and a major Japanese carrier for their RRH solutions. RFHIC will deliver around 500,000 GaN power amplifiers for LTE roll-outs in 2012, equivalent to more than 135 million watts. For more information, contact us at sales@rfhicusa.com

*RF & MW is our business & passion*

Worldwide
Tel : 82-31-250-5078 / E-mail : rfsales@rfhic.com

USA Office
Tel : 919-677-8780 / E-mail : sales@rfhicusa.com

RFHIC
www.rfhic.com

mote prototype was equipped with a low leakage super capacitor that was trickle charged with wireless power. Super capacitors have significant advantages over batteries through their significantly higher number of recharge cycles, low leakage, low cost and cleaner disposal. The drawback with capacitors is their unregulated voltage, which in the absence of proper supervision may discharge quickly, rendering the end device powerless. Lack of supervision of the charge-discharge mechanism of the capacitor into the end device may also cause it to undergo unnecessary power-on-resets (POR). In such a scenario, the MCU would turn on once the capacitor reached its turn on voltage drawing current from the capacitor, immediately causing the capacitor to discharge. Without sufficient voltage margin, the capacitor voltage would drop below the turn on voltage of the MCU, shutting it down before it can complete its firmware routine. With capacitors as power storage devices, there is always a risk of the MCU entering a state of constant PORs without finishing its functioning.

Preventing such a state has to be achieved through the proper design and calibration of the PMU circuit, which in essence is a voltage trigger analog switch that is set to a voltage sufficiently higher than the turn-on voltage of the MCU, but lower than the maximum operating voltage of the MCU along with proper firmware design. The operating time of the wireless mote would be the discharge time of the capacitor from the PMU triggered turn-on voltage to the turn off voltage of the MCU at 1.8 V.[22]

In order to ensure that the ambient wireless power in the UHF band (between 470 to 570 MHz) is transformed to the required voltage of 1.8 V and higher across the capacitor at a fixed distance from the power source, a topology comprising of a multistage RF voltage multiplier was used. RF Schottky diodes were used for the RF charge pumps given their lower forward voltage drop compared to conventional silicon-based PN diodes. Parasitic effects due to packaging currently limit the forward voltage of the diode to between 100 and 400 mV and forward currents of between 0.1 to 100 mA.[22] This means any voltage received across the antenna terminals below this voltage would result in the antenna seeing an open impedance towards the circuit that would cause all the incident wireless power to be reflected back without turning on the device. In order to avoid this scenario at a given distance from the wireless source, a properly designed and laid out RF charge pump circuit was designed and optimally matched to the antenna to help transform and



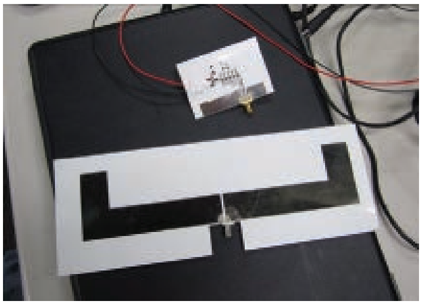

▲ *Fig. 14 Inkjet-printed ambient wireless power scavenging device.*

# MMIC AMPLIFIERS

## DC to 20 GHz from 73¢ qty.1000

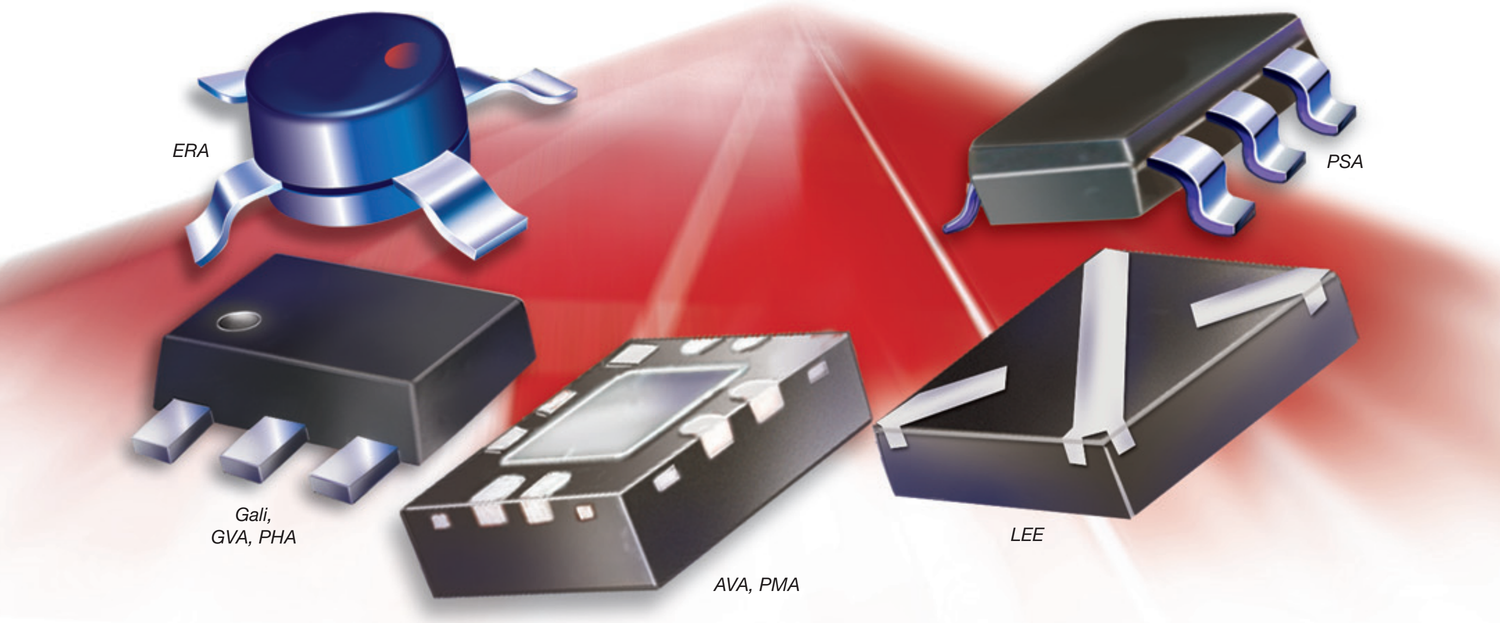


### *NF from 0.5 dB, IP3 to +48 dBm, Gain 8 to 31 dB, Pout to +30 dBm*

**Think of all you stand to gain.** With more than ~~124~~ 145 catalog models, Mini-Circuits offers one of the industry's broadest selection of low-cost MMIC amplifiers. Our ultra-broadband InGaP HBT and PHEMT amplifiers offer low noise figure, high IP3, and a wide selection of gain to enable optimization in your commercial, industrial or military application.

Our tight process control guarantees consistent performance across multiple production runs, so you can have confidence in every unit. In fact, cascading our amplifiers often results in less than 1dB total gain variation at any given frequency. These MMIC amplifiers can even meet your most critical size and power consumption requirements with supply voltages as low as 2.8 V, and current consumption down to 20 mA, and packages as small as SOT-363.

Visit our website to select the amplifier that meets your specific needs. Each model includes pricing, full electrical, mechanical, and environmental specifications, and a full set of characterization data including S-Parameters. So why wait, place your order today and have units in your hands as early as tomorrow. *RoHS compliant*

*Mini-Circuits...we're redefining what VALUE is all about!*

**Mini-Circuits®**

*ISO 9001 ISO 14001 AS9100*

P.O. Box 350166, Brooklyn, New York 11235-0003 (718) 934-4500 Fax (718) 332-4661

YONI2® ***The Design Engineers Search Engine*** *finds the model you need, Instantly* • For detailed performance specs & shopping online see **minicircuits.com**

U.S. Patents
7739260, 7761442

***IF/RF MICROWAVE COMPONENTS***

476 Rev F

rectify the incident wireless power to a higher voltage, thereby ensuring a trickle charge into the end capacitor. The complete prototype capable of scavenging power from ambient TV signals at long ranges of over 6 km was fabricated using inkjet printing technology and is shown in ***Figure 14***. The low turn on power of 35 μW in air is enough for the power scavenger to generate over 1.8 V at its output super capacitor. This is possible due to its low series dissipative losses (< 1.1 ohms)[9,22] and almost exclusive charge pump capacitive reactance as shown by the input impedance of the power scavenger[22] (see ***Figure 15***). An output voltage of 1.8 V is capable of powering on most low power MCUs and wireless transceivers. Field measurements of the prototype carried out in Tokyo, Japan show the prototype capable of scavenging enough wireless power from a TV tower 6.5 km away.[22]



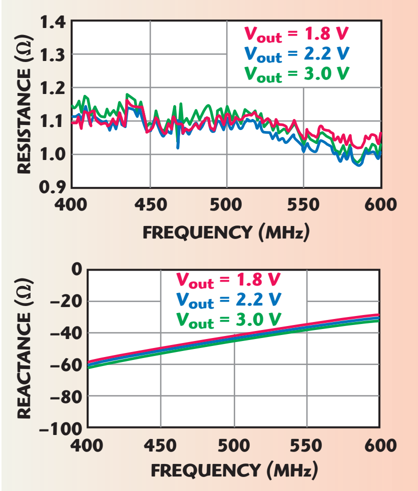


▲ *Fig. 15 Input impedance of the ambient TV power scavenging device.*

## CONCLUSION

While batteries may be essential for reliable operation of applications requiring a more reliable and steadier supply, power scavenging techniques and zero-power nanostructure (e.g., CNT, graphene) based sensors can be reliably used for powering on a number of ubiquitous RFID and remote wireless sensing applications without the need for a battery, as shown in the prototypes presented in this article. By utilizing an optimized, selective metallization process such as inkjet printing, integrated 2D/3D battery-less power scavenging wireless sensing modules/motes operating at frequencies well into the UHF range and beyond can be successfully fabricated in an environmentally friendly and cost-effective way for numerous applications including Internet of Things, Smart Skins, Smart WSNs and wearable biomonitoring systems. ■

## References


1. V. Lakafosis, A. Rida, R. Vyas, Y. Li, S. Nikolaou and M.M. Tentzeris, "Progress Towards the First Wireless Sensor Networks Consisting of Inkjet-Printed, Paper-Based RFID-Enabled Sensor Tags," *Proceedings of the IEEE*, Vol. 98, No. 9, 2010, pp. 1601-1609.
2. M. Lessard, L. Nifterik, M. Masse, J. Penneau and R. Grob, "Thermal Aging Study of Insulating Papers Used in Power Transformers," Electrical Insulation and Dielectric Phenomena 1996, *IEEE Annual Report of the Conference*, Vol. 2, 1996, pp. 854-859.
3. L. Yang, A. Rida, R. Vyas and M.M. Tentzeris, "RFID Tag and RF Structures on a Paper Substrate Using Inkjet-Printing Technology," *IEEE Transactions on*

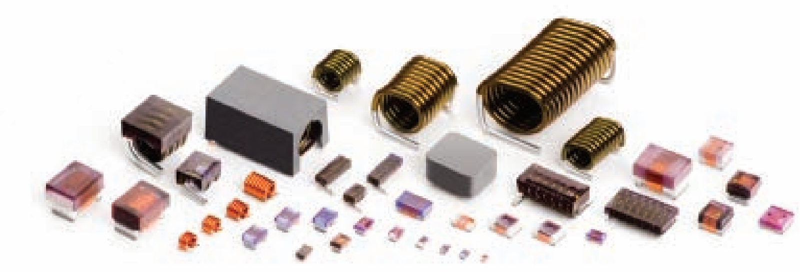



*Microwave Theory and Techniques*, Vol. 55, No. 12, December 2007, pp. 2894-2901.

4. A. Rida, L. Yang, R. Vyas, S. Basat, S. Bhattacharya and M.M. Tentzeris, "Novel Manufacturing Processes for Ultra-Low-Cost Paper-Based RFID Tags With Enhanced 'Wireless Intelligence'," *Proceedings of the 57th IEEE-ECTC Symposium*, Sparks, NY, June 2007, pp. 773-776.
5. L. Yang and M.M. Tentzeris, "3D Multilayer Integration and Packaging on Organic/Paper Low-Cost Substrates for RF and Wireless Applications," *ISSSE 2007 International Symposium on Signals*, 2007, pp. 267-270.
6. Cabot CCI-300 Conductive Nano-Silver Ink Datasheet, www.cabot-corp.com/New-Product-Development/Printed-Electronics/Products/Downloads/DL200811220115AM3822/
7. J. Mujal, E. Ramon, E. Diaz, J. Carrabina, A. Calleja, R. Martinez and L. Teres, "Inkjet Printed Antennas for NFC Systems," *Electronics, Circuits, and Systems (ICECS), 2010 17th IEEE International Conference, 2010*, pp. 1220-1223.
8. G. Shaker, S. Safavi-Naeini, N. Sangary and M.M. Tentzeris, "Inkjet Printing of Ultrawideband (UWB) Antennas on Paper-Based Substrates," *IEEE Antennas and Wireless Propagation Letters*, Vol. 10, 2011, pp. 111-113.
9. R. Vyas, V. Lakafosis, M.M. Tentzeris, H. Nishimoto and Y. Kawahara, "A Battery-Less, Wireless Mote for Scavenging Wireless Power at UHF (470 to 570 MHz) Frequencies," *IEEE Transactions on Antennas and Propagation (APSURSI)*, 2011, pp. 1069-1072.
10. G. Shaker, M.M. Tentzeris and S. Safavi-Naeini, "Low-Cost Antennas for mm-Wave Sensing Applications using Inkjet Printing of Silver Nano-particles on Liquid Crystal Polymers," *IEEE Transactions on Antennas and Propagation (APSURSI)*, 2011, pp. 1-4.
11. G. Shaker, H.S. Lee, K. Duncan and M.M. Tentzeris, "Integrated Antenna with Inkjet-Printed Compact Artificial Magnetic Surface for UHF Applications," *2010 IEEE International Conference on Wireless Information Technology and Systems (ICWITS)*, 2010, pp. 1-4.
12. S. Kim and M.M. Tentzeris, "Wearable Biomonitoring Monopole Antennas Using Inkjet Printed Electromagnetic Band Gap Structures," *Proceedings of the 6th European Conference on Antennas and Propagation (EUCAP)*, 2012, accepted.
13. R. Vyas, et al., "Paper-Based RFID-Enabled Wireless Platforms for Sensing Applications," *IEEE Transactions on Microwave Theory and Techniques*, Vol. 57, 2009, pp. 1370-1382.
14. R. Vyas, A. Rida, L. Yang and M.M. Tentzeris, "Design, Integration and Characterization of a Novel Paper-Based Wireless Sensor Module," *IEEE International Microwave Symposium*, June 2008, pp. 1305-13078.
15. "UHF Gen-2 System Overview," Texas Instruments, September 2005.
16. J. Seybold, *Introduction to RF Propagation*, John Wiley & Sons, Hoboken, NJ, 2005, pp. 111-133, 163-179.
17. Lakafosis, X.H. Yi, T.R Le, E. Gebara, Y. Wang and M.M. Tentzeris, "Wireless Sensing with Smart Skins," *IEEE Sensors 2012*.
18. Z.Y. Lin, T.R. Le, J. Song, Y.G. Yao, Z. Li, K.S. Moon, M.M. Tentzeris and C.P. Wong, "Preparation of Water-Based Carbon Nanotube Ink and its Application in Inkjet Printing of Carbon Nanotube Gas Sensor," *Journal of Electronic Packaging*, Vol. 98, No. 9, pp. 1601-1609, 2012.
19. R. Mangu, S. Rajaputra and V.P. Singh, "MWCNT-Polymer Composites as Highly Sensitive and Selective Room Temperature Gas Sensors," *Nanotechnology*, Issue 21, 2011.
20. T. Le, V. Lakafosis, Z. Lin, M.M.

# RFMD®

## Compact, Low Loss Switching for High Linearity 2G/3G/4G Applications


RFMD offers a family of high-power discrete switch products, which are available in SPDT, SP3T, and SP4T type architectures. These switches are tailored to address coexistence issues in WiFi, BT, GPS, and LTE bands, which require extremely high linearity. These switches have very low current consumption making them ideal for use in battery-powered cellular devices where talk time and standby time are critically important. Other possible applications for these switches include antenna tuning and cellular band switching.

**SPECIFICATIONS**

| | *Control Lines* | *Freq Range (MHz)* | *Power Handling (dBm)* | *Control Voltage (V)* | *Insertion Loss (dB)* | *Isolation (dB)* | *Switching Speed (uS)* | *IIP2 (dBm)* | *IIP3 (dBm)* | *Package (mm)* | *Mass Production* | *Part Number* |
|---|---|---|---|---|---|---|---|---|---|---|---|---|
| SPDT | 1 | DC to 3500 | 36 | 0 / +1.8 | 0.3 | 43 | 2.00 | 129 | 74 | 2.0 x 2.0 x 0.55 | NOW | RF1602 |
| SP3T | 2 | DC to 3500 | 36 | 0 / +1.8 | 0.4 | 40 | 2.00 | 120 | 73 | 2.5 x 2.5 x 0.55 | NOW | RF1603A |
| SP4T | 2 | DC to 3500 | 36 | 0 / +1.8 | 0.4 | 40 | 2.00 | 120 | 73 | 2.5 x 2.5 x 0.55 | NOW | RF1604 |

**Order RFMD products online at www.rfmd.com/MWJS1111.**

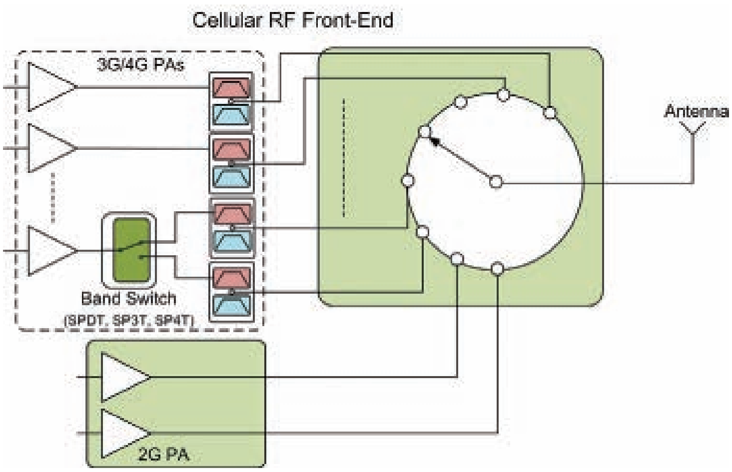


**FEATURES**

- **Very low insertion loss and high isolation**
- **Excellent linearity performance: IIP2 > 120dBm, TBR > 81dBc**
- **1.8V GPIO compatible**
- **Very low current consumption**
- **Broadband operation across multiple frequency bands and applications**



RFMD®

Mobility. Connectivity. Energy.

Tentzeris and C.P. Wong, "Graphene-Based Inkjet-Printed WISP-Enabled Wireless Gas Sensor," submitted to IMS 2012.
21. F. Schedin, et al., "Detection of Individual Gas Molecules Adsorbed on Graphene," *Nature Materials*, Vol. 6, 2007.
22. R. Vyas, H. Nishimoto, M. Tentzeris, Y. Kawahara and T. Asami, "A Battery-Less, Wireless Mote for Scavenging Wireless Power at UHF (470 to 570 MHz) Frequencies," submitted to the IEEE International Microwave Symposium, 2012.

**Manos M. Tentzeris** *received his degree in Electrical and Computer Engineering from the National Technical University of Athens (Magna Cum Laude) in Greece and MS and PhD degrees in Electrical Engineering and Computer Science from the University of Michigan, Ann Arbor, MI. He is currently a Professor with the School of ECE, Georgia Tech, Atlanta. He has published more than 420 papers in Journals and Conference Proceedings, five books and 19 book chapters. He is also an IEEE Fellow and IEEE MTT Distinguished Microwave Lecturer.*

**Rushi Vyas** *received his B.S. and M.S. degrees in Electrical Engineering from the Georgia Institute of Technology, Atlanta, in 2005 and 2010. He is currently a researcher at the ATHENA research group at the Georgia Institute of Technology while pursuing his PhD degree. He has authored/co-authored over 20 research works in peer-reviewed journals, conference proceedings and book chapters covering areas of antenna design, wireless and low power electronics, sensors, ubiquitous computing and energy harvesting. His work has been recognized in* MSN News, Engadget *and* Design World.

**Vasileios Lakafosis** *(S'07) received his Diploma degree in Electrical and Computer Engineering from the National Technical University, Athens, Greece, in 2006 and his M.Sc. degree in Electrical and Computer Engineering from the Georgia Institute of Technology, Atlanta, in 2009. He is currently pursuing his PhD degree at the Georgia Institute of Technology. Lakafosis has worked for Microsoft Research, the Cisco Research Center and the University of Tokyo. He has authored and co-authored two book chapters and over 15 papers in peer-reviewed journals and conference proceedings.*

**Taoran LE** *received her B.S. ('05) in Applied Physics from Hefei University of Technology. She received her M.S. degrees ('11) in Electronic Engineering from Politecnico di Torino in Italy and the Institut Polytechnique de Grenoble in France. She is currently a research assistant in the ATHENA group at Georgia Institute of Technology.*

**Amin Rida** *received his B.S., M.S. and Ph.D. degrees in Electrical and Computer Engineering from the Georgia Institute of Technology. He is currently a Systems Engineer at Northrop Grumman. He has authored and co-authored three books/chapter, seven journal papers, 30 conference papers in peer reviewed publications and has four pending patents.*

**Sangkil Kim** *received his bachelor's degree in Electrical and Electronic Engineering from Yonsei University, Seoul, Republic of Korea, in 2010. At present, he is pursuing his PhD degree at the Georgia Institute of Technology, Atlanta. He is now a research assistant at ATHENA group.*

MVP

Most Valuable Product

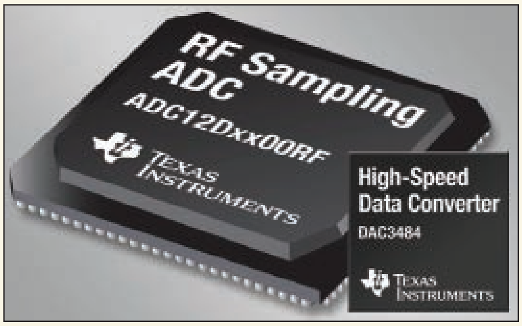


# High-Speed DAC and ADC Family

Industry analyst firm Databeans forecasts the data converter market to more than double between 2011 and 2015, with the high-speed analog-to-digital converter (ADC) and digital-to-analog converter (DAC) markets outpacing all other data converter product categories. Between 2011 and 2015, the firm expects the high-speed ADC market to grow more than 70 percent and the high-speed DAC market to grow about 60 percent.

What's driving this growth? Just think about how much technology is packed into a new car today versus ten years ago or the increasing number of consumer electronics that most of us depend on – from computers, tablets and e-readers to smartphones, cameras and MP3 players – many of which connect to the global communications network. As technology continues to advance, so too does the need to convert digital signals into the analog world in which we live. And while Databeans forecasts continued growth across all data converter market segments, the firm expects the communications market to grow the most.

To support the needs of communications, defense and aerospace manufacturers, Texas Instruments continues to develop data converters that are faster, smaller and lower power, while also providing higher resolution, ACPR and dynamic range performance. TI's new quad, 16-bit DACs and direct RF sampling ADCs are examples of how the company is pushing the limits of data conversion to enable its customers to innovate.

## DAC3484 SERIES

The 1.5 giga-samples per second (GSPS) DAC34SH84 and 1.25 GSPS DAC3484 are four-channel, 16-bit DACs combining low power consumption, high dynamic range and small size, enabling manufacturers of 3G, LTE and WiMAX base stations, repeaters and software defined radios (SDR) to push the limits of bandwidth and performance while keeping power consumption in check. A wider-input bus DAC34H84 or two-channel DAC3482 are also available to support transmit solutions with DPD linearization bandwidth up to 500 MHz.

The sample rate of the DAC34SH84 clocks in at 1.5 GSPS with a 750 MSPS input data rate per converter, enabling cellular providers to transmit wider signal bandwidths while still using adaptive digital pre-distortion loops, up to 125 MHz using fifth order feedback correction techniques. At 1.25 GSPS, the DAC3484 consumes

Texas Instruments
*Dallas, TX*

# More Power To You!

## *Our Newest "S" Series Amps Now Offers Powers From 20 To 1200 watts, And Everything In Between.*

Once again AR has turned up the power on our "S" Series 0.8-4.2 GHz solid-state amplifiers. Recently we made them smaller and lighter, with more power. Now we've added ***more*** power without increasing size or weight.

One thing we didn't change was something we call **Subampability:**™ giving you expandable power. It's a unique money-saving feature that lets you add amplifiers when you need more power. And you can use these amps independently for tests that don't require as much power.

AR products are backed by the best and most comprehensive warranty in the industry. We back them better because we build them better. And we support our customers with a global network that reaches the far corners of the world.

So when you need a new power amplifier, there are some very powerful reasons to choose an "S" Series amp from AR.

***www.arworld.us**/sSeries*

ISO 9001:2008
Certified

**rf/microwave instrumentation**

Other ar divisions: modular rf • receiver systems • ar europe

USA 215-723-8181. For an applications engineer, call 800-933-8181.
In Europe, call ar United Kingdom 441-908-282766 • ar France 33-1-47-91-75-30 • emv GmbH 89-614-1710 • ar Benelux 31-172-423-000

www.arworld.us

as little as 250 mW per channel – up to 65 percent less than the closest competitor (see ***Figure 1***) – while enabling wideband power amplifier linearization of up to 250 MHz.

The DAC3484 series simplifies the design of complex transmit architectures with 2× to 16× digital interpolation filters providing more than 90 dB of stopband attenuation to simplify data interface and reconstruction filters. Independent complex mixers allow flexible carrier placement, and a high-performance, low-jitter clock multiplier simplifies clocking without sacrificing dynamic range. The DAC3484 series also includes digital quadrature modulator correction (QMC), enabling complete IQ compensation for gain, offset, phase and group delay between channels in traditional direct up-conversion applications with quadrature modulators. Measuring 9 x 9 mm, the DAC3484 and DAC3482 multi-row QFN package is significantly smaller than comparable DACs, enabling compact designs. The higher speed DAC34SH84 ships in a 12 x 12 mm BGA package.

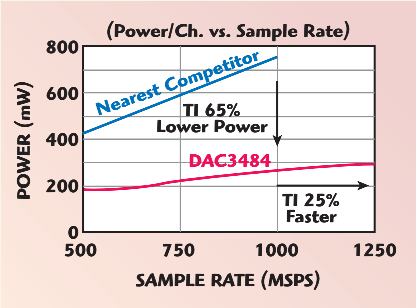


▲ *Fig. 1 1.25 GSPS, 16-bit DAC reduces power consumption and increases speed.*

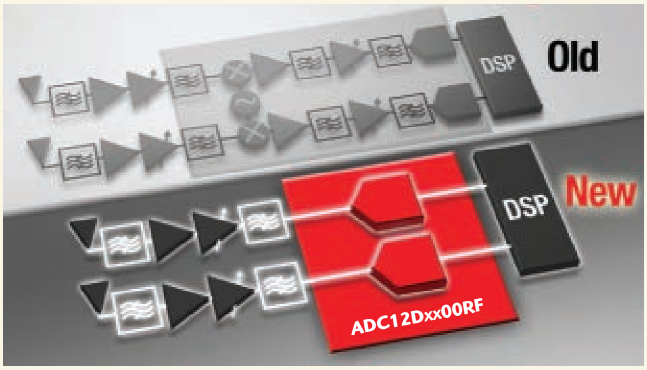


▲ *Fig. 2 RF sampling ADCs simplify radio design.*

## ADS12DXX00RF FAMILY

The ADS12Dxx00RF family of ADCs is the industry's first to directly sample RF signals beyond 2.7 GHz, with third-order intermodulation distortion (IMD3) up to -71 dBc and sampling at up to 3.6 GSPS. The family includes five 12-bit ADCs that enable system designers to eliminate multiple intermediate frequency (IF) down-conversion stages, including amplifiers, mixers, LOs and filters, as shown in ***Figure 2***. By replacing entire signal chain subsystems, the ADC12Dxx00RF drastically reduces bill of materials (BOM) cost, board size and weight in 3G/4G wireless base stations as well as microwave backhaul, military and wideband SDR applications.

The ADC12Dxx00RF family provides excellent noise and linearity performance at RF frequencies up to and above 2.7 GHz, extending the usable range beyond the 11th Nyquist zone. The devices provide a flexible LVDS interface with multiple SPI-programmable options for board design and FPGA/ASIC data capture. The LVDS outputs are compatible with IEEE 1596.3-1996 and support programmable common mode voltage.

The ADS12Dxx00RF family includes:

- ADC12D1800RF, providing interleaved single-channel sampling rates up to 3.6 GSPS, or dual-channel rates up to 1.8 GSPS, with IMD3 of -64 dBc at 2.7 GHz.
- ADC12D1600RF, providing interleaved single-channel sampling rates up to 3.2 GSPS, or dual-channel rates up to 1.6 GSPS, with IMD3 of -70 dBc at 2.7 GHz.
- ADC12D1000RF, providing interleaved single-channel sampling rates up to 2.0 GSPS, or dual-channel rates up to 1.0 GSPS, with IMD3 of -69 dBc at 2.7 GHz.
- ADC12D800RF, providing interleaved single-channel sampling rates up to 1.6 GSPS, or dual-channel rates up to 800 MSPS, with IMD3 of -71 dBc at 2.7 GHz.
- ADC12D500RF, providing interleaved single-channel sampling rates up to 1.0 GSPS, or dual-channel rates up to 500 MSPS, with IMD3 of -69 dBc at 2.7 GHz.

**Texas Instruments,
Dallas, TX (972) 644-5580,
www.ti.com.**

Connect Here.
For complete
Vertical Integration
2D/3D Design Tools
ANSYS HFSS™
Electrical Simulation Modeling
At Delta Electronics Manufacturing, we control every aspect of every process, from product inception through final inspection. The result, is a RF/microwave or millimeter wave interconnect solution that meets your expectations, first time, every time.
CNC Turning Centers
In house state-of-the-art automated electroplating
Precision assembly, test and inspection
With over eighty standard connector lines and value-added products such as cable assemblies, all you need to do is ...
Connect Here.
DELTA
ELECTRONICS MFG. CORP.
Connect Here.
Delta Electronics Mfg. Corp.
Tel: (978) 927-1060 • Fax: (978) 922-6430
P.O. Box 53 • 416 Cabot St.
Beverly, MA 01915 USA
DeltaRF.com
ISO 9001:2008 CERTIFIED
RoHS COMPLIANT
SOMWBA Woman Owned CERTIFIED

# 3D LDS Components for New Production Opportunities

NILS HEININGER
*LPKF Laser & Electronics AG, Garbsen, Germany*

The trend that has been dominating electronic and mechatronic products for many years is clear: components must get smaller in size, while packing in more functions. Also, in order to maintain their market positions, manufacturers in the communications technology sector are under tremendous pressure to continuously launch new products in shorter intervals, while still making them stand out from the crowd. Technologies such as 3D Molded Interconnect Devices (MID) enable new products to be produced with unprecedented functionality. In particular, LPKF's Laser Direct Structuring (LDS) technology offers the benefits of reliable, efficient and productive technology, with the added advantages of economic prototyping processes and a short production lead time.

The technology's current main application is the production of smartphone antennas, but significant growth in tablet or laptop antennas as well as new applications in the automotive and medical fields are expected. For the handset business, LDS offers the opportunity to minimize the footprint of the radiator by integrating it directly on the carrier, which negates assembly steps and enables several antennas to be integrated on the same carrier. To improve RF performance, it is also possible to place the antennas either on the covers, middle decks or on both sides of a component, depending on the intended RF and mechanical properties.

The flexibility and design freedom that comes with utilizing full 3D enables manufacturers to easily tune the antennas during the design and build process. All radiator areas, especially the RF tuning areas, can be easily modified during the pre-production stages, leading to short lead times. Approximately 40 percent of high level smartphones come with at least one LDS component. ***Figure 1***[1] illustrates the differentiation of the use of LDS systems by market segments.

## 3D MID

MID is all about integrating electronic circuits and components directly on three-dimensional plastic components. This enables chips to be elegantly stacked in their assemblies, and the antennas in smartphones or netbooks to be incorporated directly within the housing, thus saving space. Integrating functions also decreases the number of individual components required, eliminates a whole range of production steps, automatically saves additional costs and creates higher quality components.

The LDS method (patented by LPKF) provides significant advantages, both technically and economically, over common methods for integrating electronic circuits directly on plastic components. It uses a thermoplastic polymer doped with a laser-activatable metal-polymer additive. When the laser beam hits this polymer it activates the metal complex and creates a precise track with a roughened up surface.

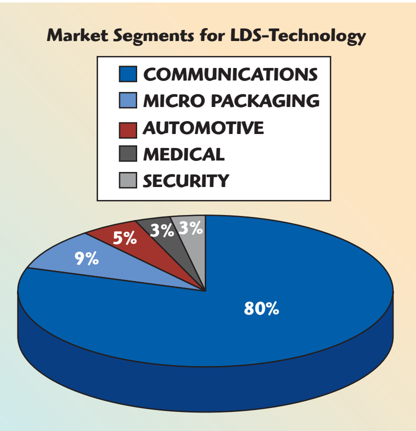


▲ *Fig. 1 The differentiation of the use of LDS systems by market segments (3D-MID e.V.).*

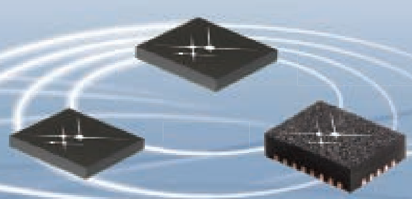

SKYWORKS®

# 3G / 4G Cellular Power Amplifier and Front-End Modules

## GPRS

| | |
|---|---|
| **SKY77350** | Quad-band GPRS PA with Fixed Gain / Input Power Control |
| **SKY77554, SKY77559** | Quad-band GPRS BiFET iPAC™ FEMs for GSM / GPRS with Dual- and Tri-band 3G Antenna Switch |
| **SKY77562** | Quad-band GPRS FEM with Fixed Gain / Input Power Control with Tri-band 3G Antenna Switch |

## EDGE

| | |
|---|---|
| **SKY77351, SKY77354** | Quad-band GPRS / EDGE PAs with Fixed Gain / Input Power Control |
| **SKY77551** | Quad-band GPRS / EDGE FEM |
| **SKY77553** | Quad-band GPRS / EDGE FEM with Tri-band 3G Antenna Switch |
| **SKY77558, SKY77570** | Quad-band GPRS / EDGE FEMs with Fixed Gain / Input Power Control, Including 6-band 3G / 4G Antenna Switch |

## CDMA

| | |
|---|---|
| **SKY77732, SKY77735, SKY77722** | PAMs for CDMA2000 / EVDO |

## WCDMA / LTE

| | |
|---|---|
| **SKY77701, SKY77702, SKY77703, SKY77704, SKY77705** | PAMs for CDMA / WCDMA / HSDPA / HSUPA / HSPA+ / LTE |
| **SKY77706, SKY77709** | PAMs for LTE FDD (Bands VII and XL) |
| **SKY77707, SKY77708** | PAMs for LTE / EUTRAN (Bands XIII and XVII) |
| **SKY7776x, SKY7775x, SKY7774x** | High PAE PAMs for Next Generation 3G / 4G in Single- and Dual-band Configurations |

## MMMB

| | |
|---|---|
| **SKY77601, SKY77604** | Multiband / Multimode PAMs for Quad-band GPRS / EDGE and Penta-band 3G (Bands I, II, IV, V, and VIII) |
| **SKY77603, SKY77611** | Multiband / Multimode PAMs for Quad-band GPRS / EDGE / 3G / 4G (Bands I–V, VIII, and XX) |
| **SKY77606** | Multiband / Multimode PAM for Quad-band GPRS / EDGE and Tri-band 3G (Bands I, V, and VIII) |

## TD-SCDMA

| | |
|---|---|
| **SKY77198, SKY77712** | PAMs for TD-SCDMA |

Skyworks Green™ products are compliant to all applicable materials legislation and are halogen-free. For additional information, refer to Skyworks Definition of Green™, document number SQ04-0074.

***Visit us at MWC 2012 – Hall 8, Stand C132 • February 27–March 1 • Barcelona, Spain***

**USA: 781-376-3000 • Asia: 886-2-2735 0399 • Europe: 33 (0)1 4144366 • Email: sales@skyworksinc.com**
**www.skyworksinc.com • NASDAQ: SWKS**

### THE LDS PROCESS STEP BY STEP

*The plastic part, made by a LDS doped thermoplast.*

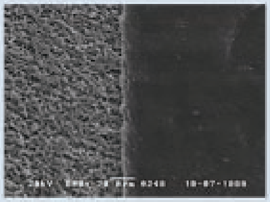

*The laser beam has structured the blank and has activated the additive.*

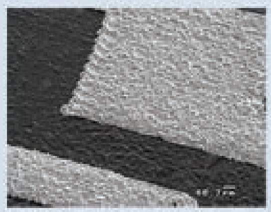

*In a currentless metallization bath copper grows on the structured parts.*

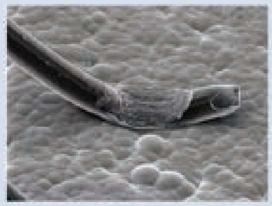

*The structure may be connected via bonding or can be assembled with electronic components.*

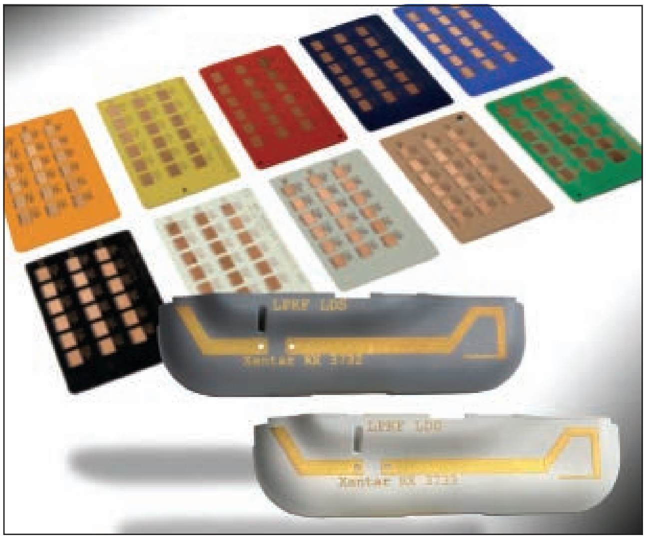

▲ *Fig. 2 The colorful world of LDS using Xantar LDS from Mitsubishi Engineering Plastics (Source: MEP).*

Exposed metal particles that are created in the process form the nuclei for the subsequent metal coating process. The laser beam therefore draws the structures required on the component so that the conductor layers are created precisely along these tracks in an electroless metal coating bath. Copper, nickel and gold finishes can be applied with this method.

The special attributes of lasers such as high flexibility, speed, resolution and precision, work to their strengths in this process. If the circuit has to be reconfigured, all that is needed is a new set of control data to be fed into the laser unit. This means that one basic component can be used to create a range of parts with different functions merely by changing the design of the circuits drawn by the laser beam. And because the control data can also be changed during production, companies can produce small and medium-sized series and even one-off products cost efficiently.

## MATERIALS

With regards to materials, the main prerequisite is that the metal oxide containing the LDS additive has to be evenly distributed and sufficiently concentrated in the thermoplast. Most

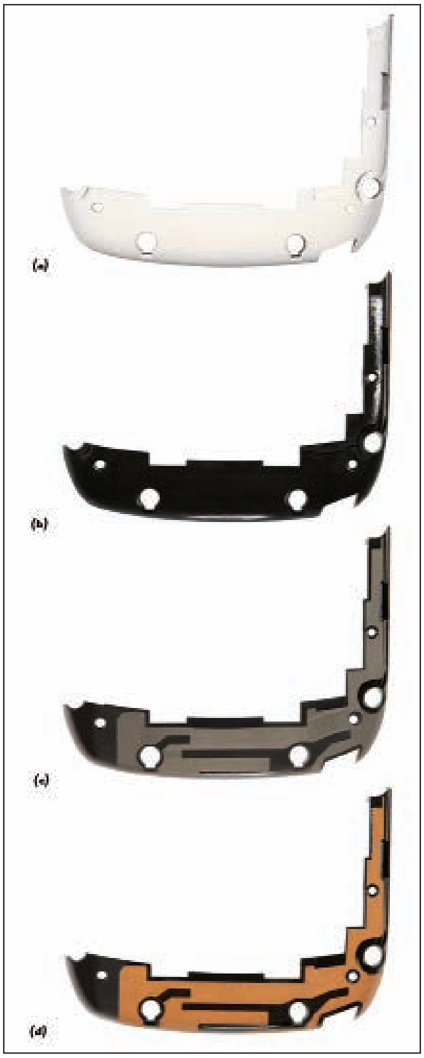


▲ *Fig. 3 Results of the ProtoPaint LDS and electroless bath process.*

of the leading plastic manufacturers offer LDS versions of their thermoplastics. The spectrum consists of amorphous and partially crystalline polymers whose thermal stability ranges from standard to high temperature thermoplastic. These include numerous types of materials that are suitable for lead-free soldering.

In the past, LDS plastics were black because the LDS additives were inherently black, but this has changed recently with SABIC and Mitsubishi Engineering Plastics offering LDS materials that can be adapted to nearly any customer need using pigments. ***Figure 2*** shows the colorful world of LDS using Xantar LDS from Mitsubishi Engineering Plastics.

## LDS PROTOTYPING

Between the layout of a MID part and series production there are several prototype stages. Up until now prototyping and low volume production has either been expensive or impossible. In generative manufacturing, processed parts are generated layer-by-layer directly from CAD data and without the use of forming tools. The most important procedures are Fused Deposition Modeling (FDM), Selective Laser Sintering (SLS) and Stereolithography (SLA). The range of plastics available for the different process technologies is expanding. In this way, developers obtain MID prototypes whose characteristics are iteratively optimized for later use.

LDS prototyping is based on a special paint that is used to coat a surface of a plastic body created by rapid prototyping. ProtoPaint LDS incorporates laser activatable additives, enabling almost any plastic surface to be treated with a laser-activatable coating. It is currently available as a primer and hardener, but a one-component version is planned that can be applied using a simple spray can.

For painting, first a blank is made and coated with a layer thickness of about 30 to 40 µm. In practice, two or three consecutive finishes are ideal for a homogeneous layer. Later this component can be structured like any LDS series part. The adhesive strength of the conductors after metallization is similar to plastic components made of LDS plastic. After the building up of a body in rapid prototyping, the painting is carried out. The laser transmits the projected circuit structures, metal layers being built up in an electroless bath. The process is shown in ***Figure 3***.

The last step in the prototyping process is to metallize the plastic parts. In collaboration with Enthone GmbH, LPKF has developed a very simple solution: LPKF ProtoPlate LDS is a copper bath that can be used without chemical expertise. The copper chemistry is put into a beaker and heated up to approximately 45°C; the activator is then added and the structured parts put into the bath. It is active for approximately two hours and can build up copper layers between 3 and 10 µm.

The fully developed prototyping process closes the gap between layout and series production in an effective way. It becomes easy, fast and economical using the same technology as the mass production. ■

## Reference

1. MID Survey 2011, 3D-MID e.V., Germany, Nuremberg 2011, www.3dmid.de.

# RF Amplifiers and Sub-Assemblies for Every Application

**Delivery from Stock to 2 Weeks ARO from the catalog or built to your specifications!**

- Competitive Pricing & Fast Delivery
- Military Reliability & Qualification
- Various Options: Temperature Compensation, Input Limiter Protection, Detectors/TTL & More
- Unconditionally Stable (100% tested)

ISO 9001:2000 and AS9100B CERTIFIED

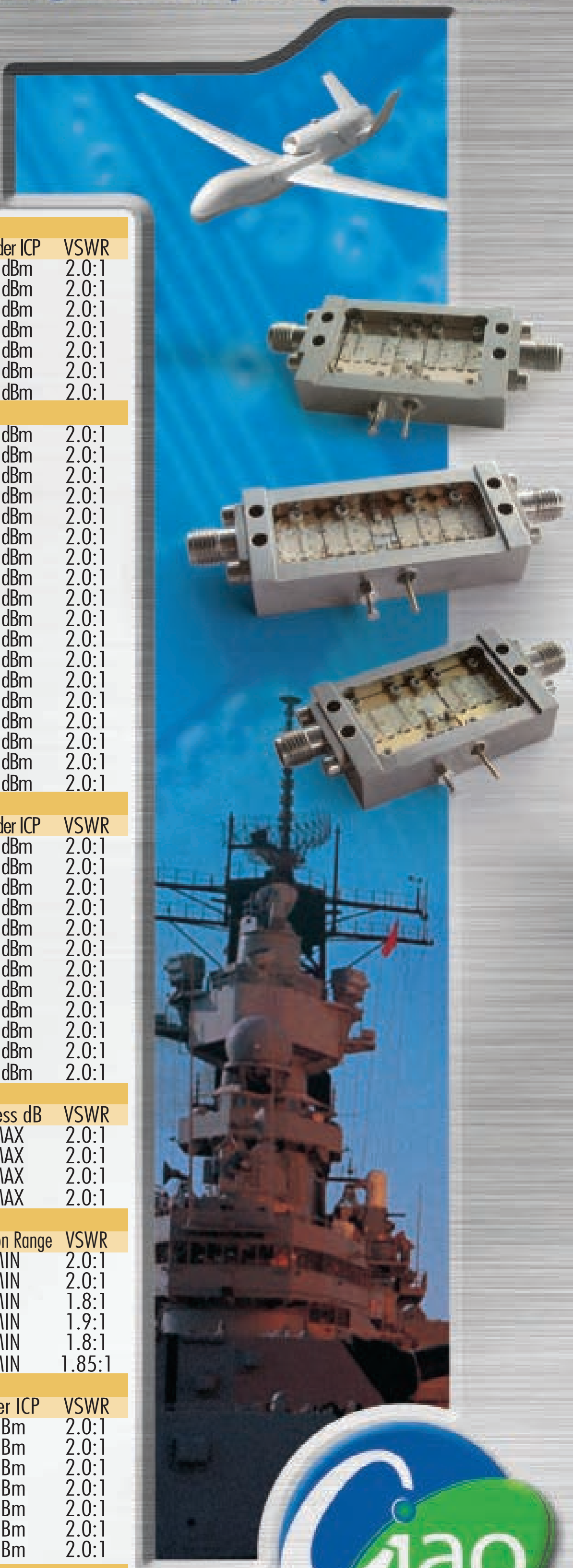

## OCTAVE BAND LOW NOISE AMPLIFIERS

| Model No. | Freq (GHz) | Gain (dB) MIN | Noise Figure (dB) | Power-out @ P1-dB | 3rd Order ICP | VSWR |
|---|---|---|---|---|---|---|
| CA01-2110 | 0.5-1.0 | 28 | 1.0 MAX, 0.7 TYP | +10 MIN | +20 dBm | 2.0:1 |
| CA12-2110 | 1.0-2.0 | 30 | 1.0 MAX, 0.7 TYP | +10 MIN | +20 dBm | 2.0:1 |
| CA24-2111 | 2.0-4.0 | 29 | 1.1 MAX, 0.95 TYP | +10 MIN | +20 dBm | 2.0:1 |
| CA48-2111 | 4.0-8.0 | 29 | 1.3 MAX, 1.0 TYP | +10 MIN | +20 dBm | 2.0:1 |
| CA812-3111 | 8.0-12.0 | 27 | 1.6 MAX, 1.4 TYP | +10 MIN | +20 dBm | 2.0:1 |
| CA1218-4111 | 12.0-18.0 | 25 | 1.9 MAX, 1.7 TYP | +10 MIN | +20 dBm | 2.0:1 |
| CA1826-2110 | 18.0-26.5 | 32 | 3.0 MAX, 2.5 TYP | +10 MIN | +20 dBm | 2.0:1 |

## NARROW BAND LOW NOISE AND MEDIUM POWER AMPLIFIERS

| Model No. | Freq (GHz) | Gain (dB) MIN | Noise Figure (dB) | Power-out @ P1-dB | 3rd Order ICP | VSWR |
|---|---|---|---|---|---|---|
| CA01-2111 | 0.4 - 0.5 | 28 | 0.6 MAX, 0.4 TYP | +10 MIN | +20 dBm | 2.0:1 |
| CA01-2113 | 0.8 - 1.0 | 28 | 0.6 MAX, 0.4 TYP | +10 MIN | +20 dBm | 2.0:1 |
| CA12-3117 | 1.2 - 1.6 | 25 | 0.6 MAX, 0.4 TYP | +10 MIN | +20 dBm | 2.0:1 |
| CA23-3111 | 2.2 - 2.4 | 30 | 0.6 MAX, 0.45 TYP | +10 MIN | +20 dBm | 2.0:1 |
| CA23-3116 | 2.7 - 2.9 | 29 | 0.7 MAX, 0.5 TYP | +10 MIN | +20 dBm | 2.0:1 |
| CA34-2110 | 3.7 - 4.2 | 28 | 1.0 MAX, 0.5 TYP | +10 MIN | +20 dBm | 2.0:1 |
| CA56-3110 | 5.4 - 5.9 | 40 | 1.0 MAX, 0.5 TYP | +10 MIN | +20 dBm | 2.0:1 |
| CA78-4110 | 7.25 - 7.75 | 32 | 1.2 MAX, 1.0 TYP | +10 MIN | +20 dBm | 2.0:1 |
| CA910-3110 | 9.0 - 10.6 | 25 | 1.4 MAX, 1.2 TYP | +10 MIN | +20 dBm | 2.0:1 |
| CA1315-3110 | 13.75 - 15.4 | 25 | 1.6 MAX, 1.4 TYP | +10 MIN | +20 dBm | 2.0:1 |
| CA12-3114 | 1.35 - 1.85 | 30 | 4.0 MAX, 3.0 TYP | +33 MIN | +41 dBm | 2.0:1 |
| CA34-6116 | 3.1 - 3.5 | 40 | 4.5 MAX, 3.5 TYP | +35 MIN | +43 dBm | 2.0:1 |
| CA56-5114 | 5.9 - 6.4 | 30 | 5.0 MAX, 4.0 TYP | +30 MIN | +40 dBm | 2.0:1 |
| CA812-6115 | 8.0 - 12.0 | 30 | 4.5 MAX, 3.5 TYP | +30 MIN | +40 dBm | 2.0:1 |
| CA812-6116 | 8.0 - 12.0 | 30 | 5.0 MAX, 4.0 TYP | +33 MIN | +41 dBm | 2.0:1 |
| CA1213-7110 | 12.2 - 13.25 | 28 | 6.0 MAX, 5.5 TYP | +33 MIN | +42 dBm | 2.0:1 |
| CA1415-7110 | 14.0 - 15.0 | 30 | 5.0 MAX, 4.0 TYP | +30 MIN | +40 dBm | 2.0:1 |
| CA1722-4110 | 17.0 - 22.0 | 25 | 3.5 MAX, 2.8 TYP | +21 MIN | +31 dBm | 2.0:1 |

## ULTRA-BROADBAND & MULTI-OCTAVE BAND AMPLIFIERS

| Model No. | Freq (GHz) | Gain (dB) MIN | Noise Figure (dB) | Power-out @ P1-dB | 3rd Order ICP | VSWR |
|---|---|---|---|---|---|---|
| CA0102-3111 | 0.1-2.0 | 28 | 1.6 Max, 1.2 TYP | +10 MIN | +20 dBm | 2.0:1 |
| CA0106-3111 | 0.1-6.0 | 28 | 1.9 Max, 1.5 TYP | +10 MIN | +20 dBm | 2.0:1 |
| CA0108-3110 | 0.1-8.0 | 26 | 2.2 Max, 1.8 TYP | +10 MIN | +20 dBm | 2.0:1 |
| CA0108-4112 | 0.1-8.0 | 32 | 3.0 MAX, 1.8 TYP | +22 MIN | +32 dBm | 2.0:1 |
| CA02-3112 | 0.5-2.0 | 36 | 4.5 MAX, 2.5 TYP | +30 MIN | +40 dBm | 2.0:1 |
| CA26-3110 | 2.0-6.0 | 26 | 2.0 MAX, 1.5 TYP | +10 MIN | +20 dBm | 2.0:1 |
| CA26-4114 | 2.0-6.0 | 22 | 5.0 MAX, 3.5 TYP | +30 MIN | +40 dBm | 2.0:1 |
| CA618-4112 | 6.0-18.0 | 25 | 5.0 MAX, 3.5 TYP | +23 MIN | +33 dBm | 2.0:1 |
| CA618-6114 | 6.0-18.0 | 35 | 5.0 MAX, 3.5 TYP | +30 MIN | +40 dBm | 2.0:1 |
| CA218-4116 | 2.0-18.0 | 30 | 3.5 MAX, 2.8 TYP | +10 MIN | +20 dBm | 2.0:1 |
| CA218-4110 | 2.0-18.0 | 30 | 5.0 MAX, 3.5 TYP | +20 MIN | +30 dBm | 2.0:1 |
| CA218-4112 | 2.0-18.0 | 29 | 5.0 MAX, 3.5 TYP | +24 MIN | +34 dBm | 2.0:1 |

## LIMITING AMPLIFIERS

| Model No. | Freq (GHz) | Input Dynamic Range | Output Power Range Psat | Power Flatness dB | VSWR |
|---|---|---|---|---|---|
| CLA24-4001 | 2.0 - 4.0 | -28 to +10 dBm | +7 to +11 dBm | +/- 1.5 MAX | 2.0:1 |
| CLA26-8001 | 2.0 - 6.0 | -50 to +20 dBm | +14 to +18 dBm | +/- 1.5 MAX | 2.0:1 |
| CLA712-5001 | 7.0 - 12.4 | -21 to +10 dBm | +14 to +19 dBm | +/- 1.5 MAX | 2.0:1 |
| CLA618-1201 | 6.0 - 18.0 | -50 to +20 dBm | +14 to +19 dBm | +/- 1.5 MAX | 2.0:1 |

## AMPLIFIERS WITH INTEGRATED GAIN ATTENUATION

| Model No. | Freq (GHz) | Gain (dB) MIN | Noise Figure (dB) | Power-out @ P1-dB | Gain Attenuation Range | VSWR |
|---|---|---|---|---|---|---|
| CA001-2511A | 0.025-0.150 | 21 | 5.0 MAX, 3.5 TYP | +12 MIN | 30 dB MIN | 2.0:1 |
| CA05-3110A | 0.5-5.5 | 23 | 2.5 MAX, 1.5 TYP | +18 MIN | 20 dB MIN | 2.0:1 |
| CA56-3110A | 5.85-6.425 | 28 | 2.5 MAX, 1.5 TYP | +16 MIN | 22 dB MIN | 1.8:1 |
| CA612-4110A | 6.0-12.0 | 24 | 2.5 MAX, 1.5 TYP | +12 MIN | 15 dB MIN | 1.9:1 |
| CA1315-4110A | 13.75-15.4 | 25 | 2.2 MAX, 1.6 TYP | +16 MIN | 20 dB MIN | 1.8:1 |
| CA1518-4110A | 15.0-18.0 | 30 | 3.0 MAX, 2.0 TYP | +18 MIN | 20 dB MIN | 1.85:1 |

## LOW FREQUENCY AMPLIFIERS

| Model No. | Freq (GHz) | Gain (dB) MIN | Noise Figure dB | Power-out @ P1-dB | 3rd Order ICP | VSWR |
|---|---|---|---|---|---|---|
| CA001-2110 | 0.01-0.10 | 18 | 4.0 MAX, 2.2 TYP | +10 MIN | +20 dBm | 2.0:1 |
| CA001-2211 | 0.04-0.15 | 24 | 3.5 MAX, 2.2 TYP | +13 MIN | +23 dBm | 2.0:1 |
| CA001-2215 | 0.04-0.15 | 23 | 4.0 MAX, 2.2 TYP | +23 MIN | +33 dBm | 2.0:1 |
| CA001-3113 | 0.01-1.0 | 28 | 4.0 MAX, 2.8 TYP | +17 MIN | +27 dBm | 2.0:1 |
| CA002-3114 | 0.01-2.0 | 27 | 4.0 MAX, 2.8 TYP | +20 MIN | +30 dBm | 2.0:1 |
| CA003-3116 | 0.01-3.0 | 18 | 4.0 MAX, 2.8 TYP | +25 MIN | +35 dBm | 2.0:1 |
| CA004-3112 | 0.01-4.0 | 32 | 4.0 MAX, 2.8 TYP | +15 MIN | +25 dBm | 2.0:1 |

CIAO Wireless can easily modify any of its standard models to meet your "exact" requirements at the Catalog Pricing.

Visit our web site at **www.ciaowireless.com** for our complete product offering.

Ciao wireless

**Ciao Wireless, Inc.** 4000 Via Pescador, Camarillo, CA 93012

Tel (805) 389-3224   Fax (805) 389-3629   sales@ciaowireless.com

## Raytheon Awarded Contract for Two AN/TYP-2 Radars

The Missile Defense Agency is awarding Raytheon a contract to provide two AN/TPY-2 radars to the U.S. Army, as the radar component to the Terminal High Altitude Area Defense (THAAD) missile defense system. The firm-fixed-price contract is for $363.9M.

"The AN/TPY-2 is the world's most advanced, mobile X-Band radar," says Dave Gulla, Vice President for Global Integrated Sensors at Raytheon Integrated Defense Systems. "It serves as the radar for the THAAD System, an important component of MDA's Ballistic Missile Defense System."

*"The AN/TPY-2 is the world's most advanced, mobile X-Band radar."*

The AN/TPY-2 is a multi-functional radar that searches, detects, tracks and discriminates ballistic missile threats, seamlessly integrating with a variety of ballistic defense systems. In addition to supporting the U.S. Army in a terminal defense role as part of a THAAD Battery, AN/TPY-2 radars are deployed around the world providing continuous forward-based ballistic missile defense as a key component of the global Ballistic Missile Defense Architecture.

The most recent deployment of the AN/TPY-2 radar represents a major milestone in achieving the Administration's European Phased Adaptive Approach (EPAA), which aims to deter, dissuade, and, if necessary, defeat enemy ballistic missiles that threaten the U.S., deployed forces, friends and allies. The AN/TPY-2 is the critical sensor component of the EPAA. Work on the AN/TPY-2 radars for this contract will be performed at Raytheon facilities in Massachusetts and by suppliers in 33 states.

## LONGBOW Receives $181M US Army Contract

The LONGBOW Limited Liability Co., a joint venture of Lockheed Martin and Northrop Grumman Corp., received a $181M contract from the U.S. Army for AH-64D Apache Block III LONGBOW systems. The contract includes the first international purchase of the Block III LONGBOW Fire Control Radar (FCR) by Taiwan, which will receive 15 Block III LONGBOW FCR systems. LONGBOW LLC will also produce 18 Radar Electronic Units (REU), 14 Unmanned Aerial System Tactical Common Data Link Assembly (UTA) systems and spares to equip the U.S. Army's new fleet of Block III Apaches.

"The Army's investment in the FCR enhancements with the Block III Fire Control Radar REU illustrates our commitment to face the challenges of the ever-adapting threats around the world," says Col. Shane Openshaw, U.S. Army Project Manager for Apache Helicopters. "The Longbow Apache is the world's premier attack helicopter, and the FCR is one of the key elements that make it that way."

For more than a decade, the LONGBOW FCR has provided Apache aircrews with target detection, location, classification and prioritization. In all weather, over multiple terrains and through any battlefield obscurant, the radar allows automatic and rapid multi-target engagement. The LONGBOW FCR integrates with the LONGBOW HELLFIRE missile, enhancing the Apache's lethality four-fold and increasing survivability sevenfold.

*The new LONGBOW Block III FCR REU provides reduced size, weight, maintenance and power requirements of the radar system.*

The new LONGBOW Block III FCR REU provides reduced size, weight, maintenance and power requirements of the radar system. The LONGBOW Block III UTA provides a two-way, high-bandwidth data link, enabling aircrews to control Unmanned Aircraft Systems' (UAS) flight path, sensors and lasers at long ranges. The system also provides the ability to receive high-quality UAS imagery on displays. Prime mission equipment and spares production, as well as engineering services and integrated logistics, will be performed at Lockheed Martin facilities in Ocala and Orlando, Fla., and Northrop Grumman facilities in Baltimore, Md. Deliveries began in fall 2011. The contract includes options to extend the period of performance from 2015 to 2017.

## Boeing and Northrop Grumman Receive Contract from US Missile Defense Agency

The Boeing Co. and industry partner Northrop Grumman Corp. have received the development and sustainment contract (DSC) from the U.S. Missile Defense Agency for future work on the Ground-Based Midcourse Defense (GMD) element of the United States' ballistic missile defense system.

"The award is the culmination of a two-year proposal process that brought together a broad industry group committed to delivering innovative solutions and a cost-effective approach to program management and execution," says Dennis Muilenburg, President and CEO of Boeing Defense, Space & Security. "We are privileged to have been partners with the Missile Defense Agency through development and deployment of the GMD system, and now with Northrop Grumman, we are honored to continue that partnership in this next phase of the program."

**Go to www.mwjournal.com for more defense news items**

Under the DSC, Boeing will continue to lead the industry team for GMD development, integration, testing, operations and sustainment activities, building on the company's experience of supporting the Missile Defense Agency as prime contractor for the program since 2001. As strategic partner, Northrop Grumman will oversee the ground system elements, as well as provide key support in operations and sustainment, system engineering and system test.

"The DSC ushers in a new era for the GMD program, and our partnership with Boeing brings together the very best minds in the industry for this national security capability," says Wes Bush, Chairman, CEO and President, Northrop Grumman. "By combining Northrop Grumman's 50-year experience and success on the nation's Minuteman ICBM program with Boeing's heritage GMD leadership, we provide the optimum mix of integrated development and sustainment capabilities for a system that demands nothing less."

The Boeing-led team currently operates and sustains the deployed GMD weapon system while developing and testing new technologies to provide increased reliability and to meet evolving customer needs and requirements. Northrop Grumman has been part of the team since 1998, responsible for designing and deploying the command-and-control systems that form the backbone of the GMD ground system.

"In selecting the Boeing and Northrop Grumman GMD team, the Missile Defense Agency retains the knowledge, skill and expertise of the world-class men and women who developed this one-of-a-kind system – the only industry team capable of affordable innovation for GMD's future," says Norm Tew, Boeing Vice President and Program Director of GMD. "We believe the government conducted a fair and open competition, making the right decision for the future of the program."

*An integral element of the Global Ballistic Missile Defense System, GMD uses radars… command-and-control facilities… and a 20,000-mile fiber optic communications network.*

An integral element of the Global Ballistic Missile Defense System, GMD uses radars, other sensors, command-and-control facilities, communications terminals and a 20,000-mile fiber optic communications network. There are more than 20 operational interceptors at Vandenberg Air Force Base, Calif., and Fort Greely, Alaska, to defend the United States against long-range ballistic missile threats.

## Forty Nine Commercial LTE Networks Confirmed by GSA

The Global mobile Suppliers Association (GSA) has published an update (5 January 2012) to its Evolution to LTE report, which covers LTE FDD and LTE TDD system modes, and confirms 49 LTE operators have now launched commercial services. Two hundred and eighty five operators, over 30 percent higher than the previous six months, committed to commercial LTE network deployments or are engaged in trials, technology testing or studies.

The GSA report confirms 226 firm commercial LTE network deployments, 36 percent higher than six months previous, are in progress or planned in 76 countries, including 49 networks, which are now launched, and another 59 operators in 17 additional countries are engaged in LTE technology trials, tests or studies.

Forty nine LTE networks, which is more than double the number six months ago, have launched commercial services in 29 countries: Armenia, Australia, Austria, Bahrain, Belarus, Brazil, Canada, Denmark, Estonia, Finland, Germany, Hong Kong, Hungary, Japan, Kuwait, Latvia, Lithuania, Norway, Philippines, Poland, Puerto Rico, Saudi Arabia, Singapore, South Korea, Sweden, UAE, Uruguay, USA and Uzbekistan.

Alan Hadden, President of the GSA, said, "Operators around the world in both mature and emerging economies strengthened their commitments and investments in LTE technology in 2011. The number of commercial networks more than doubled as operators obtained new spectrum, and many were also able to re-farm existing spectrum (particularly in the 1800 MHz band) for LTE deployments."

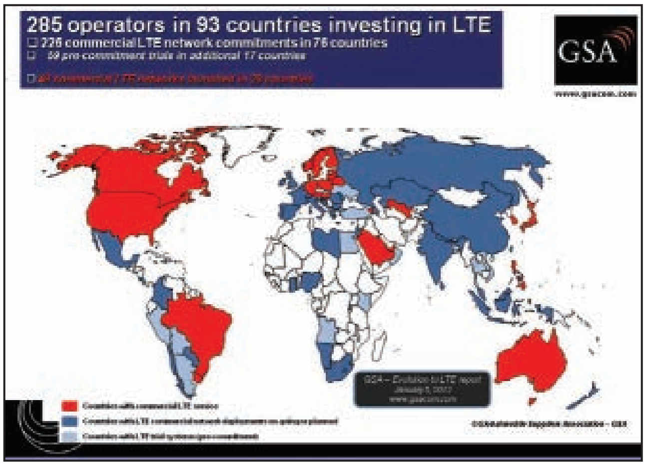


*Source: Global mobile Suppliers Association*

## TSB Launches Satellite Applications Catapult Centre

The UK's Technology Strategy Board (TSB) is to establish a new Catapult centre in Satellite Applications. This new technology and innovation centre, the fourth Catapult to be set up, will help UK businesses develop new satellite-based products and services and stimulate growth across the UK economy. The Catapult will focus on applications of R&D in four growth areas: communications, broadcasting, positioning and observation.

*"The Satellite Applications Catapult will help the UK stay at the leading edge of space technology..."*

Satellite services are expected to be an important growth area for the UK economy in the next decade and beyond. Worldwide, the space sector is expected to grow to £400B by 2030. The Satellite Applications Catapult will help to achieve targets set out in the UK Space Innovation and Growth Strategy to grow UK market share from 6 percent to 10 percent by 2030 and create 100,000 new high value jobs.

The Catapult will provide in-orbit test facilities, allowing innovative UK organisations to demonstrate new satellite technologies. It removes significant cost barriers and shortens the time UK businesses will wait to achieve a first flight demonstration for new equipment and technologies in space. The Catapult, expected to open in autumn 2012, will also provide UK businesses, including SMEs, unique access to advanced systems for data capture and analysis to support the development of new services delivered by satellites.

David Willetts, UK Minister for Science and Higher Education, said, "The new Catapult centres will help turn today's emerging technologies into tomorrow's industries. The Satellite Applications Catapult will help the UK stay at the leading edge of space technology and help us achieve the potential we set out in the Space Innovation and Growth Strategy."

## RadioNet3 Focuses on European Radio Astronomy

RadioNet3, a four-year, €9.5M project offering unprecedented access to 18 state-of-the-art European radio telescopes, including the Atacama Large Millimetre Array (ALMA) in Chile and the James Clerk Maxwell Telescope in Hawaii, has been launched. The project will ensure that European radio astronomy facilities remain globally competitive by increasing expertise in the research community and developing new instruments for current and proposed telescopes.

RadioNet3, which began on 1 January 2012, builds on the success of previous radio astronomy projects, RadioNet1 and 2, and is a collaboration of 27 world class European organisations. Led by the Max Planck Institute for Radio Astronomy (MPIfR), it is combining the best equipment available with the top radio astronomical expertise.

The new program will stimulate new activities in research and development of both the existing radio infra-

Go to www.mwjournal.com for more international news items

*"Our aim is to establish a long-term strategy for structuring radio astronomy in Europe."*

structures as well as telescopes of the future, including the largest radio telescope in the world – the Square Kilometre Array (SKA) – due to be completed within the next decade.

"Our aim is to establish a long-term strategy for structuring radio astronomy in Europe," said Prof. Anton Zensus, Director at MPIfR and coordinator of the RadioNet3 project. "We will make sure the results are available to the outside world and that the next generation of scientists and engineers are prepared for the advent of the new generation radio telescopes."

## Analysis Predicts Wireless Test Equipment Expansion in Latin America

New analysis from Frost & Sullivan focused on Latin America Wireless Test & Equipment Markets estimates the markets to expand from $158.5M in 2010 to $342.0M in 2017, growing at a compound annual growth rate (CAGR) of 11.6 percent during the forecast period.

"A key factor driving demand for wireless test equipment is the continuous development of wireless communication standards from 2 and 2.5G to 3G, 3.5G, HSPA and 4G," noted Frost & Sullivan Research Analyst Mariano Kimbara. "There are several 4G trials and deployments slated to begin by the end of 2011 and the beginning of 2012, which are expected to generate growth for this market."

The evolution from 2G to 3G wireless standards has contributed significantly to the uptake of wireless test and equipment in the Latin American region. Operators in the region are in the initial phase of 3G HSPA deployments and very few are introducing HSPA+. The new HSPA technologies allow increased data transmission in the region without the need for massive investment. Imminent LTE deployments also augur well for market prospects.

*"… driving demand for wireless test equipment is the continuous development of wireless communication standards…"*

"The major reason for deploying LTE in the region is the promise of reduced operating costs and savings in terms of frequency spectrums over the long term," explained Kimbara. "As a result, operators are favouring the implementation of LTE, instead of blindly following the parameters of developed markets such as those in North America and Europe."

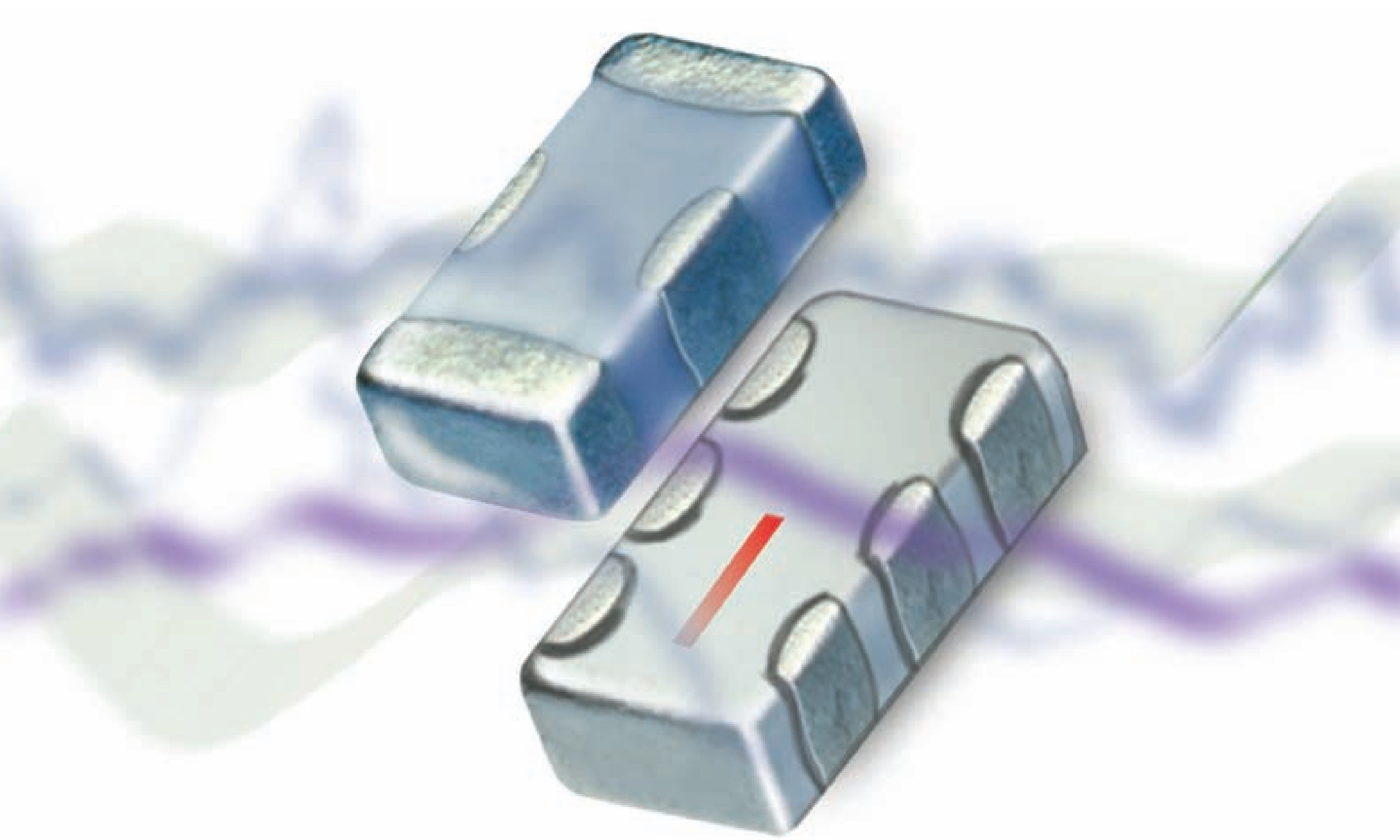

# CERAMIC FILTERS

## LOW PASS BANDPASS HIGH PASS

*45 MHz to 13 GHz from* 99¢ *ea. qty.3000*

***Over ~~141~~ 167 models...only 0.12 x 0.06"*** These tiny hermetically sealed filters utilize our advanced Low Temperature Co-fired Ceramic **(LTCC)** technology to offer superior thermal stability, high reliability, and very low cost, making them a must for your system requirements. Visit our website to choose and view comprehensive performance curves, data sheets, pcb layouts, and everything you need to make your choice. You can even order direct from our web store and have a unit in your hands as early as tomorrow!

***Wild Card** KWC-LHP LTCC Filter Kits only $98*

*Choose any 8 LFCN or HFCN models*
*Receive 5 of ea. model, for a total of 40 filters*
*Order your KWC-LHP FILTER KIT TODAY!*

***RoHS compliant*** U.S. Patents 7,760,485 and 6,943,646

***Now available in small-quantity reels*** at *no extra charge:*
Standard counts of 20, 50, 100, 200, 500, 1000 or 2000. Save time, money, and inventory space!

*Mini-Circuits...we're redefining what VALUE is all about!*

**Mini-Circuits®**
*ISO 9001 ISO 14001 AS 9100*

P.O. Box 350166, Brooklyn, New York 11235-0003 (718) 934-4500 Fax (718) 332-4661

YONI2® ***The Design Engineers Search Engine*** *finds the model you need, Instantly* • For detailed performance specs & shopping online see **minicircuits.com**
U.S. Patents 7739260, 7761442

***IF/RF MICROWAVE COMPONENTS***

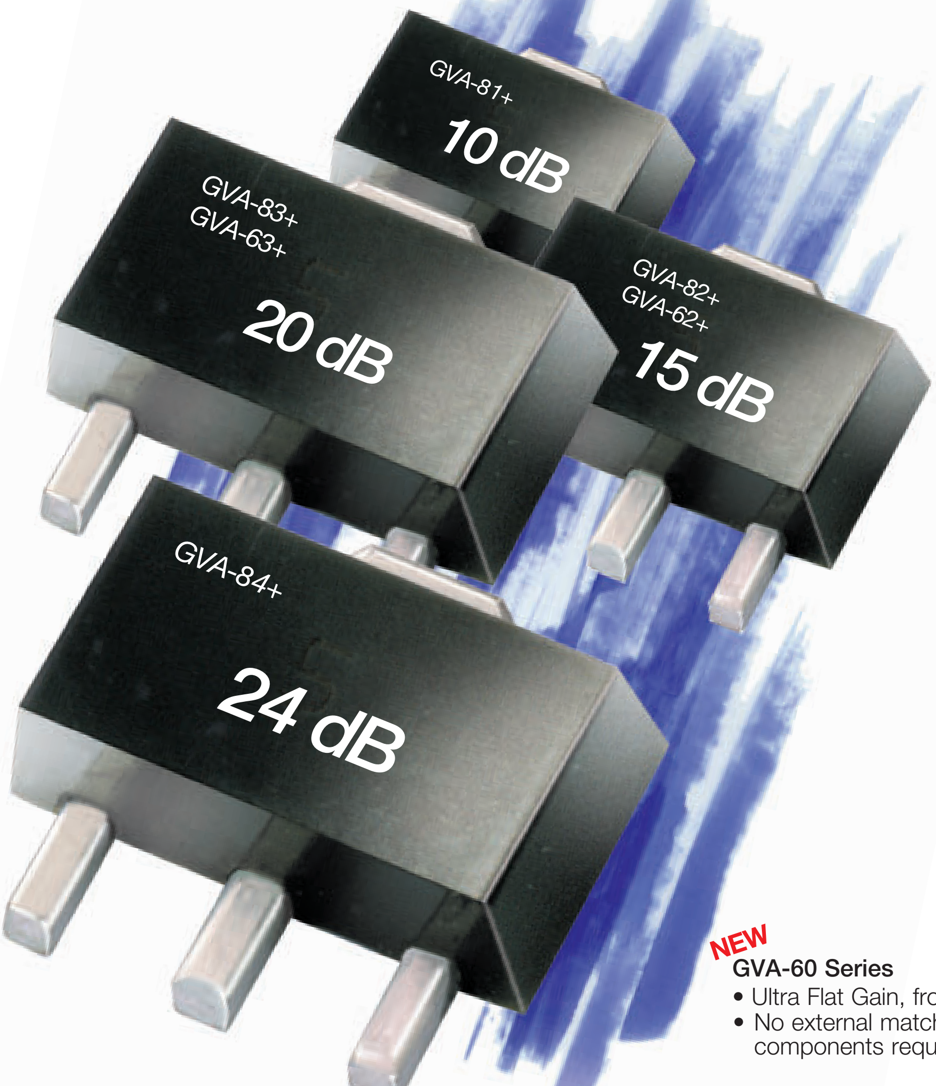


**NEW**
**GVA-60 Series**
- Ultra Flat Gain, from 0.1-6 GHz
- No external matching components required

*+20 dBm Power Amplifiers with a choice of gain*

# GVA AMPLIFIERS

## DC* to 7 GHz

*from $1.59 ea. (qty. 1000)*

Mini-Circuits' monolithic, surface-mount GVA amplifiers are extremely broadband, with wide dynamic range and the right gain to fit your application. Based on high-performance InGaP HBT technology, patented GVA amplifiers cover DC* to 7 GHz, with a selection of gain choices 10, 15, 20 or 24dB, (measured at 1 GHz). And our new **GVA-62+ and -63+** deliver improved gain flatness, with no matching components required! All GVA models provide better than +20 dBm typical output power, with typical IP3 performance as high as +41 dBm at 1 GHz. Supplied in RoHS-compliant, SOT-89 housings, low-cost GVA amplifiers feature excellent input/output return loss and high reverse isolation. With built-in ESD protection, GVA amplifiers are unconditionally stable and designed for a single 5V supply. Just go to minicircuits.com for technical specifications, performance data, export info, pricing, and everything you need to choose your GVA today!

*Mini-Circuits…we're redefining what VALUE is all about!*

**Low frequency cut-off determined by coupling cap.*

*US patent 6,943,629*

Dan Massé, Associate Technical Editor

## Revenue for IEEE 802.15.4 IC Market to Grow to Over $1.1B

The IEEE 802.15.4 IC market is projected to grow to over $1.1B in 2016, up from just $90M in 2010. Advanced Metering Infrastructure (AMI) is still a key adoption market and there is significant impetus behind the continuation of this market. Some concerns have been raised around mass deployments ahead of IP support and the planned ZigBee Smart Energy 2.0, but recent announcements by ZigBee to migrate its portfolio of profiles into IP-based solutions should allay such concerns.

The home entertainment market has also seen significant uptake, helping to drive up shipment numbers over the past 12 months or so with the development and adoption of ZigBee RF4CE. Initial products leveraging 802.15.4 are still led by P2P deployments using proprietary software stacks, but the transition to standard software implementations is well underway and the market positions of both approaches will be reversed by the end of the forecast period with standardized implementations dominating. In addition, P2P deployments also dominate usage, but that too will shift over to mesh network configurations during the forecast period.

*The IEEE 802.15.4 IC market will grow to over $1.1B in 2016, up from just $90M in 2010.*

Chipset shipment will continue to grow at expanding rates as the 802.15.4 technology reaches a level of deployment maturity and price point that enables WSN to extend more broadly across markets, not just in AMI and home entertainment, where the bulk of the market is currently, but also across the building automation and healthcare sectors around the world. New markets are also emerging, such as traffic monitoring, smart parking and flood alert systems within the smart city concept.

Kelvin Chan, Industry Analyst, says, "Standard WSN protocols based on IEEE 802.15.4 will face a confluence of challenges from existing wireless technologies such as Low Power Wi-Fi, Low Energy Bluetooth, and a more recent addition, Low Energy DECT, as these technologies look to capitalize on their installed base and ubiquity stature, especially in the home area network (HAN) environment, to penetrate the smart energy market segment."

## Wireless Infrastructure Drives RF Power Semiconductor Markets to Over $1B

Spending on RF power semiconductors for the wireless infrastructure market has experienced significant growth in 2011, according to ABI Research. Other markets – notably the military – are seeing some moderation in growth as the global economic picture and political factors come into play. Also, gallium nitride (GaN) – long seen as the promising new "material of choice" for RF power semiconductors – is continuing its march to capture share.

"GaN has the promise of increased market share in 2012 and is forecast to be a significant force by 2017," notes Lance Wilson, Research Director, Mobile Networks. "It bridges the gap between two older technologies, exhibiting the high-frequency performance of gallium arsenide combined with the power-handling capabilities of Silicon LDMOS. It is now a mainstream technology that has achieved measurable market share and in the future will capture a significant part of the market."

*"GaN has the promise of increased market share in 2012 and is forecast to be a significant force by 2017."*

The vertical market showing the strongest uptick in the RF power semiconductor adoption business, outside of wireless infrastructure, is commercial avionics and air traffic control, which Wilson describes as now being "a significant market." While the producers of these chips' devices are located in the major industrialized countries, this sub-segment market is now so global that end equipment buyers can be from anywhere.

ABI Research's new study, "RF Power Semiconductors," examines RF power semiconductor devices that have power outputs of greater than four watts and operate at frequencies of up to 3.8 GHz, which represent the bulk of applications in use today. With the current release, analysis of the six main vertical segments (wireless infrastructure; military; industrial, scientific and medical (ISM); broadcast; commercial avionics and air traffic control; and non-cellular communications), which were previously subdivided into 24 sub-segments, are expanded to 29 sub-segments.

## Half a Million TD-LTE Base Stations Will Be Deployed by 2016

At least half a million base stations will be installed or upgraded for TD-LTE by the end of 2016. "It was only two years ago that nearly every WiMAX operator, including operators with unpaired Time-Division Duplex (TDD) frequency spectrum, were planning to deploy WiMAX 2," says Aditya Kaul, Practice Director, Mobile Networks. "Today, almost all of them have switched plans and are deploying TD-LTE instead." TD-LTE is the TDD variant of the fourth-generation (4G) Long Term Evolution (LTE) wireless standard.

WiMAX operators today are generally offering fixed WiMAX service based on the IEEE 802.16d specification, or mobile WiMAX service based on IEEE 802.16e. The IEEE 802.16m standard (also known as WiMAX

Go to www.mwjournal.com for more commercial market news items

2) was developed to provide higher data rates and increased capacity and the members of the WiMAX Forum committed to follow this evolution path for 4G.

"A funny thing happened on the way to the forum," says Jim Eller, Principal Analyst, Wireless Infrastructure. "Despite starting two years later than WiMAX 2, TD-LTE emerged as a viable alternative." China Mobile was the early promoter of TD-LTE technology, as a 4G evolution path for its 3G network based on TD-SCDMA technology. Other operators, however, saw better advantages in aligning with the global LTE standards.

*The 600-pound gorilla in TD-LTE is still China.*

TD-LTE commercial service has been launched in Brazil, Japan, Poland, Saudi Arabia and other countries. TD-LTE deployments are underway in Australia and Scandinavia and large-scale TD-LTE networks are planned in the United States and India.

The 600-pound gorilla in TD-LTE is still China. China Mobile started its second phase of the TD-LTE Large Scale Trial Initiative (LSTI) in December and will run until June 2012. According to Jake Saunders, Vice President of Forecasting, "China Mobile announced plans last month to install an additional 10,000 to 20,000 TD-LTE base stations in 2012 and perhaps another 60,000 in 2013."

## Disruptive MM-MB PAs Take Off with Smartphones

Multimode, multiband power amplifiers (MM-MB PA) took off in 2011 with adoption by Nokia, Apple, Samsung and LG in several popular smartphones, as seen in the Strategy Analytics RF & Wireless Components (RFWC) report, "Multimode, Multiband PAs Change the Game for PA Suppliers." Strategy Analytics predicts that the market for MM-MB PAs will exceed $150M in 2012, growing rapidly through 2016, irrevocably transforming the PA market.

According to Christopher Taylor, author of the report, "Increasing band count in 3G and 4G mobile devices has led to adoption of MM-MB PAs to save space and reduce PA count, as in the Apple iPhone 4S. Not all PA suppliers have the broad range of process, circuit, switch, filter and module capabilities needed for MM-MB PAs. So far, Renesas, whose PA business unit will soon transfer to Murata, Skyworks, RFMD and Avago Tech, have captured the highest share with their MM-MB PAs."

Neil Mawston, Director of the Strategy Analytics Wireless Device Strategies (WDS) market research service, adds, "Shipments of 3G/4G devices will grow to more than 1.2 billion devices in 2016; a high proportion of these will be smartphones. It is clear that MM-MB PAs will benefit from this growth, and play a key role in enabling it."

# Around the Circuit

Kerri Germani, Staff Editor

## WALTER CROFUT REMEMBERED

The industry mourns the passing of its friend and colleague, Walter Crofut. Walter joined Narda Microwave in 1981 and spearheaded the company's new product development and marketing efforts throughout his career. His education at Princeton and Brown, combined with his soaring intellect and drive for perfection made him highly respected, both within the company, and throughout the industry. All this, combined with a soft-spoken, congenial personality made Walter a valued co-worker and friend to all.

## INDUSTRY NEWS

**Mercury Computer Systems Inc.**, a provider of commercially developed application-ready ISR subsystems for defense prime contractors, has completed its acquisition of **KOR Electronics** and its wholly owned subsidiary, **Paragon Dynamics Inc.** The $70M all-cash transaction closed on December 30, 2011. KOR Electronics is a supplier of system level solutions to the worldwide Defense and Intelligence communities. KOR is headquartered in Cypress, Calif. with principal locations in Aurora, Colo., and Rome, N.Y. Mercury is based in Chelmsford, Mass.

**Telit Wireless Solutions**, a global machine-to-machine (M2M) wireless technology company, has entered into a binding agreement to purchase **Navman Wireless OEM Solutions**, a designer and manufacturer of Global Positioning System (GPS) modules and solutions, for $3M in cash. This latest Telit acquisition comes on the heels of its March 2011 acquisition of Motorola Solutions' M2M business and its July 2011 acquisition of GlobalConect Ltd., an M2M services and connectivity business.

**Thales** has signed an agreement to acquire **Tampa Microwave**, a privately held company specializing in tactical satellite communications (SATCOM) terminals and related products for government and commercial customers. The acquisition is expected to close in the first quarter of 2012. Tampa Microwave's core capabilities include the design, development and manufacturing of SATCOM terminals as well as custom SATCOM engineering and customer support. The company's strategic focus areas complement Thales' existing product portfolio and will expand its capabilities in the wideband SATCOM domain. Tampa Microwave will operate as a subsidiary of Thales Communications Inc., a Thales USA company that operates under a proxy agreement with the U.S. Department of Defense (DoD). The business will maintain its location in Tampa, Fla. and the current Tampa Microwave management team will remain unchanged.

**Molex Inc.** announced that it has completed the acquisition of South Grafton, Mass.-based **Temp-Flex Cable Inc.** Temp-Flex designs and manufactures specialty wire and cable products that provide technological solutions for the medical, aerospace, military, computer, electronics, test and measurement, and industrial markets. According to Mike Miskin, Vice President and General Manager, Cable Products Business Unit of Molex Inc.'s Global Integrated Products Division, this is a strategic acquisition that will give Molex access to development and manufacturing expertise for specialty wire and cable products thereby expanding its high performance cable assembly business.

**Astrium** is to acquire a majority stake (66.78 percent) in **Space Engineering**, the Italian specialist in telecommunications and radar technology, focusing on digital telecommunications, RF and antenna equipment engineering for both space and ground-based applications. The acquisition of the Rome-headquartered company will enhance Astrium's capability to develop and manufacture sophisticated telecommunications hardware and demonstrates the company's commitment to the Italian space market. With sites in Rome and near Potenza in southern Italy, Space Engineering and its main subsidiary, **Teleinformatica e Sistemi**, specialize in the development of telecommunications, navigation and remote sensing applications and engineering services for both the civilian and defense sectors. Becoming part of Astrium will enable Space Engineering to make the next step forward in terms of development by giving it access to new markets.

**DragonWave Inc.** has completed the required consultation process with Italian trade union representatives for the planned acquisition of **Nokia Siemens Networks'** microwave transport business. DragonWave and Nokia Siemens Networks have also determined that no merger control filings are required in relation to the proposed acquisition. Subject to fulfillment of remaining closing conditions, DragonWave and Nokia Siemens Networks plan to close the transaction in the first quarter of 2012.

**Skyworks Solutions Inc.**, an innovator of high reliability analog and mixed signal semiconductors enabling a broad range of end markets, announced that it has opened a design center in Korea to support the company's increasing demand for 3G and 4G front-end solutions. In fiscal 2011, Skyworks grew its 3G front-end module shipments by more than 150 percent year-over-year. The site will support integrated circuit and multi-chip-module designs and layouts, RF laboratory work and customer support through early manufacturing.

**SemiGen Inc.**, an RF/microwave assembly and automated PCB manufacturing house, has opened its new RF supply

**For up-to-date news briefs, visit www.mwjournal.com**

# WIDEBAND TRANSFORMERS

## Features

> Low Cost
> Wide Bandwidth
> Good Amplitude / Phase Unbalance
> Rugged Welded Construction
> RoHS Compliant
> Patented REL-PRO® Technology
> 0.150" x 0.150" x 0.150"

RoHS COMPLIANT


| Model Number | Frequency (MHz) | Impedance Ratio | Schematic |
|---|---|---|---|
| TM4-0 | 0.2 - 350 | 4:1 | |
| TM1-0 | 0.3 - 1000 | 1:1 | |
| TM1-1 | 0.4 - 500 | 1:1 | |
| TM1.5-2 | 0.5 - 550 | 1.5:1 | |
| TM2-1 | 1 - 600 | 2:1 | |
| TM1-6 | 5 - 3000 | 1:1 | |
| TM2-GT | 5 - 1500 | 2:1 | |
| TM4-GT | 5 - 1000 | 4:1 | |
| TM8-GT | 5 - 1000 | 8:1 | |
| TM4-1 | 10 - 1000 | 1:4 | |
| TM4-4 | 10 - 2500 | 1:4 | |
| TM1-2 | 20 - 1200 | 1:1 | |
| TM1-9 | 100 - 5000 | 1:1 | |
| TM1-8 | 800 - 4000 | 1:1 | |

SYNERGY®
MICROWAVE CORPORATION

For additional information, contact Synergy's sales and application team.

Phone: (973) 881-8800 Fax: (973) 881-8361 E-mail: sales@synergymwave.com

***Visit Our Web Site At WWW.SYNERGYMWAVE.COM***

center and is accepting orders for epoxies, bonding tools, gold wire and other supplies used in the manufacture and test of microwave modules and components. The center is fully stocked and located adjacent to the SemiGen manufacturing center in Manchester, N.H. It will be ready to provide immediate delivery of epoxy paste and sheets, epoxy preforms, gold wire, bonding tools and supplies from all major suppliers. No minimum order is required, saving consumers from traditionally long lead times and higher minimum orders when they buy direct from manufacturers.

**TriQuint Semiconductor Inc.**, a RF solutions supplier, has been recognized by **Raytheon Co.** for exceptional performance in supporting its Space and Airborne Systems (SAS) business during 2011. TriQuint was honored by Raytheon for the fourth consecutive year at the company's 2011 SAS Supplier Excellence Award (SEA) recognition event. Winning suppliers represent less than one percent of the SAS supply base. Only 39 companies that supply Raytheon SAS received awards in 2011. Winning companies were chosen by Raytheon for meeting demanding standards in the areas of quality and delivery performance, customer satisfaction, total business and financial health. Evaluations from Raytheon buyers and material program managers who interact with TriQuint every day were also part of the selection process.

**Anritsu Co.** announced it has donated 26 handheld radios to the Boy Scouts of America (BSA) that will be used by Boy Scouts seeking to get involved with amateur radio and earn their Radio Merit Badge. The donation, made possible by an upgrade to Anritsu's onsite two-way radio system, is part of Anritsu's ongoing global commitment to foster wireless technology education and support worthy community organizations.

## CONTRACTS

**Lockheed Martin** has been awarded work by the U.S. Army's Product Manager, Joint-Automatic Identification Technology organization to provide operations and maintenance for the Radio Frequency In-Transit Visibility (RF-ITV) system. If all options are exercised over the course of five years, the contract is valued at $126M. RF-ITV sites exist worldwide in support of combatant commands, making this a massive and complex effort because sites must be maintained at optimal levels of operational readiness to support joint forces. Through RF-ITV technology, the system provides last known locations and in-the-container visibility for shipments that have active RF tags attached to pallets, containers or equipment.

**Kratos Defense & Security Solutions Inc.** announced that its **Herley Industries Inc.** subsidiary has received a contract valued at $11.5M from a major prime contractor for the continuing production of electronic hardware for a U.S. ballistic missile program. Herley designs, develops and manufactures microwave technology solutions for the defense, aerospace and medical industries worldwide. Based in Woburn, Mass., Herley has seven manufacturing locations and approximately 1000 employees.

**API Technologies Corp.**, a provider of electronic systems, subsystems, RF and secure solutions for the defense, aerospace and commercial industries, announced that it has received a new $1.4M order for precision position sensors to be used in air-to-surface missiles. API's RF Solutions division was awarded the order by a Fortune 100 defense contractor.

## PERSONNEL

As part of its continuing expansion to meet growing customer demands, **AR RF/Microwave Instrumentation** has added three engineers in its Souderton, Penn. headquarters. **Anthony Peroni** is an experienced design engineer, having served in that position at Motorola, M/A-COM and Spectrum Microwave. Peroni holds a master of science degree in electrical engineering from Pennsylvania State University. At AR, he will be involved in the development of solid-state amplifiers for the company's expanding line of high-power microwave products. **Dave Bains** also joins AR's engineering department as a microwave design engineer. He has over 20 years experience in the microwave industry, with emphasis on amplifier technology. Bains, who earned a degree in microwave engineering from England's Sheffield University, has worked for Microwave Semiconductor Corp., Amplidyne and Witron. **Keith Miller**, a design engineer with over 35 years experience, will be responsible for developing designs from initial concept through final approval. He holds an associate degree in mechanical engineering from Pennsylvania State University and a bachelor of science degree in mechanical engineering technology from the University of Pittsburgh.

**Giga-tronics** announced that **Robert Waldeck** has joined the company as Vice President of Business Development for Switching Solutions. Waldeck has held sales positions in the T&M instrument industry during the past 15 years and, prior to that, worked in the defense and space industry. Waldeck spent more than 16 years developing automated test equipment for various branches of the military at a prominent defense contractor. He holds a bachelor's degree in electronic engineering from the N.Y. Institute of Technology and a master's of business administration from CW Post, Long Island University.

▲ Robert Waldeck

**Trilithic Inc.**, has promoted two employees. **John Bush** has been named Senior Systems Sales Engineer within the Broadband Instruments group. In his new expanded role, Bush will be responsible for working directly with customers at the senior level and bringing their ideas to fruition, contributing to new initiatives and leading product development for the Broadband Instruments group. Bush joined Trilithic in 2004 and has quickly advanced through his many roles in technical applications support and sales engineering. **Mark Darragh** has been named Product Manager for Trilithic's

▲ John Bush

▲ Mark Darragh


SERIES
San-tron
San-tron
San-tron
San-tron
San-tron

## Around the Circuit

Leakage Systems in the Broadband Instruments Group. Darragh joined Trilithic in July 2007 as an Applications Engineer. Prior to joining Trilithic, Darragh served multiple companies in product support roles. Darragh is a graduate of ITT Technical Institute with an electronic engineering technology degree.

▲ *Leonard Humes Jr.*

**M2 Global Technology** announced that **Leonard Humes Jr.** has joined the company as Senior Manager of Continuous Improvement Programs. The expansion of M2 Global's management team is the latest step in the company's quest to become the supplier of choice for the defense, aerospace and communications markets. Humes is a senior management professional with more than 20 years of diverse experience in industrial engineering, manufacturing operations, plant management, lean manufacturing and six sigma implementation. He is proficient at restructuring companies and developing and implementing business, manufacturing, and lean strategies that achieve rapid turnarounds and dramatic improvements in productivity and profits. He holds a master's of business administration degree from Texas A&M University and a bachelor's degree in mechanical engineering from the University of Texas.

**NEC Corp.** announced that **Kaoru Kenyoshi** was appointed to the Board of Directors of ETSI, the European Telecommunications Standards Institute, during its 58th General Assembly held in Cannes, France, in November. Kenyoshi will join ETSI's Board of Directors for the 2012 – 2014 term as the first member from the NEC Group and first member from Japan. ETSI's General Assembly is the Institute's highest decision-making body that meets twice a year to discuss issues that include strategy, operations and financial affairs.

## REP APPOINTMENT

**MI Technologies** announced an agreement for the establishment of **MI-Japan** to serve as the exclusive sales and service channel for that country. Formerly, MI Technologies had been represented in Japan by an unaffiliated distributor. With this new arrangement, MI Technologies established an exclusive channel to provide the needed focus in that dynamic marketplace. The contact person at MI-Japan's main office in Toyko is Nobuhiko Mukaida. The phone number is 81-3-6721-8854 and email is nobuhiko@mi-japan.co.jp.

## WEBSITE

**Renaissance Electronics** and **HXI** unveiled its revamped website for HXI products (www.hxi.com). Among its offerings is a comprehensive catalog of products. It also offers options to search datasheets by keywords, send enquiries online and sign up for the newsletter that provides regular product updates.


# HAND FLEX™ CABLES

Hand Flex Cables conform to any shape required.

from $8^{69}$ ea. (qty.1-9) IN STOCK DC to 18 GHz

***Get the performance of semi-rigid cable, and the versatility of a flexible assembly.*** Mini-Circuits Hand Flex cables offer the mechanical and electrical stability of semi-rigid cables, but they're easily shaped by hand to quickly form any configuration needed for your assembly, system, or test rack. Wherever they're used, the savings in time and materials really add up!

***Excellent return loss, low insertion loss, DC-18 GHz.*** Across their entire bandwidth, Hand Flex cables deliver excellent return loss (>27 dB for up to 24" runs) and low insertion loss (0.2 dB typ at 9 GHz for a 3-inch cable). So why waste time measuring and bending semi-rigid cables, when you can easily install a Hand Flex interconnect?

***Two popular diameters to fit your needs.*** Hand Flex cables are available in 0.086" or 0.141" diameters, with a turn radius of 6 or 8 mm, respectively. Straight SMA connectors are standard, and now we've added right-angle connectors to our Hand Flex lineup, for applications with tightly-packed components.

***Standard lengths in stock, custom models available.*** Standard lengths from 3 to 24" are in stock for same-day shipping. You can even get a Designer's Kit, so you always have a few on hand. Custom lengths, or two-right-angle models, are also available by preorder. Check out our website for details, and simplify your high-frequency connections with Hand Flex! *RoHS compliant*

*Mini-Circuits...we're redefining what VALUE is all about!*

**Mini-Circuits®**
*ISO 9001 ISO 14001 AS 9100*
P.O. Box 350166, Brooklyn, New York 11235-0003 (718) 934-4500 Fax (718) 332-4661

# Proper Stack-Up in a Multilayer PCB to Reduce Noise Coupling and Improve EMI

*As digital circuits became faster, direct coupling among power planes in multilayer printed circuit boards (PCB) became a major concern for signal integrity/power integrity and electromagnetic interference (EMI). Fast signals produce electromagnetic waves that can propagate by means of the parallel plates in the PCB, induce noise on the signals passing through the power bus (vias) and radiate from the edge of the board. The present study focuses on the analysis of the noise that propagates from a power plane to another power plane due to their proximity. To mitigate this problem, proper design of both power and ground planes in the stack-up is illustrated. A test board is fabricated and measurements are performed in order to validate the numerical electromagnetic model.*

With the ever-increasing speed and density of a digital integrated circuit system, the effects due to field interaction among IC chips, packages and PCBs have become more and more the limiting factors in high-speed system design.[1] Signal and power integrity (SI/PI) effects, such as propagation delay, crosstalk and simultaneous switching noise (SSN), require accurate and efficient electromagnetic analysis and modeling beyond the traditional static methods with a few lumped circuit elements.

Modeling a power plane, using equivalent lumped inductors[2] or inductive networks, can give erroneous results for computing power supply noise, because the model may only take into account the effect of slower current transient. Moreover, in many methods that have been applied in the past to analyze multilayered power distribution networks (PDN) containing several planes, the plane-pair have always been assumed to be isolated from each other. A method for analyzing the field penetration in package power distribution net-

Antonio Ciccomancini Scogna
*CST of America, Framingham, MA*
Jianmin Zhang
*CISCO Systems, San Jose, CA*

works is proposed[3] but also, in this case only, coupling of power/ground (PWR/GND) planes is studied. The importance of the topic is confirmed by recent publications focused on the modeling of PWR/GND planes and PDN in multilayer PCBs.[4,5]

On modern high performance digital circuits, the energy increases and is provided by PWR planes embedded in the multilayer structure of the PCB. These PWR planes can induce noise causing SI problems for drivers/receivers mounted on the board and power supply noise during input/output (I/O) switching. This last aspect often causes voltage fluctuations and circuit delay due to the transient currents injected into the PDN.

Decoupling capacitors connected to the PWR/GND leads are added to mitigate the effect of SSN; they help to stabilize the power distribution bus by supplying current that opposes any change in the power bus voltage. On the other hand, it has been demonstrated that all noise mitigation techniques that employ discrete capacitor components have a fundamental limitation, due to the inherent inductance arising from the leads of the capacitor.[6] Conventional PWR planes structures should be treated as dynamic electromagnetic systems in which waves can propagate between the PWR/GND planes. For this reason, a full wave modeling, which includes the vias, connectors and all the planes, is necessary to adequately detail the effects that are necessary to quantify the PCB from a SI and EMI point of view. This article investigates the effect of noise propagation in a multilayer PCB, due to the close proximity of two PWR planes and provides an overview on the design of the power bus location on multilayer PCBs.

## TEST STRUCTURE AND MODEL TO HARDWARE VALIDATION

The test board used for this study is illustrated in ***Figure 1***. It is an eight layer board of total thickness t = 2.088 mm and the dimensions are 260 × 210 mm; the dielectric material is standard FR-4 with nominal relative electric permittivity, $\varepsilon_r$ = 4.5 and loss tangent, tg$\delta$ = 0.02 at 1 GHz. The conductor is copper with conductivity $\sigma_c$ = 5.5×10$^7$ S/m and the thickness of all the PWR/GND planes is 0.018 mm.

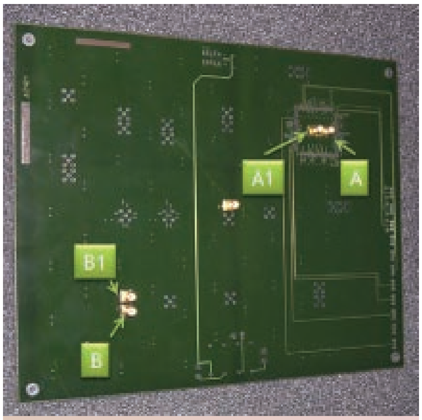


(a)

| | |
|---|---|
| COPPER FOIL-0.018 | 1 |
| PREPEG-0.208 | |
| COPPER FOIL-0.018 | 2 |
| C-STAGE-0.100 | |
| COPPER FOIL-0.018 | 3-PWR1 |
| PREPEG-0.720 | |
| COPPER FOIL-0.018 | 4-PWR2 |
| C-STAGE-0.100 | |
| COPPER FOIL-0.018 | 5 |
| PREPEG-0.300 | |
| COPPER FOIL-0.018 | 6 |
| C-STAGE-0.200 | |
| COPPER FOIL-0.018 | 7 |
| PREPEG-0.280 | |
| COPPER FOIL-0.018 | 8 |

2.088 mm

(b)

▲ *Fig. 1 Fabricated test board used for the model to hardware correlation (a) and stack-up of the PCB (b).*

Four SMA connectors, named respectively A1, A, B1 and B, are mounted on the top plane of the board in order to perform S-parameter measurements. SMA A1 and B1 are connected to the power plane PWR1. SMA A and B are soldered on the power plane named PWR2. PWR1 and PWR2 are two power planes, which are located in the stack-up one next to the other and separated by a 0.72 mm dielectric thickness. S-parameters are measured between SMA A1 and SMA B1 with an Anritsu 37247C vector network analyzer (VNA) and a full two-port calibration has been made at the ends of the probes.

A full wave field solver CST STUDIO SUITE®, based on the finite integration technique (FIT)[7], is employed to calculate $S_{21}$ between A1 and B1 on the same test board and the calculated results are compared with

You Have Our Undivided
ATTENTION
EWT
www.ewtfilters.com
We understand how critical your applications are. That's why you'll always have our *Undivided Attention*.
Offering more than 40 years of experience in custom design & manufacturing of RF and Microwave filters and filter based products to 50 GHz.
Military • Commercial
Wireless • Space
Eastern Wireless TeleComm, Inc.
Tel: 410.749.3800 Fax: 410.749.4852
sales@ewtfilters.com

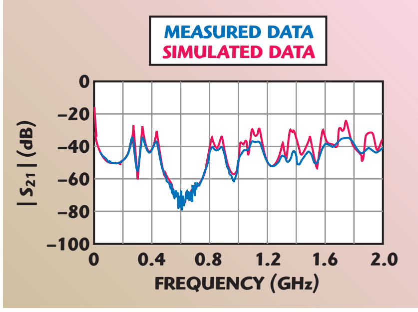


▲ *Fig. 2 $S_{21}$ correlation between measured and simulated results (A1-B1).*

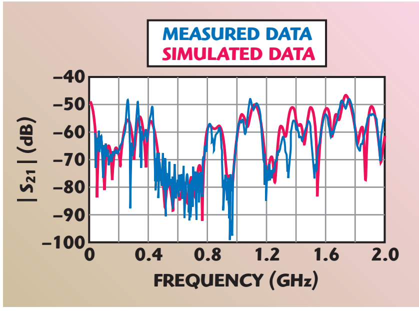


▲ *Fig. 3 $S_{21}$ correlation between measured and simulated results (B-A1).*

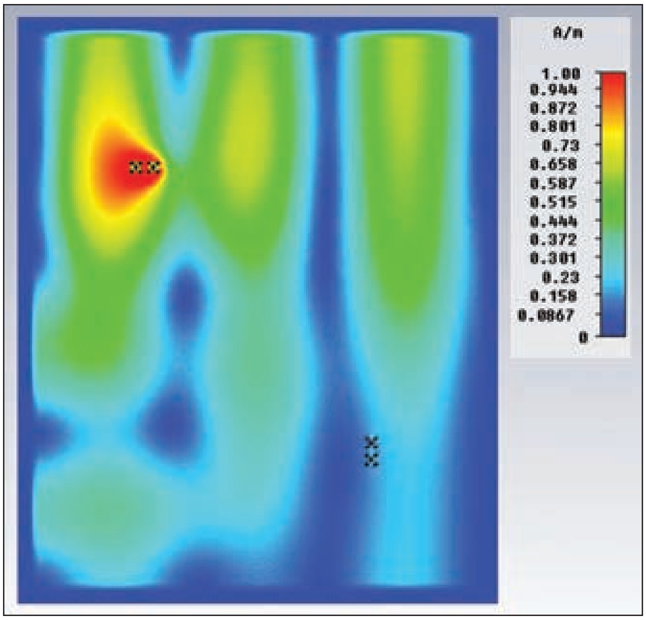


▲ *Fig. 4 Current distribution at 1 GHz in the cross section of the considered board stack-up.*

the measurements, as shown in ***Figure 2***. In the equivalent electromagnetic model, it is important to point out that the SMA connectors are also modeled and particular attention has been given to the excitation: the two ports at which the S-parameters are evaluated are the upper surface of the SMA A1 and SMA B1. In order to ensure a TEM structure of the electromagnetic field (essential condition for a meaningful interpretation of the scattering matrix) the TEM excitation has been realized by considering waveguide ports at the top of the SMA.

Good agreement can be observed between the measured and the numerically calculated data. The considered frequency range is 20 MHz to 2 GHz, which is a typical value used for PI analysis. The small difference in the amplitude of the measured and simulated $S_{21}$ is due to the fact that, in the actual board, there are multiple vias with different diameters, which subtract useful area to the PWR/GND plane pair, therefore increasing the $S_{21}$. ***Figure 3*** shows $S_{21}$ on the PWR2 due to a wave propagating on PWR1 (B-A1). It can be noted that the magnitude is only about 10 times attenuated with respect to the original wave on PWR1 and this value is certainly not enough to guarantee a good SI immunity. To confirm this, ***Figure 4*** is a picture of the current field distribution on a cross section of the board calculated at 1 GHz, which shows the amount of current on the other PWR plane, causing coupling with it. This phenomenon is due to the fact that the two PWRs are separated by only 710 μm of dielectric material.

This is not the worst case scenario. As in realistic high speed PCBs, the coupling effect is more accentuated, due to the presence of multiple antipads and islands, which are necessary to design through/buried vias as well as to isolate the sensitive circuitry parts. As seen in Figures 2 and 3, the size and shape of the board introduce few resonant frequencies whose amplitude can be, in principle, reduced by using a thinner dielectric material between the two planes. In particular, the reduction of the amplitude in dB is proportional to the ratio between the two layers and the $S_{21}$ decreases according to the quality

factor of the cavity formed by them. The quality factor, determined by the total loss and the energy storage is linearly dependent on the height of the cavity formed by the two metal layers. Although S-parameters are evaluated, the general S-parameter matrix can be simply transformed into the impedance matrix using the following equation:

$$[Z] = Z_0 \frac{[I]+[S]}{[I]-[S]} \quad (1)$$

[I] is the identity matrix and $Z_0$ is the characteristic impedance of the network analyzer. The transfer impedance $Z_{21}$ on the off diagonal of the impedance matrix, gives indications about the open circuit voltage at a victim location on the power bus generated by the current injected at a source location. From Equation 1, if the following conditions are fulfilled,

$$|S_{21}|,|S_{12}| << 1 \quad (2a)$$

$$S_{11}, S_{22} \approx -1 \quad (2b)$$

as it normally happens for a PWR/GND plane pair, the magnitude of $Z_{21}$ is related to the $S_{21}$ measurements as the following:

$$|Z_{21}|\,dB \approx |S_{21}|\,dB + 28\,dB \quad (3)$$

Consequently $S_{21}$ simulations and/or measurements can be used to study the transfer impedance between two selected points' places on the power bus.

Due to the CPU time, when performing full-wave analysis, alternative methods can be employed to evaluate the noise coupling among multiple points on a PCB. If the PWR/GND layers have a rectangular shape, the resonant frequencies for the TMnm modes are given by the equation:

$$f_{nm} = \frac{c}{2\pi\sqrt{\varepsilon_r}} \sqrt{\left(\frac{m\pi}{L}\right)^2 + \left(\frac{n\pi}{W}\right)^2} \quad (4)$$

where m and n are the mode number, L is the length of the board, W is the width and $\varepsilon_r$ is the relative permittivity of the dielectric between the plane, and c is the speed of the light in free space. The resonances of the frequencies where the measured $S_{21}$ levels reach their peaks (see Figures 2 and 3) match almost perfectly with the frequencies calculated with Equation 4.

## NOISE PROPAGATION REDUCTION BY MODIFYING THE STACK-UP

In this section, it is demonstrated how the changing of the location for the plane PWR1 as far as shown in ***Figure 5*** will allow it to drastically reduce the effect of coupling between the two PWR planes. From the transmission coefficient $S_{21}$, which can be measured or calculated on PWR2 when a wave propagates on the other, it is evident how, in this case, the reduction is approximately four to five times, with respect to the previously examined case. This situation allows it to ensure an efficient isolation level between the two PWR planes, when a wave propagates on one. The value of the $S_{21}$ magnitude, calculated by means of the FIT code when PWR1 is located between the TOP plane and a GND plane, is compared with the results obtained between SMA B1 and SMA A of the original stack-up.

The advantage of this concept is that without any additional metal layer the coupling between the two PWR planes is reduced to extremely

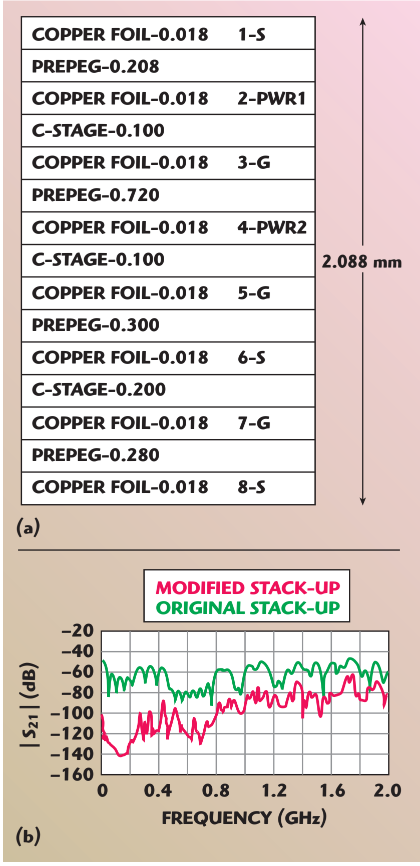


▲ *Fig. 5 Modified stack-up (a) and comparison of $S_{21}$ magnitude with the modified stack-up (b).*

# OPTICAL DRIVER SOLUTION

***Ideal for Driving MZ Optical Modulator With Electrical NRZ Data!***

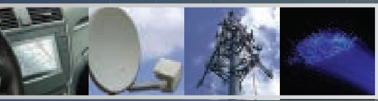

Analog, Digital & Mixed-Signal
ICs, Modules, Subsystems & Instrumentation

## *HMC1050 & HMC1051 Optical Modulator Drivers, DC to 30 GHz!*

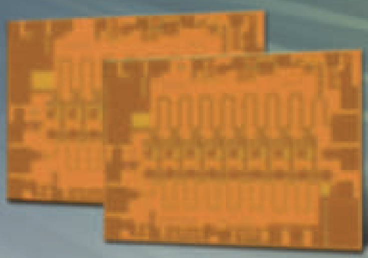

- ***Complete Driver Chain Solution For Low-Power Designs***
- ***Ideal For 100G DWDM & 40G DQPSK Transmitters***
- ***Up to 32 Gbps Operation***
- ***Peak Detect Feature***
- ***Requires Minimal External Components***

**Cascaded Configuration for Driving MZ Modulator**

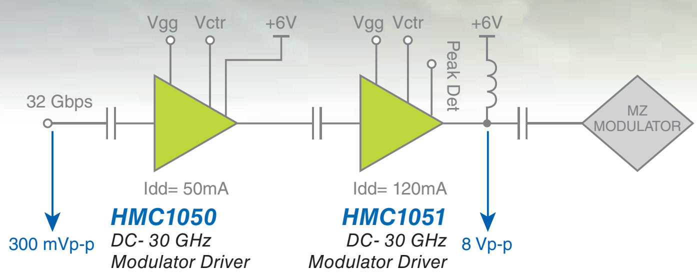


Total Power Consumption: 1 W

**32 Gbps NRZ Output Eye Diagram @ +6V**

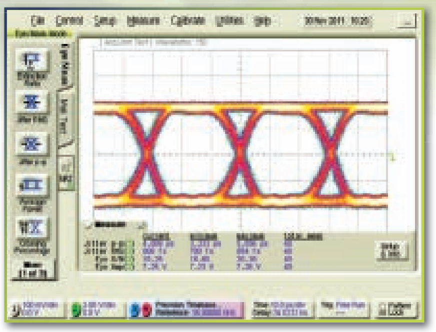

| | Frequency (GHz) | Function | Gain (dB) | Group Variation Delay (ps) | Additive Jitter (ps) | P1dB (dBm) | Output Voltage Level (Vp-p) | Part Number |
|---|---|---|---|---|---|---|---|---|
| | DC - 20 | MZ Optical Modulator Driver | 18 | ±15 | 0.3 | 22 | 2.5 - 8 | HMC870LC5 [1] |
| | DC - 20 | EA Optical Modulator Driver | 15 | ±15 | 0.3 | 16.5 | 2.5 - 4 | HMC871LC5 [1] |
| NEW! | DC - 30 | 3Vpp Optical Modulator Driver / Wideband Amplifier | 14 | ±5 | 0.3 | 14 | 3 | HMC1050 [2] |
| NEW! | DC - 30 | 8Vpp Optical Modulator Driver / Wideband Amplifier | 16 | ±5 | 0.3 | 20 | 8 | HMC1051 [2] |

*[1] Drivers that benefit from Hittite Active Bias Controllers*
*[2] Request Data Sheet: FO@hittite.com*

***Ideal For Wideband Electronic Warfare Systems, Test & Measurement and NRZ Applications Up to 32 Gbps!***

Hittite MICROWAVE CORPORATION

2 Elizabeth Drive • Chelmsford, MA 01824
978-250-3343 tel • 978-250-3373 fax • sales@hittite.com

**Order On-Line at: www.hittite.com**
Receive the latest product releases - click on "My Subscription"

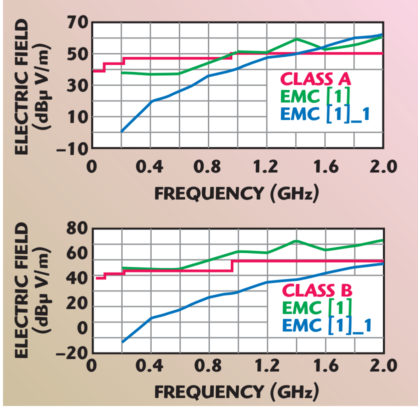


▲ *Fig. 6 EMI emission for original (EMC [1]) and modified stack-up (EMC[1]_1) at a distance of 3 m (a) and 10 m (b).*

small values. However, in some cases, a minimum number of layer and position in the stack-up is required in order to maintain the PCB functionality. In such cases, an extra metal layer is required to guarantee a lower coupling level, which unfortunately introduces extra costs. Alternative solutions can be obtained by introducing effective power islands[8] and shorting vias, which provide some isolation among the layer or more advanced filtering structures, such as two-dimensional (2D) electromagnetic bandgap structures (EBG)[9] or new techniques based on photonics crystals.[10]

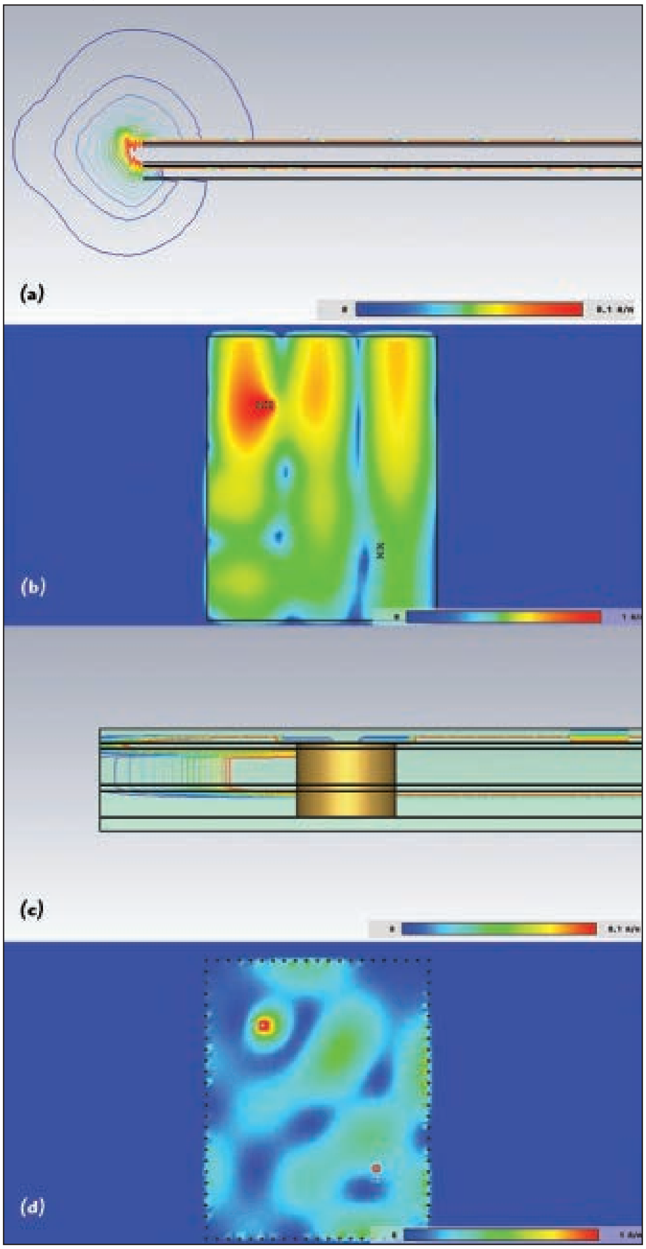


▲ *Fig. 7 Surface current distribution at 1 GHz on the PWR1 and fringing field of the H-field for original PCB (a, b) and PCB with stitching vias (c, d).*

## EMC/EMI ANALYSIS

The EMC/EMI of the proposed test board is also investigated. ***Figure 6*** shows the absolute radiated emission at 3 and 10 m away from the board when an input current $I_{noise}$ = 1 mA is used to inject noise in the position A1. To understand whether the GND plane via stitching, placed around the board edges, has any effect with respect to the EMI produced by the fringing fields on the power bus, a new board is designed. It assumes the presence of stitching vias among the layers at the periphery of the board, 5 mm distant from the edge and with a pitch value of 6 mm. The emission profile is calculated and compared to the original board and the results are illustrated.

It can be observed that the 3 m radiated field is below the FCC level up to 1.4 GHz, which represents a substantial

improvement with respect to the case of the original board without stitching vias. The radiated emissions at 10 m are even lower and below the FCC levels over the whole frequency range of interest 0 to 2 GHz. The presence of the board ground ring represented by the stitching vias also provides protection against ESD generated during the board handling; therefore, it serves two purposes. ***Figure 7*** confirms the additional coupling on PWR1, when no stiching vias are present as well as the strong fringing field predicted at the edge of the board, which causes increased emissions. By adding the ring of stitching vias, both noise coupling (represented by the lower value of the surface current on the PWR1) and the fringing field are consistently reduced.

## CONCLUSION

A GND-PWR1-PRW2-GND board stack-up is studied from both a PI and SI point of view. Numerical simulations, validated by means of measurements on a given test board, demonstrate that the PWR planes location in multilayer PCBs can be very important. Both experimentally and numerically calculated results have pointed out that when two PWR planes are too close, there is excessive coupling between them and this generates a propagation of noise on one PWR plane when the other is excited. The concept is also shown by means of current distribution on the board planes. This can be avoided by changing the PWR plane location and realizing a different stack-up. Using PWR layers, sandwiched between GND layers stitched together, has beneficial effects on the board signal integrity due to a more stable reference offered to the signal paths. The radiated emissions of the board are also studied and it is demonstrated how the electrostatic ring placed all around the board can significantly decrease the maximum value of field radiated from the edge of the board. ■

## References

1. M. Swaminathan, J. Kim, I. Novak and J.P. Libous, "Power Distribution Networks for System-on-package: Status and Challenges," *IEEE Transactions on Advanced Packaging*, Vol. 27, No. 2, May 2004, pp. 286-300.
2. N. Na, J. Choi, S. Chum and M. Swaminathan, "Modelling and Transient Simulation of Planes in Electronic Package," *IEEE Transactions on Advanced Packaging*, Vol. 23, No. 3, August 2000, pp. 340-352.
3. J. Mao and M. Swaminathan, et al., "Modelling of Field Penetration Through Planes in Multilayered Packages," *IEEE Transactions on Advanced Packaging*, Vol. 24, No. 3, August 2001, pp. 326-333.
4. E. Engin and M. Swaminathan, *Power Integrity Modeling and Design for Semiconductors and Systems*, Prentice Hall, Upper Saddle River, NJ, 2008.
5. I. Novak and J. Miller, *Frequency Domain Characterization of Power Distribution Networks*, Artech House, Norwood, MA, 2007.
6. X. Ye, D.M. Hockanson, M. Li, Y. Ren, W. Cui, J.L. Drewniak and R.E. DuBroff, "EMI Mitigation with Multilayer Power Bus Stacks and Via Stitching of Reference Plane," *IEEE Transactions on Electromagnetic Compatibility*, Vol. 43, No. 4, November 2001, pp. 538-548.
7. CST STUDIO SUITE 2012®, www.cst.com.
8. A. Ciccomancini Scogna, "PPW Noise Mitigation in Multilayer PCBs by Means of Virtual Island and/or Array of Shorting Vias," *2007 Proceedings of the Electromagnetic Compatibilty Conference*.
9. O.M. Ramahi and V. Granastein, "Novel Planar Electromagnetic Bandgap Structures for Mitigation of Switching Noise and EMI Reduction in High-Speed Circuits," *IEEE Transactions on Electromagnetic Compatibility*, Vol. 49, No. 3, 2007, pp. 661-669.
10. A. Ciccomancini Scogna, A. Orlandi and T.L. Wu, "Noise Coupling Mitigation in PWR/GND Plane Pair by Means of Photonic Crystal Fence: Sensitivity Analysis and Design Parameters Extraction," *IEEE Transactions on Advanced Packaging*, to be published.

**Antonio Ciccomancini Scogna** *received his doctorate in electrical engineering from the University of L'Aquila, Italy in 2005. He is Principal Engineer at Computer Simulation Technology (CST) of America, Framingham, Mass. His research interests include EMC numerical modeling, printed and integrated circuits, electromagnetic packaging effects, signal integrity and power integrity analysis in high speed digital systems.*

**Jianmin Zhang** *received his master's degree and doctorate both in electrical engineering from the University of Missouri-Rolla in 2003 and 2007, respectively. He first joined Cisco Systems as a Senior Hardware Engineer after graduation in 2007 and as a technical leader in 2011 subsequently. He has been focusing on signal integrity and power integrity R&D for high-speed interconnects and involving in design and analysis of high-performance networking products at printed circuit board, package, and system levels. His research interests include signal integrity, power integrity, SerDes modeling, EMI/EMC, PCB material characterization and de-embedding techniques.*

# PLL CHIPSET

## New PLL Chipset for Ultimate Spurious & Phase Noise Performance!

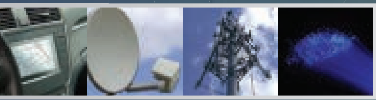

Analog, Digital & Mixed-Signal
ICs, Modules, Subsystems & Instrumentation

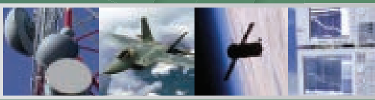

### HMC983LP5E & HMC984LP4E Used as a PLL Chipset !

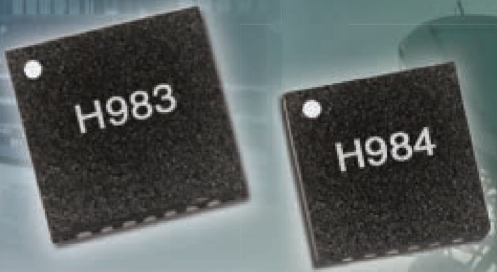


**180 nHz Fractional Frequency Resolution!**

- **Programmable 48-Bit 100 MHz Delta-Sigma Modulator**
- **User-Defined, Automatic or Triggered FMCW Frequency Sweeps**
- **High Phase Detector Frequencies:**
  **125 MHz in Fractional Mode**
  **175 MHz in Integer Mode**
- **Phase Noise Figure of Merit:**
  **-227 dBc/Hz in Fractional Mode**
  **-231 dBc/Hz in Integer Mode**

**HMC983LP5E**
**Built-in Automatic FMCW Sweeper Feature**

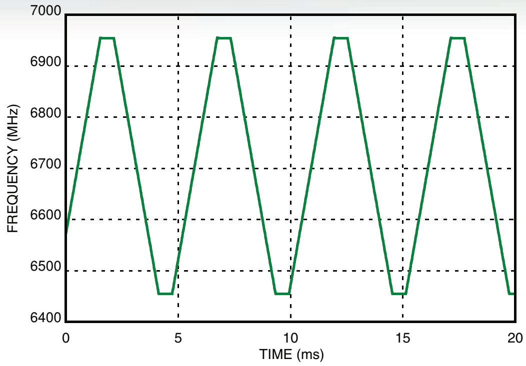


**HMC983LP5E & HMC984LP4E World's Lowest Spur Fractional-N PLL Chipset (7000.01MHz, 50MHz PFD)**

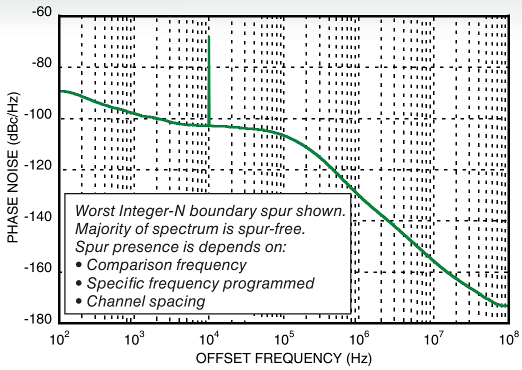


| Input Frequency (GHz) | Function | Input Power (dBm) | Output Level | Floor FOM (dBc/Hz) | Bias Supply | Part Number |
|---|---|---|---|---|---|---|
| DC - 7 | 48-Bit Delta Sigma Programmable Fractional Divider with Sweeper | -15 to -3 | 0.75 Vp-p to 2 Vp-p into 100 Ohm | -160 | +5V @ 1 mA<br>+3V @ 244 mA | **HMC983LP5E** |
| DC - 0.35 | Phase Frequency Detector & Charge Pump | 3 to 12 | 0.02 to 2.5 mA | -231 | +5V @ 97mA<br>+3V @ 27mA | **HMC984LP4E** |

**Ultimate Performance Chipset Targeting PLL & FMCW Sweeper Applications!**

Hittite MICROWAVE CORPORATION

2 Elizabeth Drive • Chelmsford, MA 01824
978-250-3343 tel • 978-250-3373 fax • sales@hittite.com

**Order On-Line at: www.hittite.com**
Receive the latest product releases - click on "My Subscription"

# RF Characteristics of a Short Wavelength Comb-Type Capacitive Transmission Line on MMICs

*In this work, the basic characteristics of the comb-type capacitive transmission line (CCTL) structure were investigated for application to the development of miniaturized on-chip passive components. According to the results, the CCTL structure showed short wavelength characteristics, due to its periodically added capacitance. The wavelength of the CCTL structure was only 10 percent of that of a conventional microstrip line on a MMIC. The CCTL structure showed a propagation constant much higher than a conventional microstrip line, due to the slow-wave propagation on a periodic structure. Using the CCTL structure, a highly miniaturized impedance transformer was fabricated on a GaAs MMIC. The impedance transformer showed good RF performances in a broadband from S- to X-Band, and its size was 0.042 mm², which is 0.95 percent of the size of the transformer fabricated by a conventional microstrip line.*

With the evolution of integrated circuit (IC) technology, the demands for on-chip RF passive components on ICs have increased in the wireless communication systems market.[1-8] However, bulky RF passive components, such as conventional impedance transformers and dividers, have been fabricated outside of the ICs, due to their large sizes. According to a previous report,[5] of all the slow-wave structures,[3-8] the CCTL structure showed the shortest wavelength. For application to various on-chip components on a MMIC, the basic characteristics of the CCTL structure should be explored thoroughly. In

Jang-Hyeon Jeong, Young Yun, Hong-Seung Kim and Nat-Won Jang
*Korea Maritime University, Busan, Korea*
Yunju Baek
*Pusan National University, Busan, Korea*


© 2012 AWR Corporation. All rights reserved. AWR is a National Instruments Company.
AWR®
The AWR mmWave design flow.
Often MMIC'd.
Never duplicated.
When you're racing toward important targets, design performance is paramount. Don't let yourself be duped. Nobody does more for mmWave MMIC design than AWR. You can do circuit, system, and EM simulations faster, easier, and more accurately. What's more, with schematic and layout in the same UI, you're more efficient and avoid the manual mistakes associated with running multiple tools. Tackle today's high-end, mission-critical mmWave MMIC designs with ease. Grab a test copy at www.awrcorp.com/mwo.
Stop waiting and start designing™
MICROWAVE OFFICE™

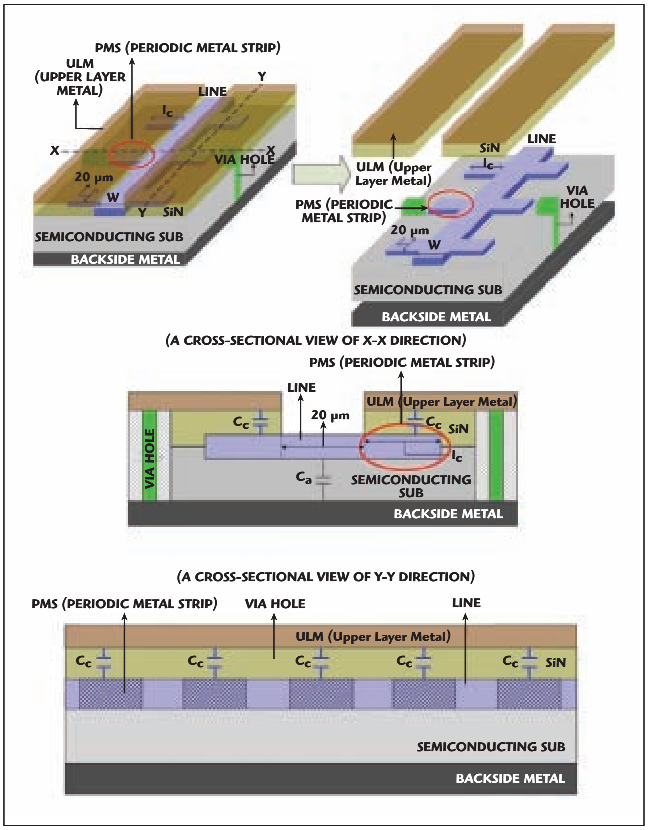


▲ *Fig. 1 Structure of a CCTL.*

this work, using theoretical and experimental analyses, the basic characteristics of the short wavelength CCTL structure on a GaAs MMIC were investigated to the development of miniaturized on-chip passive components. In addition, using the CCTL structure, a highly miniaturized on-chip passive component was fabricated on a GaAs MMIC.

## BASIC CHARACTERISTICS OF CCTL

***Figure 1*** shows the structure of a CCTL.[5] As shown, a comb-type line is fabricated on the semiconducting substrate. The comb-type line consists of a line and periodic metal strips (PMS), which are connected to both sides of the line. The upper layer metal (ULM) is placed on the top side of the CCTL structure and is electrically connected to the backside ground plane through the via-holes. Therefore, the ULM serves as a ground plane, together with the backside ground plane. A SiN film is deposited between the ULM and PMS for tight coupling. As is well known, a conventional microstrip line has only a periodic capacitance $C_a$ (shown in Figure 1) between the line and the backside ground plane, while the CCTL structure has an additional capacitance $C_c$ as well as $C_a$, due to a strong electromagnetic coupling between PMS and ULM. Therefore, the CCTL structure exhibits a much shorter wavelength ($\lambda g$) than conventional ones, because $\lambda g$ is inversely proportional to the periodic capacitance; in other words, $\lambda g = 1/[f\,(LC)^{0.5}]$.

### Short Wavelength Characteristics of CCTL

***Figure 2*** shows a comparison of the wavelength for CCTL and a conventional transmission line. The spacing L between the strips and the line width, W, which are shown

# Bigger screen. Faster rise/fall time. Twice the sampling rate.

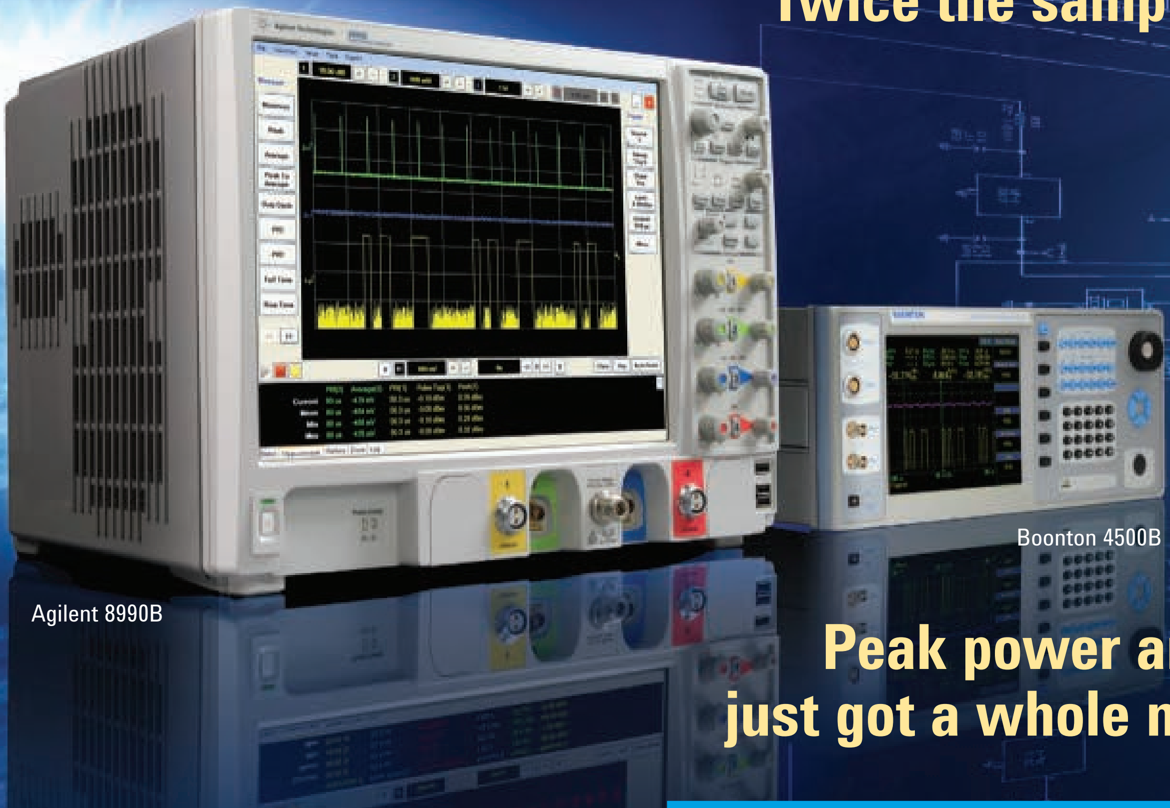

Boonton 4500B

Agilent 8990B

# Peak power analyzers just got a whole new look.

Radar and wireless communications are increasingly complex, demanding higher performances than ever. The new Agilent peak power analyzer features 15 pulse characterization measurements, including automated pulse droop and delay measurements. Plus a vivid 15-inch touch-screen display to reveal even elusive signal trace details.

**That's thinking ahead. That's Agilent.**

| | Agilent 8990B | Boonton 4500B** |
|---|---|---|
| Rise/fall time* | 5 ns | 7 ns |
| Sampling rate | 100 MSa/s | 50 MSa/s |
| Dynamic range* | -35 to +20 dBm | -50 to +20 dBm |
| Internal zero and calibration | Yes | No |
| USB sensor support | Yes | No |

*Sensor dependent

**Data for competitive peak power analyzer from competitor publication PN B/4500B/0311/EN updated 2011

**Trade-in your Boonton 4500B or HP 8990A/8991A**
**Receive a 10% credit on a new Agilent 8990B**
www.agilent.com/find/8990tradein

Test & Measurement World's TOP 50 2011



u.s. 1-800-829-4444 canada 1-877-894-4414

Agilent Technologies

in Figure 1, are all 20 μm. The length of PMS $l_c$ varies from 10 to 30 μm. The CCTL structure was fabricated on a GaAs substrate with a height of 100 μm. Compared with a conventional microstrip line, the wavelength of the CCTL structure is only 10 percent of the one of a conventional microstrip line on a MMIC. In short, at 10 GHz, the wavelengths of the CCTL and the conventional microstrip line are 1.06 and 10.56 mm, respectively.

## Characteristic Impedance of CCTL

It can easily be seen that an increase of $l_c$ results in an enhancement of the periodic capacitance $C_c$, due to an increase of the capacitive area. Therefore, the characteristic impedance $Z_0$ of the CCTL can be easily controlled by changing $l_c$, because $Z_0$ depends on the periodic capacitance of the transmission line; in other words, $Z_0 = (L/C)^{0.5}$.[9] The dependence of $Z_0$ on $l_c$ is shown in ***Figure 3***, where the line width, W, was fixed to a value of 20 μm. The above results indicate that highly miniaturized passive components with various impedances can be realized by using the CCTL structure.

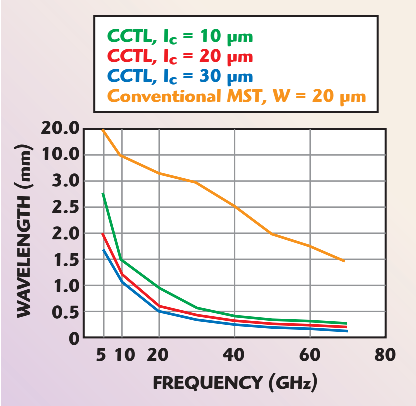


▲ *Fig. 2 CCTL and conventional microstrip line wavelengths.*

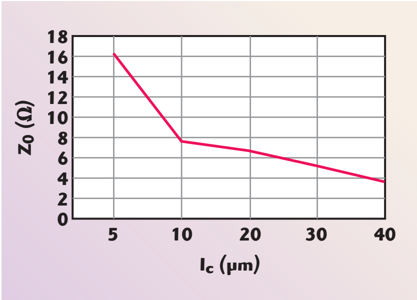


▲ *Fig. 3 Characteristic impedance of the CCLT.*

## Loss, Propagation Constant and Dielectric Constant

For a fair loss comparison, the loss of a CCTL and a conventional microstrip line with the same electrical length should be compared with each other, because the wavelength of a CCTL structure is much shorter than for a conventional microstrip line. Accordingly, the loss of the CCTL structure and the conventional microstrip line with a length of λ/4 were compared; the results are shown in ***Table 1***. As shown, for an electrical length of λ/4, the CCTL structure shows a little higher loss than the conventional microstrip line. The CCTL structure shows a loss of 1.0 to 1.3 dB, while the conventional microstrip line shows a loss of 0.6 to 0.8 dB. Although the CCTL structure shows a little higher loss, it is preferable for the development of miniaturized passive components on a MMIC, due to its short wavelength.

**TABLE I**
**INSERTION LOSS COMPARISON FOR A λ/4 CCTL STRUCTURE AND CONVENTIONAL MICROSTRIP LINE**

| | 3 GHz | 4 GHz | 5 GHz | 6 GHz | 7 GHz |
|---|---|---|---|---|---|
| Conventional Microstrip Line (dB) | 0.80 | 0.701 | 0.645 | 0.616 | 0.606 |
| CCTL (dB) | 1.17 | 1.08 | 1.14 | 1.21 | 1.32 |

***Figures 4*** and ***5*** show the effective propagation constant and effective dielectric constant of the CCTL structure. As shown, the CCTL structure shows a much higher propagation constant β than the conventional microstrip line, which means that a slow wave exists on CCTL, due to its periodic structure. The effective dielectric constant was obtained from the following equation

$$\varepsilon_e = \left(\frac{2\pi}{\omega\lambda}\frac{1}{\sqrt{\varepsilon_0\mu_0}}\right)^2 \quad (1)$$

As shown, the CCTL structure shows a much higher effective dielectric constant than a conventional microstrip line, due to the slow wave on CCTL.

## EQUIVALENT CIRCUIT MODEL OF THE CCTL STRUCTURE ON MMIC

For application to the design of RF passive components in a wireless communication system, the equivalent circuit of the CCTL structure should be extracted. ***Figure 6*** shows the equivalent circuit of the unit cell of the CCTL structure, which corresponds to the equivalent circuit of the $n^{th}$ unit section of the periodic structure surrounded by a rectangular box. $C_c$ corresponds to the capacitance between ULM and PMS, which is proportional to the area $l_h l_c$, where $l_h$ and $l_c$ are the width and length of the periodic strips of PMS, respectively, and $l_h$ was fixed as 20 μm. $R_g$ and $L_g$ are the resistance and inductance originating from the loss and current flow of the PMS with a length $l_c$. $C_a$ corresponds to the ca-

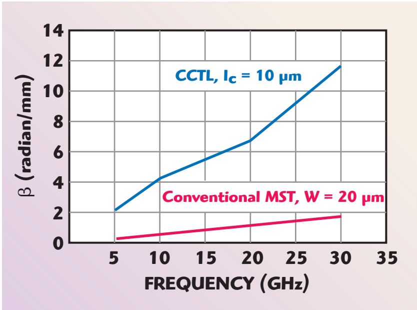


▲ *Fig. 4 Effective propagation constant of the CCTL structure and conventional microstrip line.*

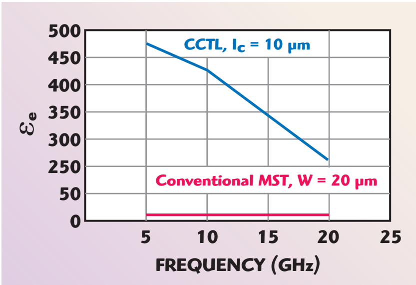


▲ *Fig. 5 Effective dielectric constant of the CCTL structure and conventional microstrip line.*

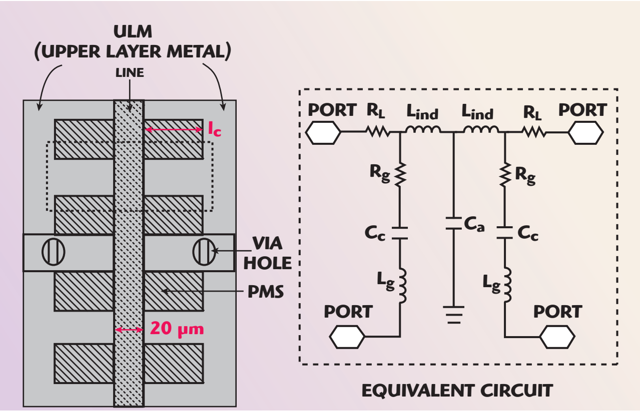


▲ *Fig. 6 Equivalent circuit of a unit cell of the CCTL structure.*

pacitance between line and ground metal. $L_{ind}$ and $R_L$ are parasitic inductance and resistance originating from the top line. The capacitances, inductances and resistances of the equivalent circuit are given by

$$L_{ind}=\left[0.0262+0.0215\left(\frac{l_c}{W}\right)-0.0215\left(\frac{l_c}{W}\right)^2\right](nH) \quad (2)$$

$$C_a=\left[0.215-0.775\left(\frac{l_c}{G}\right)+3.25\left(\frac{l_c}{G}\right)^2\right](pF) \quad (3)$$

$$C_c=\left[0.45-0.194\times10^{-2}\left(\frac{l_c}{d_i}\right)+0.48\times10^{-5}\left(\frac{l_c}{d_i}\right)^2\right](pF) \quad (4)$$

$$R_L=\left[-0.05\left(\frac{W}{l_c}\right)+0.6\right](\Omega) \quad (5)$$

$$R_g=\left[0.885-0.38\left(\frac{l_c}{l_h}\right)+0.26\left(\frac{l_c}{l_h}\right)^2\right](\Omega) \quad (6)$$

$$L_g=\left[-0.0646+0.1364\left(\frac{l_h}{l_c}\right)+0.0398\left(\frac{l_h}{l_c}\right)^2\right](nH) \quad (7)$$

where W, $l_c$ and $d_i$ are top line width, length of periodic metal strip and the thickness of the SiN layer. G is the thickness between line and ground and $l_h$ is the width of the PMS. In particular, Equation 4 includes $(l_c/d_i)^2$, because there are nonlinearity originating from parasitics due to the fringing capacitance. Using the equivalent circuit and closed-form equations, the RF characteristics of the CCTL structure were calculated and compared with measured results. ***Figure 7*** shows the measured and calculated insertion loss $S_{21}$ of the CCTL structure for two $l_c$ values. For the calculation results, the equivalent circuit and the closed form equations were used. There is a fairly good agreement between calculated and measured results up to 50 GHz.

## HIGHLY MINIATURIZED IMPEDANCE TRANSFORMER ON A GAAS SUBSTRATE

A highly miniaturized impedance transformer was fabricated on a GaAs substrate, using the CCTL structure, for application to S- to X-Band MMICs. ***Figure 8*** shows

# Xinger® Subminiature Components Selection Matrix

- Sized for both compact wireless infrastructure applications (e.g. A-to-D converters, receivers, transceivers, and amplifiers for pico or home base stations) *and* wireless consumer electronics applications (e.g. handhelds, digital/analog conversion, broadcasting, Bluetooth® devices)
- Product family supports wide array of bands and protocols, such as WiMax, WiFi, GSM, GPS, Bluetooth®, ZigBee®, 802.11a, b, g, 3G, RFID, PCS, DCS, others
- Low cost in volume with excellent performance for their size (power handling, insertion loss, etc.)
- Non-conductive surface; 100% RF-tested; RoHS compliant; shipped on tape & reel

0404 balun — 0603 balun — 0805 balun — analog-to-digital conversion balun

## Balun Transformers

| Part no. | Freq. (GHz) | Power (W) | Size inches/ (mm) | Unbal. Port Imp. (Ω) | Bal. Port Imp. (Ω) | Ins. Loss (dB) | Amp. Bal. (dB) | Phase Bal. (degrees) | RL Unbal. (dB) |
|---|---|---|---|---|---|---|---|---|---|
| B0205F50200AHF | 0.2 - 0.5 | 2.0 | 0.1 x 0.08 (4.1 x 2.1) | 50 | 50 | 1.6 | 0.4 | 3.1 | 13.9 |
| BD0205F5050AHF | 0.2 - 0.5 | 2.0 | 0.1 x 0.08 (4.1 x 2.1) | 50 | 50 | 1.1 | 0.6 | 3.0 | 11.0 |
| B0225J7575AHF | 0.2 - 2.5 | 0.5 | 0.08 x 0.05 (2 x 1.25) | 75 | 75 | 1.1 | 3.2 | 40.0 | 14.0 |
| B0310J50100AHF | 0.3 - 1.0 | 2.0 | 0.08 x 0.05 (2 x 1.25) | 50 | 100 | 1.0 | 2.8 | 36.0 | 8.1 |
| B0322J5050AHF | 0.3 - 2.2 | 2.0 | 0.08 x 0.05 (2 x 1.25) | 50 | 50 | 1.6 | 1.3 | 20.0 | 13.0 |
| B0430J50100AHF | 0.4 - 3.0 | 1.0 | 0.08 x 0.05 (2 x 1.25) | 50 | 100 | 4.0 | 1.4 | 12.0 | 8.4 |
| BD0810J50100AHF | 0.8 - 1.0 | 2.0 | 0.08 x 0.05 (2 x 1.25) | 50 | 100 | 1.0 | 0.4 | 2.0 | 13.0 |
| BD0810J50150AHF | 0.8 - 1.0 | 2.0 | 0.08 x 0.05 (2 x 1.25) | 50 | 150 | 1.1 | 0.6 | 6.0 | 13.3 |
| BD0810J50200AHF | 0.8 - 1.0 | 2.0 | 0.08 x 0.05 (2 x 1.25) | 50 | 200 | 1.0 | 1.1 | 8.0 | 14.5 |
| BD0826J50200AHF | 0.8 - 2.6 | 2.0 | 0.08 x 0.05 (2 x 1.25) | 50 | 200 | 1.5 | 1.3 | 7.0 | 8.5 |
| B0809J50ATI | 0.85 - 0.915 | 2.0 | 0.08 x 0.05 (2 x 1.25) | 50 | 50 | 0.6 | | | 15.3 |
| B0922J7575A50HF | 0.9 - 2.2 | 2.0 | 0.08 x 0.05 (2 x 1.25) | 75 | 75 | 1.1 | 1.4 | 9.0 | 12.0 |
| B0922J7575AHF | 0.9 - 2.2 | 2.0 | 0.08 x 0.05 (2 x 1.25) | 75 | 75 | 1.2 | 1.4 | 9.0 | 7.9 |
| BD0922J75100AHF | 0.9 - 2.2 | 2.0 | 0.08 x 0.05 (2 x 1.25) | 75 | 100 | 1.64 | 0.8 | 4.67 | 9.1 |
| B0922N7575AHF | 0.95 - 2.15 | 0.75 | 0.04 x 0.04 (1 x 1) | 75 | 75 | 0.76 | 2.1 | 20.95 | 13.2 |
| BD1222J50200A00 | 1.2 - 2.2 | 2.0 | 0.08 x 0.05 (2 x 1.25) | 50 | 200 | 0.6 | 0.9 | 6.0 | 14.0 |
| BD1631J50100AHF | 1.6 - 3.1 | 2.0 | 0.08 x 0.05 (2 x 1.25) | 50 | 100 | 1.0 | 1.0 | 5.0 | 10.0 |
| BD1722J50100AHF | 1.7 - 2.2 | 2.0 | 0.08 x 0.05 (2 x 1.25) | 50 | 100 | 1.2 | 1.2 | 6.0 | 12.0 |
| BD1722J50200A00 | 1.7 - 2.2 | 2.0 | 0.08 x 0.05 (2 x 1.25) | 50 | 200 | 0.7 | 0.9 | 8.0 | 15.0 |
| BD1722N5050AHF | 1.7 - 2.2 | 0.8 | 0.04 x 0.04 (1 x 1) | 50 | 50 | 1.1 | 0.8 | 7.0 | 13.0 |

Data current as of: January, 2012

## Balun Transformers (continued)

| Part no. | Freq. (GHz) | Power (W) | Size inches/ (mm) | Unbal. Port Imp. (Ω) | Bal. Port Imp. (Ω) | Ins. Loss (dB) | Amp. Bal. (dB) | Phase Bal. (degrees) | RL Unbal. (dB) |
|---|---|---|---|---|---|---|---|---|---|
| BD2040J50100A00 | 2.0 - 4.0 | 2.0 | 0.08 x 0.05 (2 x 1.25) | 50 | 100 | 1.0 | 1.1 | 17.0 | 10.5 |
| BD2130J5050AHF | 2.1 - 3.0 | 2.0 | 0.08 x 0.05 (2 x 1.25) | 50 | 50 | 1.2 | 1.0 | 5.0 | 10.0 |
| BD2326L50200AHF | 2.2 - 2.6 | 2.0 | 0.06 x 0.03 (1.5 x 0.75) | 50 | 200 | 1.1 | 0.8 | 9 | 12 |
| BD2327N50100AHF | 2.3 - 2.7 | 1.0 | 0.04 x 0.04 (1 x 1) | 50 | 100 | 0.8 | 1.0 | 7.0 | 17.0 |
| BD2425J50100AHF | 2.4 - 2.5 | 2.0 | 0.08 x 0.05 (2 x 1.25) | 50 | 100 | 0.8 | 0.5 | 5.0 | 14.0 |
| BD2425J50200AHF | 2.4 - 2.5 | 2.0 | 0.08 x 0.05 (2 x 1.25) | 50 | 200 | 0.8 | 0.5 | 6.0 | 9.5 |
| BD2425N100ATI | 2.4 - 2.5 | 1 | 0.04 x 0.04 (1 x 1) | 50 | Matched | 0.8 | — | — | 17.3 |
| BD2425N50100AHF | 2.4 - 2.5 | 1.0 | 0.04 x 0.04 (1 x 1) | 50 | 100 | 0.7 | 0.6 | 3.0 | 18.0 |
| BD2425N50200AHF | 2.4 - 2.5 | 1.0 | 0.04 x 0.04 (1 x 1) | 50 | 200 | 0.7 | 1.0 | 6.0 | 21.0 |
| BD2425N5050AHF | 2.4 - 2.5 | 0.8 | 0.04 x 0.04 (1 x 1) | 50 | 50 | 0.9 | 0.9 | 7.0 | 15.0 |
| BD2425N5075AHF | 2.4 - 2.5 | 1.0 | 0.04 x 0.04 (1 x 1) | 50 | 75 | 0.9 | 0.9 | 3.0 | 14.0 |
| BD2425N50ATI | 2.4 - 2.5 | 1.0 | 0.04 x 0.04 (1 x 1) | 50 | 127+j34 | 0.6 | x | x | 13.0 |
| BD2425NCSR | 2.4 - 2.5 | 1.0 | 0.04 x 0.04 (1 x 1) | 50 | Matched | 1.0 | 0.5 | 6.0 | 10.0 |
| BD2425NNRF | 2.4 - 2.5 | 1.0 | 0.04 x 0.04 (1 x 1) | 50 | Matched | 1.3 | x | x | 10.2 |
| BD2425P50100AHF | 2.4 - 2.5 | 1.0 | 0.04 x 0.04 (1 x 1) | 50 | 100 | 0.9 | 1.5 | 9.0 | 19.0 |
| BD2425P5075AHF | 2.4 - 2.5 | 1.0 | 0.04 x 0.04 (1 x 1) | 50 | 75 | 1.2 | 1.6 | 7.1 | 11.0 |
| BD3150N50100AHF | 3.1 - 5.0 | 1.0 | 0.04 x 0.04 (1 x 1) | 50 | 100 | 0.7 | 1.3 | 7 | 16 |
| BD2425N50AIR | 4.8 - 5.9 | 1.0 | 0.04 x 0.04 (1 x 1) | 50 | 50 | 0.7 | 1.2 | 7.0 | 16.0 |
| BD4859N50100AHF | 4.8 - 5.9 | 1.0 | 0.04 x 0.04 (1 x 1) | 50 | 100 | 0.6 | 1.5 | 8 | 15 |
| BD4859N50150AHF | 4.8 - 5.9 | 1.0 | 0.04 x 0.04 (1 x 1) | 50 | 150 | 0.6 | 1.4 | 10.0 | 12.0 |
| BD4859N5050AHF | 4.8 - 5.9 | 1.0 | 0.04 x 0.04 (1 x 1) | 50 | 50 | 0.7 | 1.2 | 7.0 | 16.0 |

Data current as of: January, 2012

# Xinger® Subminiature Components Selection Matrix

## 3dB Hybrid Couplers

| Part no. | Freq. (GHz) | Power (W) | Size inches/ (mm) | Ins. Loss (dB) | Amp. Bal. (dB) | Phase Bal. (degrees) | RL Unbal. (dB) | Isolation |
|---|---|---|---|---|---|---|---|---|
| C0810J5003AHF | 0.8 - 1.0 | 4.0 | 0.08 x 0.05 (2x1.25) | 0.6 | 0.9 | 7.0 | 21.0 | 18.0 |
| C1720J5003AHF | 1.7 - 2.0 | 4.0 | 0.08 x 0.05 (2x1.25) | 0.4 | 1.0 | 5.0 | 21.0 | 24.0 |
| C2023J5003AHF | 2.3 - 2.7 | 4.0 | 0.08 x 0.05 (2x1.25) | 0.4 | 0.8 | 6.0 | 18.0 | 21.0 |
| C2327J5003AHF | 2.3 - 2.7 | 4.0 | 0.08 x 0.05 (2x1.25) | 0.4 | 0.9 | 8.0 | 15.0 | 18.0 |
| C3337J5003AHF | 3.3 - 3.7 | 4.0 | 0.08 x 0.05 (2x1.25) | 0.3 | 1.0 | 7.0 | 15.0 | 18.0 |

## Directional Couplers

| Part no. | Freq. (GHz) | Power (W) | Size inches/ (mm) | Ins. Loss (dB) | Mean Coupling (dB) | RL Unbal. (dB) | Directivity (dB) |
|---|---|---|---|---|---|---|---|
| DC0710J5010AHF | 0.7 - 1.0 | 2.0 | 0.08 x 0.05 (2x1.25) | 0.21 | 10.9 | 17.5 | 20.1 |
| DC0710J5020AHF | 0.7 - 1.0 | 2.0 | 0.08 x 0.05 (2x1.25) | 0.22 | 19.5 | 21.4 | 17.5 |
| DC1722J5010AHF | 1.7 - 2.2 | 2.0 | 0.08 x 0.05 (2x1.25) | 0.16 | 10.8 | 19.4 | 16.6 |
| DC1722J5015AHF | 1.7 - 2.2 | 2.0 | 0.08 x 0.05 (2x1.25) | 0.22 | 15.2 | 29.2 | 22.6 |
| DC1722J5020AHF | 1.7 - 2.2 | 2.0 | 0.08 x 0.05 (2x1.25) | 0.17 | 19.9 | 22.5 | 21.4 |
| DC2337J5010AHF | 2.3 - 3.7 | 2.0 | 0.08 x 0.05 (2x1.25) | 0.21 | 10.8 | 22.8 | 21.1 |
| DC2337J5020AHF | 2.3 - 3.7 | 2.0 | 0.08 x 0.05 (2x1.25) | 0.14 | 21.3 | 21.2 | 14.9 |
| DC4759J5020AHF | 4.7 - 5.9 | 2.0 | 0.08 x 0.05 (2x1.25) | 0.17 | 19.7 | 10.3 | 10.3 |

## RF Crossovers

| Part no. | Freq. (GHz) | Power (W) | Size inches/ (mm) | Unbal. Port Imp. (Ω) | Bal. Port Imp. (Ω) | Ins. Loss (dB) | RL Unbal. (dB) |
|---|---|---|---|---|---|---|---|
| J0060L5050A00 | 0.0 - 6.0 | 2.0 | 0.06 x 0.03 (1.5x0.75) | 50 | 50 | 0.1 | 18.0 |
| X0060L5050AHF | 0.0 - 6.0 | 2.0 | 0.06 x 0.03 (1.5x0.75) | 50 | 50 | 0.1 | 19.0 |
| J0060L7575A00 | 0.0 - 2.5 | 2.0 | 0.06 x 0.03 (1.5x0.75) | 50 | 50 | 0.13 | 22.0 |
| X0060L7575AHF | 0.0 - 2.5 | 2.0 | 0.06 x 0.03 (1.5x0.75) | 50 | 50 | 0.1 | 21.0 |

Data current as of: January, 2012

# Xinger® Subminiature Components Selection Matrix

## Power Dividers

| Part no. | Freq. (GHz) | Power (W) | Size inches/ (mm) | Unbal. Port Imp. (Ω) | Bal. Port Imp. (Ω) | Ins. Loss (dB) | Amp. Bal. (dB) | Phase Bal. (degrees) | RL Unbal. (dB) | Isolation |
|---|---|---|---|---|---|---|---|---|---|---|
| PD0409J7575S2HF | 0.4 - 0.9 | 2.0 | 0.08 x 0.05 (2 x 1.25) | 75 | 75 | 0.6 | 0.6 | 3.0 | 10.0 | 8.2 |
| PD0810J5050S2HF | 0.8 - 1.0 | 2.0 | 0.08 x 0.05 (2 x 1.25) | 50 | 50 | 0.6 | 0.6 | 4.0 | 14.0 | 17.0 |
| PD0922J5050D2HF | 0.9 - 2.2 | 2.0 | 0.08 x 0.05 (2 x 1.25) | 50 | 50 | 0.8 | 0.5 | 3.0 | 9.3 | 10.5 |
| PD0922J5050S2HF | 0.9 - 2.2 | 2.0 | 0.08 x 0.05 (2 x 1.25) | 50 | 50 | 0.7 | 0.3 | 3.0 | 10.4 | 9.0 |
| PD0922J7575D2HF | 0.9 - 2.2 | 2.0 | 0.08 x 0.05 (2 x 1.25) | 75 | 75 | 1.0 | 0.7 | 3.0 | 9.5 | 14.0 |
| PD1722J5050D2HF | 1.7 - 2.2 | 2.0 | 0.08 x 0.05 (2 x 1.25) | 50 | 50 | 0.7 | 0.3 | 3.0 | 11.0 | 17.0 |
| PD1722J5050S2HF | 1.7 - 2.2 | 2.0 | 0.08 x 0.05 (2 x 1.25) | 50 | 50 | 0.8 | 0.3 | 3.0 | 10.0 | 15.0 |
| PD1722J5050S3HF | 1.7 - 2.2 | 2.0 | 0.08 x 0.05 (2 x 1.25) | 50 | 50 | 1.2 | 1.1 | 12.0 | 8.9 | 14.0 |
| PD2328J5050S2HF | 2.3 - 2.8 | 2.0 | 0.08 x 0.05 (2 x 1.25) | 50 | 50 | 0.5 | 0.3 | 2.0 | 15.0 | 17.0 |
| PD2425J5050S2HF | 2.4 - 2.5 | 2.0 | 0.08 x 0.05 (2 x 1.25) | 50 | 50 | 0.4 | 0.2 | 2.0 | 18.0 | 22.0 |
| PD2425N5050S2 | 2.4 - 2.5 | 0.5 | 0.04 x 0.04 (1 x 1) | 50 | 50 | 0.5 | 0.4 | 1.3 | 21.0 | 20.0 |
| PD3150J5050S2HF | 3.1 - 5.0 | 2.0 | 0.08 x 0.05 (2 x 1.25) | 50 | 50 | 1.3 | 0.4 | 2.0 | 6.8 | 13.0 |
| PD4859J5050S2HF | 4.8 - 5.9 | 2.0 | 0.08 x 0.05 (2 x 1.25) | 50 | 50 | 1.0 | 0.3 | 4.0 | 7.9 | 14.0 |

Data current as of: January, 2012

**Xinger® subminiature component sample kits are available from some authorized stocking distributors; call 800.411.6596 for details.**

**Visit www.anaren.com to learn more about Anaren's *other* components for wireless infrastructure, consumer electronics & other assorted applications!**

Anaren Integrated Radio (AIR) modules for low-power RF applications

High-power resistive components for military & instrumentation applications

Low-cost wireless resistive components

Subminiature, high-frequency resistors

Xinger®-III brand couplers, baluns, power dividers & more

Anaren®

What'll we think of next?®

| | |
|---|---|
| **Website** | **www.anaren.com** |
| **USA/Canada** | **(315) 432-8909** |
| **Toll free** | **(800) 411-6596** |
| **Europe** | **+44 2392-232392** |

a photograph of the impedance transformer. The characteristic impedance $Z_0$ of the transformer is given by $Z_0 = (Z_{c1} Z_{c2})^{0.5}$ where $Z_{c1}$ and $Z_{c2}$ are the source and load impedance, respectively.[9] In this work, $Z_{c1}$ and $Z_{c2}$ are 12 and 5 Ω, respectively and $Z_0$ is 7.7 Ω. For a $Z_0$ of 7.7 Ω, $l_c$ is 10 µm. For a center frequency of 7 GHz, the length of the λ/4 transformer, which was determined from Figure 2, is 0.6 mm, and the line width, W is 70 µm.

The size of the transformer employing CCTL is 0.042 mm, which is 0.95 percent of the size of a transformer fabricated using a conventional microstrip line on a MMIC.[9] In other words, if λ/4 transformer with a $Z_0$ of 7.7 Ω is fabricated by a conventional microstrip line on a GaAs substrate, the line width, W and a length of λ/4 are 1,170 µm and 3.77 mm, respectively, and its size is 4.41 mm$^2$. ***Figure 9*** shows the measured return loss

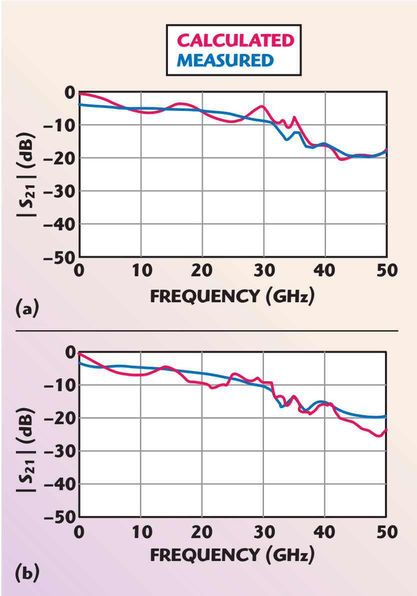


▲ *Fig. 7 Insertion loss of the CCTL structure (a) $l_c$ = 20 µm and (b) $l_c$ = 30 µm.*

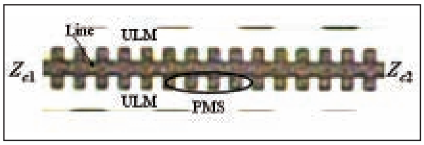


▲ *Fig. 8 Photograph of the impedance transformer using a CCTL structure.*

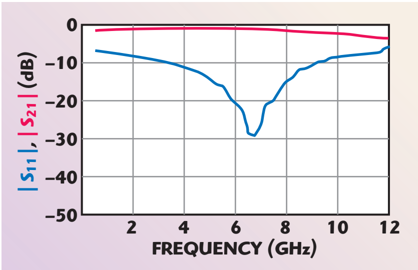


▲ *Fig. 9 RF characteristics of the impedance transformer using a CCTL structure.*

$S_{11}$ and insertion loss $S_{21}$ of the transformer. The insertion and return loss were measured at a port impedance of 50 Ω and was normalized to source and load impedance, $Z_{c1}$ and $Z_{c2}$. As shown in this figure, a good transformer RF performance can be observed. The return and insertion loss are 28 and 1.4 dB, respectively, at a center frequency of 7 GHz, and return loss values better than 10 dB and insertion loss values of 1.5 ± 0.5 dB in the 3.2 to 9.2 GHz range.

## CONCLUSION

In this work, the basic characteristics of a CCTL structure were investigated for the development of miniaturized on-chip passive components. According to the results, the CCTL

Microsemi

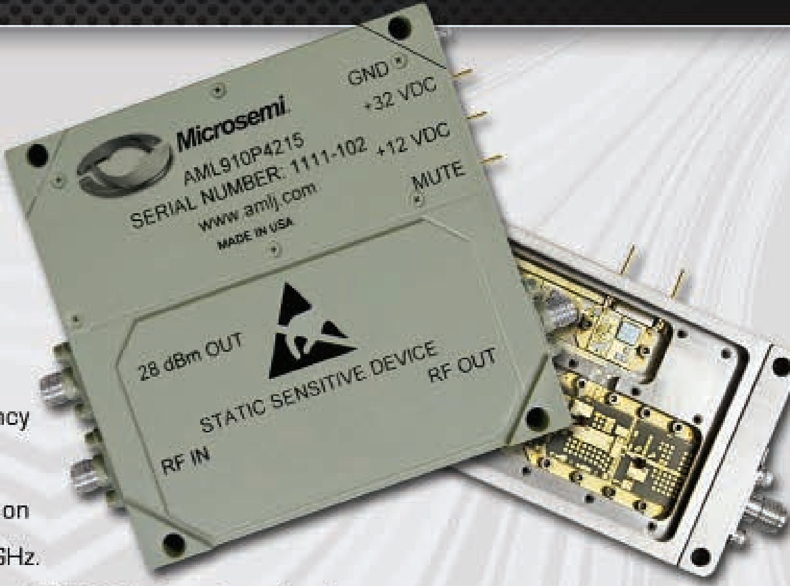


Our Gallium Nitride (GaN) amplifier products employ the latest semiconductor technologies and present the very best performance to our customers. Gallium Nitride (GaN) technology, coupled with our chip and wire die level expertise maximize power added efficiency and high power density characteristics of GaN in small convenient packages. Multi-octave amplifiers and application specific narrow band amplifiers cover frequencies to 18 GHz. GaN amplifiers operate with voltages between +28VDC to +50VDC (design dependent). Catalog designs offer power levels up to 100 Watts; custom designs to 200 Watts are available.

# GaN Power Amplifiers

| Model Number | Frequency (GHz) | Gain (dB min) | Psat (dBm min) | Psat (dBm typ) | Psat (Watts typ) | Voltage (V) Current (A) | PAE | ECCN |
|---|---|---|---|---|---|---|---|---|
| AML056P4013 | 0.5 - 6.0 | 40 | 35 | 36 | 4 | 28V, 0.75A | 22% | EAR99 |
| AML056P4014 | 0.5 - 6.0 | 40 | 37 | 38 | 6 | 28V, 1.0A | 20% | EAR99 |
| AML056P4511 | 0.5 - 6.0 | 45 | 39 | 40 | 10 | 28V, 1.3A | 25% | EAR99 |
| AML056P4512 | 0.5 - 6.0 | 45 | 43 | 44 | 25 | 40V, 2.7A | 23% | EAR99 |
| AML13P5013 | 1.0 - 3.0 | 50 | 46 | 47 | 50 | 28V, 4.8A | 25% | EAR99 |
| AML26P4011 | 2.0 - 6.0 | 40 | 40 | 41 | 12 | 28V, 1.5A | 30% | EAR99 |
| AML26P4012 | 2.0 - 6.0 | 45 | 43 | 44 | 25 | 28V, 3.0A | 30% | EAR99 |
| AML26P4013 | 2.0 - 6.0 | 50 | 46 | 47 | 50 | 28V, 6.0A | 30% | EAR99 |
| AML59P4512 | 5.5 - 9.0 | 45 | 45 | 46 | 40 | 28V, 4.0A | 35% | 3A001.b.4.b |
| AML59P4513 | 5.5 - 9.0 | 45 | 48 | 49 | 80 | 28V, 8.0A | 35% | 3A001.b.4.b |
| AML910P4213 | 9.9 - 10.7 | 43 | 37 | 38 | 6 | 32V, 0.5A | 30% | EAR99 |
| AML910P4214 | 9.9 - 10.7 | 43 | 39 | 40 | 10 | 32V, 0.8A | 30% | EAR99 |
| AML910P4215 | 9.9 - 10.7 | 46 | 41.5 | 42 | 15 | 32V, 1.3A | 30% | EAR99 |
| AML910P4216 | 9.9 - 10.7 | 46 | 42 | 43 | 20 | 32V, 1.3A | 30% | 3A001.b.4.b |
| AML811P5011 | 7.8 - 11.0 | 45 | 43 | 44 | 25 | 28V, 2.8A | 30% | 3A001.b.4.b |
| AML811P5012 | 7.8 - 11.0 | 50 | 46 | 47 | 50 | 28V, 5.5A | 30% | 3A001.b.4.b |
| AML811P5013 | 7.8 - 11.0 | 50 | 48 | 49 | 80 | 28V, 11.5A | 25% | 3A001.b.4.b |
| AML1416P4511 | 14.0 - 16.0 | 45 | 42 | 43 | 20 | 35V, 3.2A | 18% | ITAR |
| AML1416P4512 | 14.0 - 16.0 | 45 | 45 | 46 | 40 | 35V, 6.2A | 18% | ITAR |
| AML618P4014 | 6.0 - 18.0 | 40 | 39 | 40 | 10 | 32V, 2.8A | 12% | ITAR |
| AML618P4015 | 6.0 - 18.0 | 40 | 42 | 43 | 20 | 32V, 4.9A | 12% | ITAR |
| AML218P4012 | 2.0 - 18.0 | 35 | 37 | 38 | 6 | 32V, 1.5A | 13% | ITAR |
| AML218P4011 | 2.0 - 18.0 | 40 | 39 | 40 | 10 | 32V, 2.8A | 12% | ITAR |
| AML218P4013 | 2.0 - 18.0 | 38 | 42 | 43 | 20 | 32V, 4.9A | 12% | ITAR |

Features: Fast TTL On/Off (Rise/Fall < 100ns);
Wide operating temperature range: -54° to +85°C (hermetically sealed)

Microsemi Corporation | 1000 Avenida Acaso | Camarillo, CA 93012
Tel: 805-388-1345 | Fax: 805-484-2191 | Email: sales@amlj.com | www.amlj.com

structure showed short wavelength characteristics, due to its periodically added capacitance. The wavelength of the CCTL structure was only 10 percent of that of a conventional microstrip line on a MMIC. The CCTL structure showed a propagation constant much higher than a conventional microstrip line, due to the slow wave propagation on the periodic structure. Using the CCTL structure, a highly miniaturized impedance transformer was fabricated on a GaAs MMIC. The impedance transformer showed good RF performances in a broadband from S- to X-Band, and its size was 0.042 $mm^2$, which is 0.95 percent of the size of the transformer fabricated with a conventional microstrip line. The above results mean that the CCTL is a promising candidate for the development of highly miniaturized passive components on a MMIC. ■



## ACKNOWLEDGMENTS

This research was supported by the Basic Science Research Program through the National Research Foundation of Korea (NRF), funded by the Ministry of Education, Science and Technology (2010-0007452). This work was financially supported by the Ministry of Knowledge Economy (MKE) and the Korea Industrial Technology Foundation (KOTEF) through the Human Resource Training Project for Strategic Technology. This work was also partly supported by a Grant of the Korean Ministry of Education, Science and Technology (the Regional Core Research Program/Institute of Logistics Information Technology).

## References

1. A.A. Abidi, "RF-CMOS Comes of Age," *IEEE Journal of Solid State Circuits*, Vol. 39, No. 4, April 2004, pp. 840-853.
2. J.R. Long, "Passive Components for Silicon RF and MMIC Design," *IEICE Transactions on Electronics*, Vol. E86-C, No. 6, June 2003, pp. 1022-1031.
3. Y. Yun, J.W. Jung, K.M. Kim, H.C. Kim, W.J. Chang, H.G. Ji and H.K. Ahn, "Experimental Study on Isolation Characteristics Between Adjacent Microstrip Lines Employing Periodically Perforated Ground Metal for Application to Highly Integrated GaAs MMICs," *IEEE Microwave and Wireless Components Letters*, Vol. 17, No. 10, October 2007, pp. 703-705.
4. Y. Yun, K.S. Lee, C.R. Kim, K.M. Kim and J.W. Jung, "Basic RF Characteristics of the Microstrip Line Employing Periodically Perforated Ground Metal and Its Application to Highly Miniaturized On-Chip Passive Components on GaAs MMIC," *IEEE Transactions on Microwave Theory and Techniques*, Vol. 54, No. 10, October 2006, pp. 3805-3817.
5. Y. Yun, "A Short Wavelength Comb-Type Capacitive Transmission Line for Application to Miniaturized On-Chip Passive Components on MMIC," *Electronics Letters*, Vol. 46, No. 5, March 2010, pp. 352-353.
6. D. Ahn, J.S. Park, C.S. Kim, J. Kim, Y. Qian and T. Itoh, "A Design of Low Pass Filter Using the Novel Microstrip Defected Ground Structure," *IEEE Transactions on Microwave Theory and Techniques*, Vol. 49, No. 1, January 2001, pp. 86-93.
7. A. Lai and T. Itoh, "Microwave Composite Right/Left-handed Metamaterials and Devices," *Proceedings of the 2005 Asia-Pacific Microwave Conference*, pp. 31-34.
8. J. Gao and L. Zhu, "Per-Unit-Length Parameters of 1-D CPW Metamaterials with Simultaneously Series-C and Shunt-L Loading," *Proceedings of the 2005 Asia-Pacific Microwave Conference*, pp. 39-42.
9. D.M. Pozar, *Microwave Engineering*, Addison-Wesley, Reading, MA, 1990.


# *Smart* RF SWITCH MATRIX

## DC to 18 GHz from $385^{00}

***Increased efficiency for almost any electronics lab.***
Nothing beats a Mini-Circuits Switch Matrix for quick production or design lab setups. Our innovative, stand-alone GUI is so user-friendly, you'll put it to work within minutes! Highly portable, and compatible with most lab software,* these models also add capabilities to legacy systems with ease—for full automation, step-by-step control, or remote operation via the internet.

To meet different needs, we offer different models containing up to four 50 Ω SPDT switches, all of which are absorptive in the "off" state. Whichever model you choose, and wherever you use it, you'll enjoy the quick expansion of multi-unit and multi-parameter capabilities, and easily configured test automation that simply helps you get more done more quickly, and at a lower cost, than ever before.

***Outstanding performance, unmatched reliability.***
Very low insertion loss (≤0.3 dB typ.), excellent isolation (>66 dB typ.), and low VSWR (1.2:1 typ.) across the full DC-18 GHz frequency range mean accurate data, with fewer false rejects and less retesting. The rugged aluminum cases house our patented mechanical switches—the only ones available anywhere, at any price, that offer up to 10 years and 100 million cycles of guaranteed performance.† Just go to minicircuits.com for technical specifications, performance data, pricing, and real-time availability, and *consider how much time and money you'll save* with faster setup, quick automation, and results you can rely on, day after day and year after year!

* See data sheet for an extensive list of compatible software.

† The mechanical switches internal to each model are offered with an optional 10 year extended warranty. Agreement required, see data sheets on our website for terms and conditions. Switches protected by patents 5,272,458 6,650,210 6,414,577 7,633,361 7,843,289 and additional patents pending.

*Mini-Circuits...we're redefining what VALUE is all about!*

**Mini-Circuits®**
*ISO 9001 ISO 14001 AS 9100*

P.O. Box 350166, Brooklyn, New York 11235-0003 (718) 934-4500 Fax (718) 332-4661

YONI2® ***The Design Engineers Search Engine*** *finds the model you need, Instantly* • For detailed performance specs & shopping online see **minicircuits.com**

U.S. Patents 7739260, 7761442

***IF/RF MICROWAVE COMPONENTS***

# MIMO Beamforming and Its Impact on Testing TD-LTE

Recently, both wireless and business media have cast a spotlight on TD-LTE. At a conceptual level, TD-LTE is easily understood. It is simply LTE with uplink and downlink multiplexed in the time domain rather than the frequency domain. The result is an LTE system that can be realized in a single frequency band as opposed to the paired bands required in FDD-based LTE. The most immediate and obvious consequence of TD-LTE is that LTE can be deployed by operators who do not own paired frequency bands. To be more specific, it gives WiMAX and TD-SCDMA licensees a path to LTE deployment.

Just as TD-LTE solves a problem for many operators, another wireless innovation solves a separate problem for the entire industry: Multiple-Input Multiple-Output (MIMO) antenna techniques offer faster data rates and better system capacity, without expending resources in the time or frequency domains. In an m×n MIMO system (one using m transmitting antenna elements and n receiving antenna elements), the theoretical maximum data rates are limited by the smaller of {m, n}. However, larger numbers of transmitting elements can improve system coverage and quality by improving system SNR, leading to growth in the study of 8×n MIMO systems, where each base station is equipped with eight antenna elements.

None of this is a surprise to *Microwave Journal* readers, but the marriage of multiple antenna techniques and time-domain based uplink/downlink multiplexing results in an interesting and useful attribute: since the uplink and downlink share a single frequency band, uplink channel estimation can be used to make reasonable assumptions regarding downlink channel characteristics. The TD-LTE uplink and downlink are said to be "characteristically identical".

This channel reciprocity leads to a way to improve both coverage and system quality: MIMO beamforming. While MIMO beamforming is not specific to TD-LTE, channel reciprocity in a single uplink/downlink frequency provides advantages that make beamforming attractive in TD-LTE deployments.

## BEAMFORMING FUNDAMENTALS

The term "beamforming" is sometimes used without qualification, which can cause confusion. Technically, beamforming can be as simple as beam steering, where two or more antennas radiate the same signal with controlled delays or phase shifts creating directed lobes of constructive interference (see ***Figure 1***).

The beamforming used in TD-LTE systems is a somewhat more complex proposition, in part because of the mobile nature of terminal devices. A technique called Eigen beamforming uses information about the RF channel to statistically weight amplitude and phase parameters of the transmitting antenna elements. While Eigen beamforming is not the most calculation-intensive type of beamforming (a method called Maximum Ratio Transmission performs the same types of weighting but on a per-subcarrier basis), the fact that it is being used in high-element count 8×n MIMO systems makes it a challenging proposition, both in the implementation and verification stages of system development.

Kang Chen
*Spirent Communications, Sunnyvale, CA*

# PON POWER

optical node
RF amplifier


## M/A-COM TECH FTTX AMPLIFIERS

**Delivering an integrated solution for optical node and passive optical network (PON) applications**

| Part Number | MAAM-008863 | MAAM-010333 | MAAM-010361 |
|---|---|---|---|
| **FTTx Amplifiers** | | | |
| Amplifier Stages | 3 | 2 | 3 |
| Package (PQFN) | 4x4 mm, 24-lead | 4x4 mm, 24-lead | 4x6 mm, 32-lead |
| Gain 50 MHz | 37 dB | 29 dB | 37.5 dB |
| 870 MHz | 36 dB | | |
| 1000 MHz | 35 dB | 34 dB | 42 dB |
| Gain Tilt | no tilt | 5 dB, Vagc=3V<br>7 dB, Vagc=0V | 4 dB |
| Gain Control Range | 25 dB | 27 dB | 34 dB |
| Gain Voltage Control Range | 0 to 3 V | 0 to 3 V | 0 to 3 V |
| Output Return Loss | 16 dB | 18 dB | 15 dB |
| EIN | 4.8 pA/rtHz | 3.2 pA/rtHz | 3.8 pA/rtHz |
| CNR@ Max. Gain | 47 dB | 50 dB | 48 dB |
| Pout | 20 dBmV/ch | 24 dBmV/ch | 26 dBmV/ch |
| CTB | -61 | -68 | -65 |
| CSO | -62 | -65 | -70 |
| Current | 220 mA | 280 mA | 350 mA |
| Voltage | 5 V | 5 V | 5 V |
| Optical Input Power Range | -8 dBm to +2 dBm | -8 dBm to +2 dBm | -8 dBm to +2 dBm |

M/A-COM Tech announces our new MAAM-010333 optical node video amplifier. It provides high gain, low equivalent input noise (EIN), and low distortion for optical node and PON applications. The MAAM-010333 is fabricated using our GaAs pHEMT technology in a lead-free 4 mm, 24-lead package. It requires a minimum number of off-chip components, resulting in a highly integrated, low-cost solution.

Our MAAM-010333 FTTx amplifier features:

- Low equivalent input noise (EIN): 3.2 pA/rtHZ
- High linearity with CSO of -65 dBc
- 75 Ohms output impedance
- Single +5 V supply
- CNR of 50 dB at max gain

**SIGN UP FOR NEWS**

**To sign up for more news and new product announcements, visit macomtech.com**

Get more from your PON

MACOM
Technology Solutions
THE FIRST NAME IN MICROWAVE®

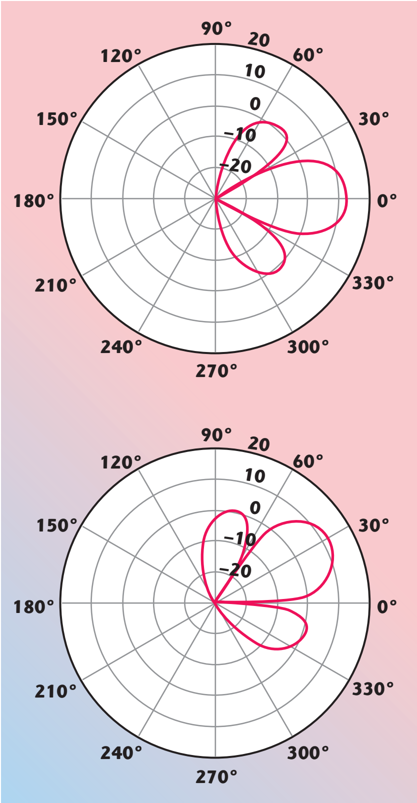


Fig. 1 *Lobes created by simple beam steering.*

## TD-LTE AND 8×N MIMO

Most planned TD-LTE deployments are designed around transmitting antennas with eight antenna elements. In these systems, four antenna elements, separated by distance, are physically oriented at one angle. Another four elements are located so that each is concentric with one of the first four, and each of these latter four is oriented at a right angle to its partner element, as shown in ***Figure 2***.

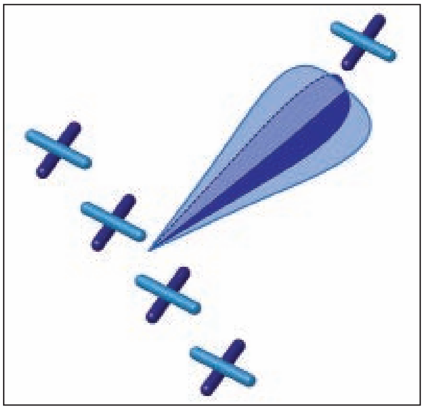

*Fig. 2 An 8 × 2 beamforming system creates orthogonally polarized beams.*

Each group of four similarly oriented elements forms a beam that can be aimed in a specific direction. Correlation between these four radio links is purposely high. The two orthogonally polarized beams exhibit low correlation with each other, acting somewhat like a 2xn MIMO system and therefore able to transmit multiple layers or data streams. The system therefore implements the data-rate maximizing benefits of a MIMO system, while taking advantage of beamforming to optimize signal strength in specific directions. This is commonly known as a dual-layer beamforming system, where each layer can represent a separate stream of data.

A dual-layer MIMO beamforming system can be used as either a single-user MIMO system (SU-MIMO), where both data streams are assigned to a single user equipment (UE), or a multi-user (MU-MIMO) system, where each stream is assigned to a separate UE. This provides tremendous flexibility to the network operator, who can choose to deploy such a system, either to maximize coverage or to maximize per-user data throughput.

## HOW BEAMFORMING WORKS

In any beamforming system, it is required that the system can estimate the direction of the targeted UE. In FDD systems, this is a function of feedback from the UE in the form of the Precoding Matrix Indicator (PMI), but once again, the channel reciprocity of TD-LTE eliminates this requirement. Instead, the UE sends a channel-sounding signal to the base station. The base station then estimates the UE's direction of arrival (DoA) by examining the relative phase difference between the co-polarized antennas. Note that while this estimation is done in the uplink, the base station uses channel reciprocity and can transmit in the downlink based on the estimation of the uplink.

Next, based on the estimated DoA, the base station dynamically adjusts the "antenna weight" (relative amplitude and phase) of each element of the antenna array so as to steer the beams towards desired users, and/or to steer nulls in the direction of sources of unwanted interference. ***Figure 3*** shows the basic concept.

The above scenario is actually simple beam steering. Eigen beamforming adds some intelligent processing,

but the desired fundamental effect is the same: the system estimates downlink channel parameters by taking advantage of reciprocity and adjusts antenna weights accordingly.

## TESTING BEAMFORMING

Many of the challenges to creating realistic MIMO test beds in the lab have previously been identified and re-

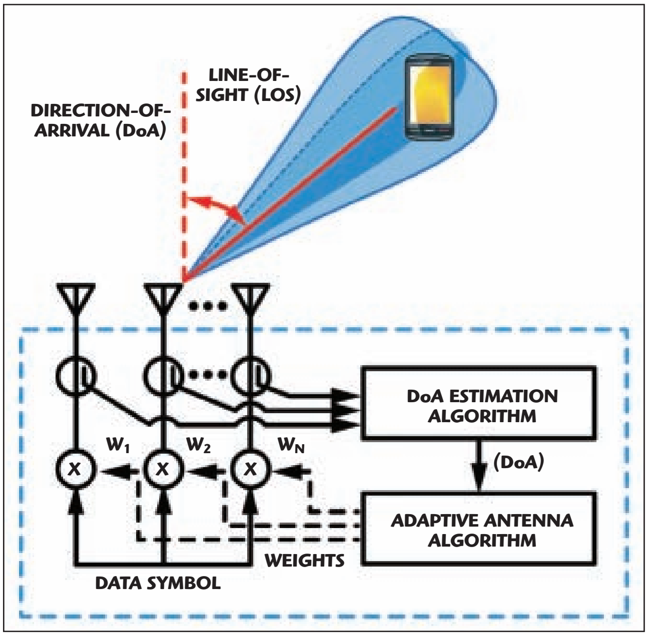


▲ *Fig. 3 Adaptive beamforming system.*

solved. Because of the spatial nature of both beams and MIMO link components, lab-based testing must implement both proper polarization and realistic antenna patterns in order to create an effective testing environment.

TD-LTE adds a requirement beyond those used in simple MIMO testing: the uplink and downlink must be reciprocal in terms of fading as well as all transfer function characteristics. In the testing lab, this is not as straightforward as it may seem. Modern channel emulators are, by necessity, made up of unidirectional RF channels. Accurately emulating reciprocal channels requires a great deal of care in producing synchronized, accurately duplicated fading. A channel emulator that works very well for most testing may not be a good match for TD-LTE testing if it cannot produce nearly identical channel conditions in the uplink and downlink.

Another critical area of concern is phase accuracy and calibration. This seemingly arcane topic has generated a lot of work in recent months, leading to new advances in state-of-the-art lab-based RF channel emulation. In practice, phase alignment is affected by:

- adjusting the channel power level
- adjusting the signal to noise ratio
- changing channel models
- adjusting frequency
- power cycling

While SISO and non-beamforming MIMO systems are relatively insensitive to the slight phase shifts caused by these procedures, MIMO beamforming is especially susceptible to phase-related inaccuracies. ***Figure 4*** shows a

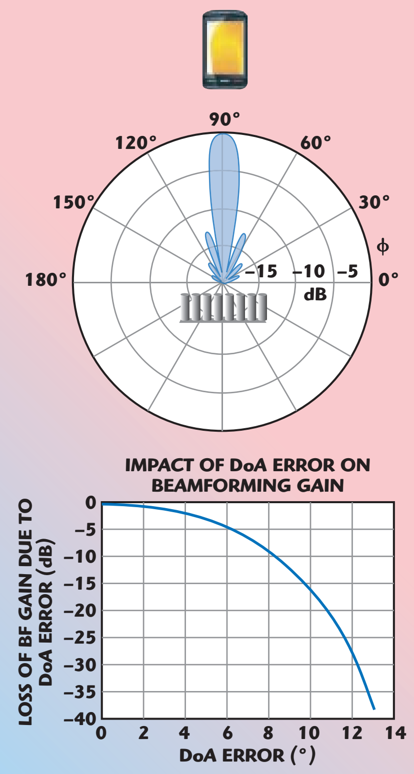


▲ *Fig. 4 Phase error and its impact on beamforming gain (eight-antenna linear array).*

radiation pattern of a typical eight-antenna uniform linear array with DoA degrees of error. An error of eight degrees results in 10 dB loss of beamforming gain; an error of 14 degrees will cause loss of the link.

Accurately testing MIMO beamforming therefore requires periodic phase calibration of the system. While it is possible to manually phase-calibrate a channel emulation system used for testing MIMO beamforming, the user can easily spend 5 to 8× more time calibrating than doing the testing. Even more importantly, manual phase-calibration requires the disconnection and re-connection of multiple RF connectors, which has an effect on long-term system stability.

The solution is automated phase calibration, which joins dynamic environments and geometric channel models as "must have" capabilities in modern channel emulators. Driven largely by fundamental research involving prototype 8×n MIMO beamforming systems, advanced channel emulation systems now offer automated phase calibration requiring no manual intervention. In an automatically phase-calibrated system, a quick button-push or mouse click fine-tunes the phase accuracy of each radio link used by the system without cable disconnection, and most importantly, ensures the validity and accuracy of test results.

## CONCLUSION

As TD-LTE attracts more attention (ABI Research recently estimated that half a million base stations will be deployed by 2016), new challenges become apparent, particularly in testing. Eight-antenna MIMO beamforming is a unique feature exploited by TD-LTE to offer both multiple layers and the directional aspects of beamforming.

In this article, the basic concept of TD-LTE was introduced and how MIMO beamforming works was explained. An analysis of error in testing beamforming was discussed and the single most critical test challenge (phase-related accuracy in the test bed) was identified. Finally, the article explored an effective solution to this challenge. ■

# Square Coaxial Lines and Materials Measurements

Coaxial lines are used to measure constitutive parameters of materials, permeability (μ) and dielectric constant (ε), with broad operating bandwidth and good mode control. Square lines are a special class that allows measurement of anisotropic materials, such as honeycomb, and periodic structures, such as pyramidal radiation absorbing material (RAM). These applications are presented (illustrated) based upon Damaskos Inc.'s experience as a provider of materials measurement solutions.

## GENERAL DESCRIPTION OF A SQUARE COAX SETUP

***Figure 1*** shows an example of a square coaxial line. Except for the shape of the inner and outer conductors, square lines are fundamentally similar to circular lines. Propagation in the TEM mode is desired, as the S-parameters of a material under test (MUT) are recorded in one- and two-port configurations. Both lines offer control of the impedance of the line via the ratio of conductor radii or edge dimensions; both are calibrated with similar standards; both require consideration of the upper useful frequency above which a change of mode may occur; both typically employ swept frequency CW measurements and subsequent processing in hardware or software to generate error corrected S-parameters; and both manipulate the S-parameters in the solution of the inverse problem for the μ and ε of the MUT by means of the same set of equations. However, the planar boundaries of the conductors of square lines can provide undistorted images of the MUT, and this can be a distinct advantage in the measurement of some materials that are spatially periodical.

▲ *Fig. 1 50 Ω, 6.0", two-port square coaxial line with square donut test sample.*

With a, the outer conductor dimension and b, the inner conductor dimension, the characteristic impedance of circular and square lines is:

Nickander J. Damaskos, Benuel J. Kelsall and James E. Powell, Jr.
*Damaskos Inc., Concordville, PA*

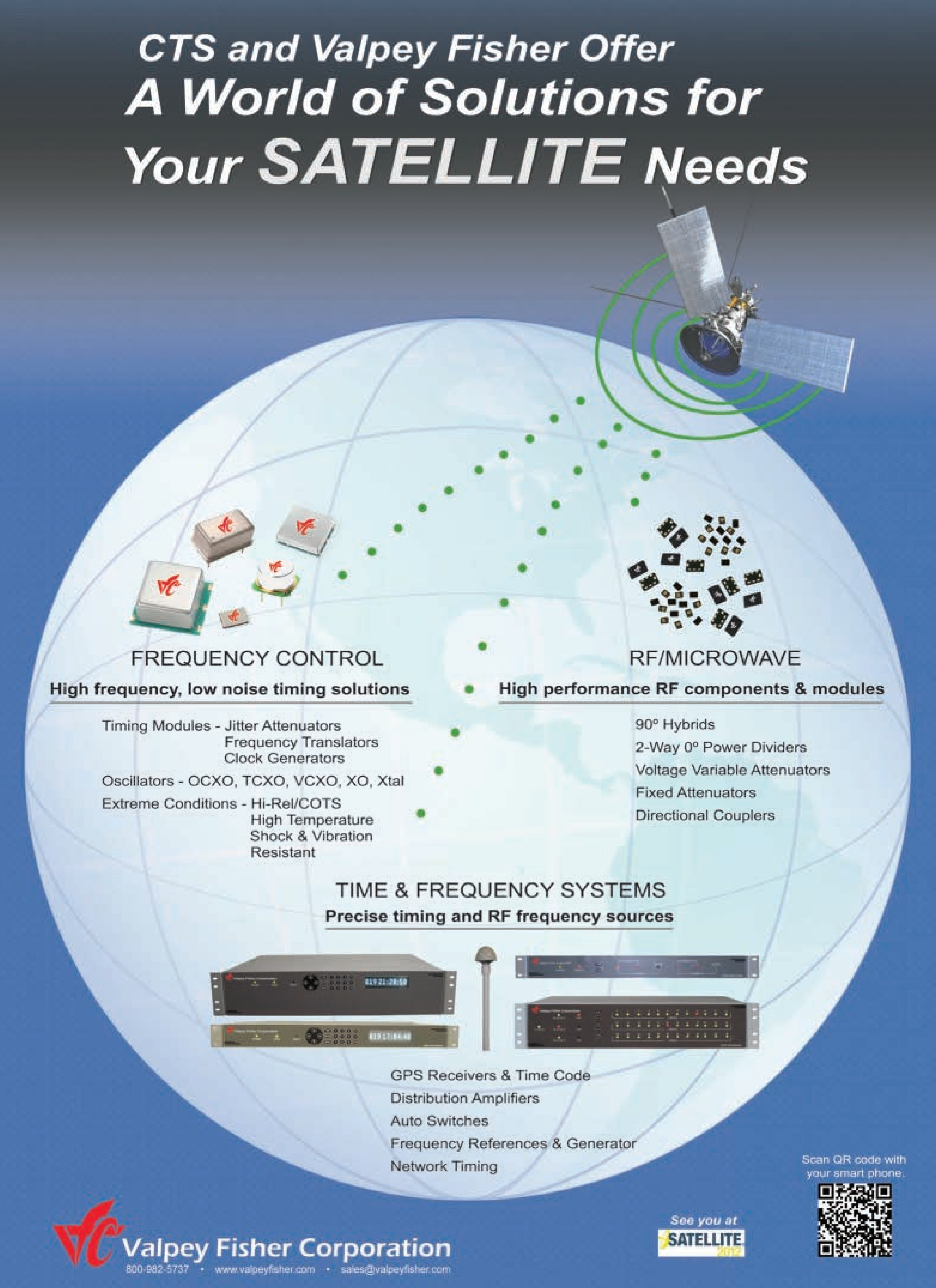
CTS and Valpey Fisher Offer
A World of Solutions for
Your SATELLITE Needs
FREQUENCY CONTROL
High frequency, low noise timing solutions
Timing Modules - Jitter Attenuators
Frequency Translators
Clock Generators
Oscillators - OCXO, TCXO, VCXO, XO, Xtal
Extreme Conditions - Hi-Rel/COTS
High Temperature
Shock & Vibration
Resistant
RF/MICROWAVE
High performance RF components & modules
90º Hybrids
2-Way 0º Power Dividers
Voltage Variable Attenuators
Fixed Attenuators
Directional Couplers
TIME & FREQUENCY SYSTEMS
Precise timing and RF frequency sources
GPS Receivers & Time Code
Distribution Amplifiers
Auto Switches
Frequency References & Generator
Network Timing
Scan QR code with your smart phone.
See you at
SATELLITE 2012
Valpey Fisher Corporation
800-982-5737 • www.valpeyfisher.com • sales@valpeyfisher.com


**TABLE I**

**REPRESENTATIVE SQUARE COAXIAL SIZES FOR MATERIAL MEASUREMENTS**

| DI Model | a (in) | b (in) | Zo (ohms) | Primary Function | First Higher Order Mode (GHz) |
|---|---|---|---|---|---|
| 100 | 10 | 4.0 | 50 | Mu Epsilon | 0.45 |
| | | 3.33 | 60 | Periodic Structures | |
| | | 6.67 | 20 | Anisotropic Materials | |
| 600 | 6 | 2.4 | 50 | Mu Epsilon | 0.75 |
| | | 2.0 | 60 | Periodic Structures | |
| | | 4 | 20 | Anisotropic Materials | |
| 300 | 3 | 1.2 | 50 | Mu Epsilon | 1.5 |
| | | 1.0 | 60 | Periodic Structures | |
| | | 2.0 | 20 | Anisotropic Materials | |

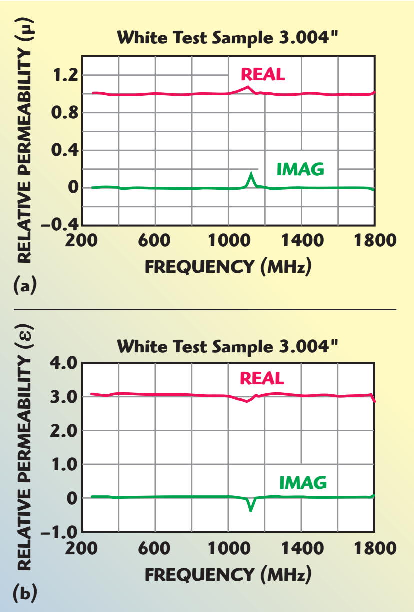


▲ *Fig. 2 μ (a) and ε (b) measurements in a 50 Ω, 10.0" square coaxial line.*

$Zo_{circ}\ (\Omega) = 60 \ln (b/a)$
$Zo_{sq}\ (\Omega) = 47.086\ (1-b/a) / (0.279+0.721b/a)$, within 1 percent for $b/a>0.25$.

***Table 1*** shows some typical square coaxial lines and their primary functions.

For 50 Ω circular lines, the cut-off frequency in GHz of the first interfering mode is 5.178/a where the diameter a is given in inches. For square coax lines, commonly used to measure material parameters, the first interfering mode is given in Table 1. Experience shows that, with carefully prepared isotropic materials samples and carefully constructed lines, the onset of moding is delayed well above these frequencies. See ***Figure 2***, for example, where the material parameters are obtained where the loss of the TEM mode is delayed well above the first possible interfering mode. The glitch at 1100 MHz may occur at a half-wavelength sample thickness for low loss materials.

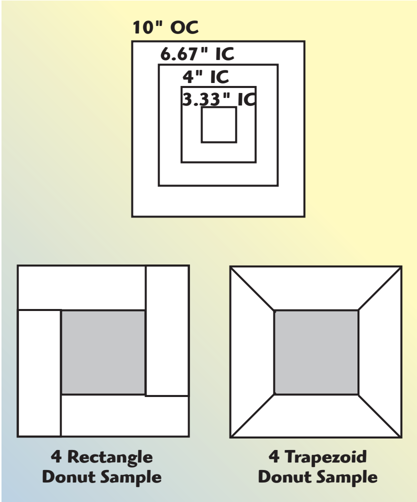


▲ *Fig. 3 Geometries of square coaxial lines and square donut samples.*

## SOME SPECIFIC USES

Some uses of square coaxial lines include the measurement of isotropic materials μ and ε; approximate measurement of anisotropic materials μ and ε; and measurement of transmission and reflection properties of periodic materials.

**Isotropic Materials:** For this class, sample preparation requires four well-machined rectangular blocks that make good contact to the conductors and also good contact to each other (see ***Figure 3***). Block to

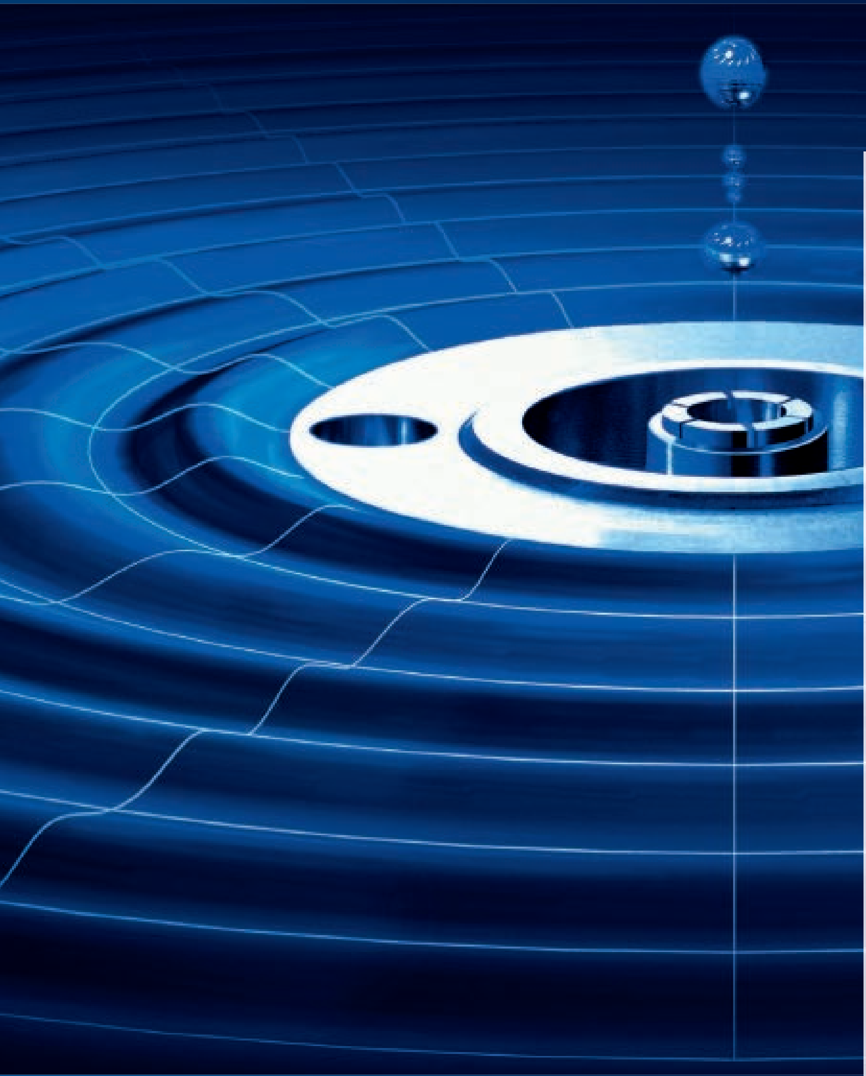

block gaps affect μ more so than ε. Any line impedance can be used.

**Anisotropic Materials:** In this instance four trapezoidal samples are prepared and again require good contact to conductors and to each other. Low impedance lines offer a better approximation to preserving the local anisotropy at the conductor corners. Honeycomb core is measured in this manner, where the modeling assumes three orthogonal directionally dependent components of ε. A low impedance waveguide is commonly employed to measure rectangular solid samples, which are simpler to prepare and more true to the modeling assumption. They become impractical to use below approximately a few hundred MHz. Square lines range lower in frequency with much smaller sample size.

**Periodic Materials:** The 3:1 edge ratio, 60 Ω lines, have eight equal area regions. When the material in each region is identical and has the proper symmetry, it is repeated infinitely in the orthogonal directions to the line. Measurement of the S-parameters of some frequency selective impedance sheets is illustrated in ***Figure 4***. The line is a two-port, 5.4" × 1.8", square coaxial line. The pyramidal RAM tester of ***Figure 5*** is a one-port, 6' × 6' × 60' long, shorted square coaxial line. For these applications, measurements down to long wavelengths are made possible using small quantities of material.

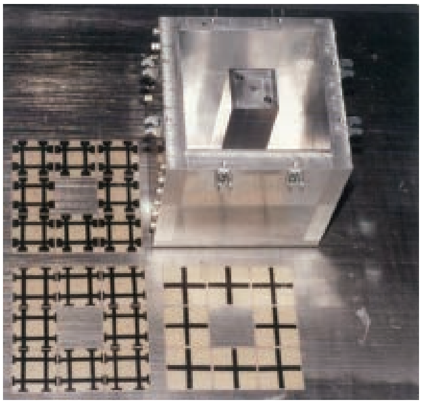

▲ *Fig. 4 Frequency selective surface samples for a 60 Ω, 5.4" × 1.8" square coaxial line.*

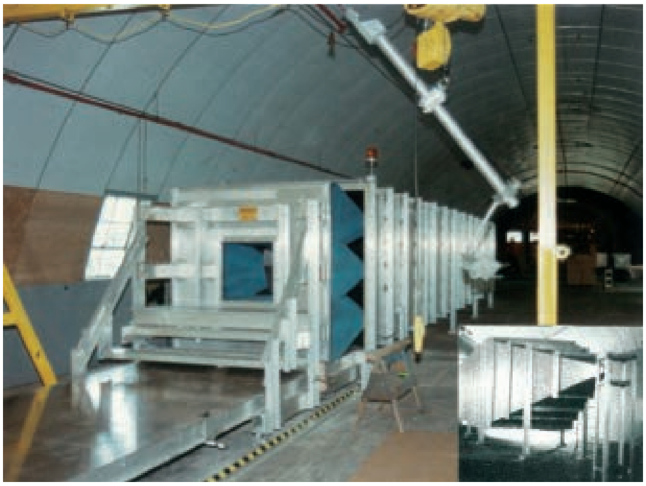

▲ *Fig. 5 60 Ω, 60' long, 6' square one-port square coaxial line for pyramidal RAM return loss measurements.*

## CONCLUSION

Several methods have been shown, in which square coaxial lines are employed to make materials properties measurements and made, for reference, comparisons to the use of the more familiar circular coax lines. Square lines permit good measurements of the properties of anisotropic materials and classes of periodic structures. They offer as high quality measurements of isotropic measurements as circular lines. ■

## References


1. J. Uher, J. Bornemann and U. Rosenberg, *Waveguide Components for Antenna Feed Systems*, Artech House Inc., Boston, MA, 1993.
2. S. Ramo, J. Whinnery and T. Van Duzer, *Fields and Waves in Communication Electronics*, John Wiley & Sons, New York, NY, 1967.



**Nickander J. Damaskos** *is President of Damaskos Inc. and Program Manager of R&D projects in microwave measurements of materials design.*

**Benuel J. Kelsall** *is Vice President of Damaskos Inc. and Manager of the microwave laboratory. He develops materials measuring setups and software.*

**James E. Powell, Jr.** *has a master's degree in mechanical engineering and has been with Damaskos Inc. for 25 years. He has been the Principal Designer of the various fabricated setups.*


# Multichannel Coax Rotary Joint / Slip Ring Assembly

**Up to 30 channels.**
Use MDL's rotary joint to transfer 3 RF signals and a 30-channel slip ring for flawless DC transmission. We make and assemble both components, so you'll save labor and testing costs. And you're assured of the highest quality and reliability from the leader in high quality cast components and waveguide packages.

**You've never been in better hands.**
Quality from CAD to crate, quick turnaround, and tight economy is what we're all about. Call an MDL specialist today at 800-383-8057 or do a little surfing of your own and visit us at **mdllab.com**.

| *RF Rotary Joint* | |
|---|---|
| *Two Channels:* | *14.4 – 15.4 Ghz* |
| *One Channel:* | *9.7 – 15.4 Ghz* |
| *VSWR:* | *<2.0:1* |
| *I.L.:* | *<2.0dB* |
| *Isolation:* | *>60 dB* |

| *Slip Ring Assembly* | |
|---|---|
| *Isolated Contacts:* | *30* |
| *Voltage:* | *20-300 Volts* |
| *Current:* | *.1 - 5 Amps* |

WAVEGUIDE CAST BENDS & TWISTS
WAVEGUIDE FEED ASSEMBLIES
MONOPULSE COMPARATORS
ROTARY JOINTS
MICROWAVE FILTERS
ROTARY SWITCHES
WAVEGUIDE TO COAX ADAPTERS
WAVEGUIDE PRESSURE WINDOWS
COMMERCIAL WAVEGUIDE ASSEMBLIES

MDL

*Microwave Development Laboratories, 135 Crescent Road, Needham Heights, MA 02494*
*V: 781-292-6680/6684   F: 781-453-8629   E-mail: mdlsales@mdllab.com   www.mdllab.com*

# A Portable USB-Controlled 2.45 GHz, 100 W Generator

Meeting the need for portable and compact laboratory equipment, Emblation's ISYSconnect is one of the smallest high power microwave generators on the market. Combining innovative design with improved functionality, this 2.45 GHz microwave system collects and manages all test data, making it an efficient desktop tool for research labs and test facilities.

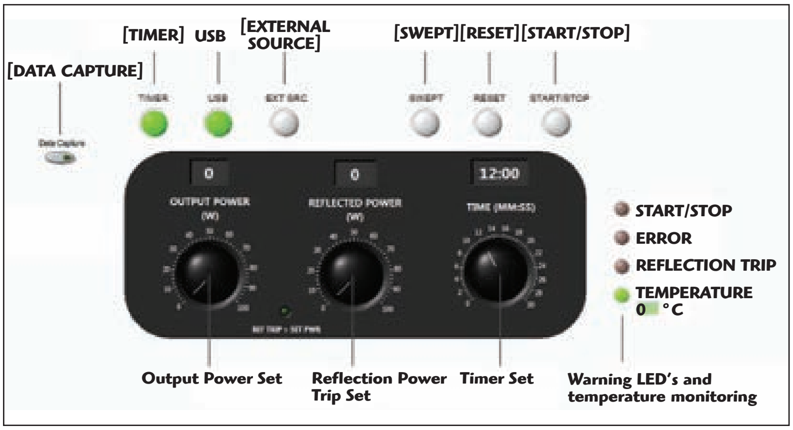


▲ *Fig. 1 The standard GUI with full system control.*

## LAPTOP OR PC CONTROL

Simple and comprehensive control is a major benefit – with no front panel controls, the ISYSconnect USB system is fully controlled via software, which is provided free of charge as a standalone executable file or a Labview VI. The Graphical User Interface (GUI) allows the user to control the output power setting in 5 W steps up to 100 W for accurate energy delivery.

The reflection power safety trip disables the microwave power when a set value of reflected power is reached (a feature that is controlled in 1 W steps). The time feature facilitates timed or continuous use. For custom specifications the software can be tailored to any user-specific needs.

## GRAPHICAL USER INTERFACE

The standard GUI for the ISYSconnect has been designed for ease of use, with an intuitive software-based interface and all controls on screen. The software controls the following modes of operation, which are shown in ***Figure 1***:

Emblation Microwave
*Alloa, Scotland, UK*

[START/STOP] – With this enabled, the system displays the real-time measurement of the output and reflected power as well as the amplifier temperature.

[SWEPT] – When used in stand-alone mode, this mode enables an improved accuracy measurement of real-time reflected power to be made and displayed. The ISYSconnect benefits from Emblation's patented safesweep reflection measurement solution, which reduces the reflection measurement error significantly when the input match of the device under test is non-optimal.

[TIMER] – Implemented when the user requires a predetermined test duration – time is clearly displayed on screen and microwave power will be disabled when the time duration has elapsed.

[EXTERNAL SOURCE] – For use in amplifier mode with the user's own signal generator via an SMA female connector on the rear panel.

[DATA CAPTURE] – When data is required for analysis this feature allows all the system parameters including settings, status and measurement to be easily captured with the option to download information to a .csv file.

## REAL TIME OPERATION

The ability to record, store and manage data is what makes the ISYSconnect such a valuable tool for researchers and technicians. By selecting data capture, all test information is automatically stored, saving time and ensuring accuracy. It is also simple to automate tests and work remotely, giving the user the opportunity to carry out multiple tasks or to safely conduct more dangerous or volatile tests. The ISYSconnect will operate at a distance in excess of 5 m between the USB connection and a microwave generator. Typical applications include microwave chemistry, microwave measurement, manufacturing, and product research and development.

## 2-IN-1 AMPLIFIER AND GENERATOR

The ISYSconnect can be used as both a microwave generator and as a standard amplifier. Using the latest technical advances in GaN on SiC solid-state technology and operating in Class AB mode, it generates microwave power in excess of 100 W CW at 2.45 GHz when used in the internally regulated standalone mode. In this mode and the swept mode, the output power can be varied in 5 W increments from 0 to 100 W using pulse width modulation techniques with power stability maintained within 5 percent of the set value.

When used as an amplifier, a small signal gain of up to 58 dB is typical. Using this mode of operation, the amplifier operates without any internal power regulation, allowing the user to have full control of the output power levels to achieve in excess of 100 W. A performance summary of the ISYSconnect can be seen in ***Figures 2*** and ***3***.

## EFFICIENCY

The efficient performance of the ISYSconnect is fundamental to a number of important features. The use of higher operating voltages on the GaN

# Quality, Performance and Reliability in Precision Coaxial Connectors


**ADAPTERS · CABLE CONNECTORS · RECEPTACLES · CUSTOM DESIGNS**

| Including These Connector Series | | | | | |
|---|---|---|---|---|---|
| 1.85mm | DC-65 GHz | 2.92mm | DC-40 GHz | 7mm | DC-18 GHz |
| 2.4mm | DC-50 GHz | 3.5mm | DC-34 GHz | SSMA | DC-40 GHz |

**ISO 9001:2008**

SGMC Microwave — The name to count on for Quality, Performance and Reliability! Please contact us today by Phone, Fax or Email.

SGMC MICROWAVE


Manufacturer of Precision Coaxial Connectors
620 Atlantis Road, Melbourne, FL 32904
Phone: 321-409-0509 Fax: 321-409-0510
sales@sgmcmicrowave.com
www.sgmcmicrowave.com

on SiC semiconductors in the system design helps reduce the drain current and the resultant Joule effect losses. The system has an amplifier efficiency of ~62 percent, resulting in a low channel temperature rise and also significantly reduced thermal loss, requiring reduced thermal management. The microwave module is cased in lightweight aluminium, designed to be significantly thinner and lighter than existing microwave modules with a reduction in airflow requirements using bespoke cooling technology.

## PORTABILITY

The ISYSconnect is an example of the transition towards compact, portable lab equipment. Emblation has developed and patented the utilization of compact high thermal capacity heat sinks in microwave generators with a novel thermal transfer interface technology, allowing the overall microwave module to become significantly smaller than current commercially available solid-state microwave modules (normally utilizing large heatsinks and fans).

The technology employed has resulted in an effective system that keeps the amplifier power transistors cool and maintains a high efficiency, which, in turn, results in lower loss and lower thermal increase. In addition to increasing overall thermal efficiency, this development reduces both the size and weight of the system considerably; in comparison to standard 19-inch systems that can weigh in excess of 50 lbs, the ISYSconnect is just under 9 lbs. This makes it particularly suitable for desk-based applications, moving between labs or transporting between research locations.

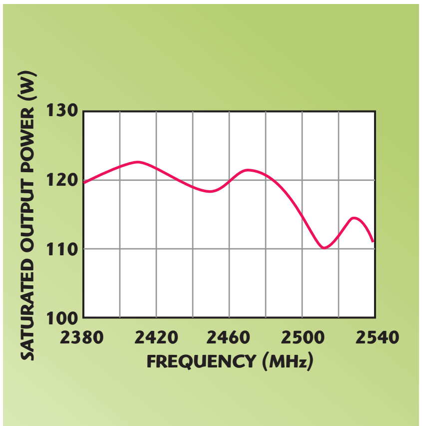


*Fig. 2 ISYSconnect output power performance.*

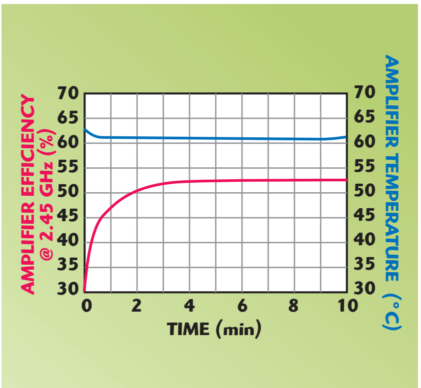


*Fig. 3 Amplifier efficiency and channel temperature performance.*

**Emblation Microwave,**
**Alloa, Scotland, UK**
**+44 (1259) 236132,**
**info@emblationmicrowave.com,**
**www.emblationmicrowave.com.**

UP TO **100 Watt**

# AMPLIFIERS

NOW! **100 kHz to 18 GHz**


from $945 ea. qty. (1-9)

**It's Watts you want? From 3 up to 100 Watts,** Mini-Circuits has high-power amplifiers built for rugged, reliable performance in heavy-duty, 100 kHz-18 GHz applications. Each model is available with or without a heat sink/fan, operating on a single integrated DC supply, with surprisingly efficient current consumption. Extensive safety features prevent amplifier damage from over-temperature, over-voltage, or open or short loads. And internal power regulation delivers high performance even when your DC power supply is fluctuating. Our manufacturing controls ensure that quality and reliability are built into every unit, to provide the **truly *robust* amplifiers that our customers demand.**

*IN STOCK! FAST DELIVERY!*

*Mini-Circuits…we're redefining what VALUE is all about!*

| Model | Freq. (MHz) | Gain (dB) | $P_{out}$ (dBm) @Comp | | Dynamic Range | | DC Pwr. | | Price | Price |
|---|---|---|---|---|---|---|---|---|---|---|
| | | | 1dB | 3dB | NF (dB) | IP3 (dBm) | Volt (V) | Current (A) | $ ea. | *X* |
| ***With Heat Sink/Fan*** | $f_L$-$f_U$ | Typ. | Typ. | Typ. | Typ. | Typ. | Nom. | Max | Qty. 1-9 | ***suffix*** |
| NEW LZY-22+ | 0.1-200 | 43 | +42.0 | +45.0 | 8.9 | +52 | 24 | 6.0 | 1495 | 1470 |
| LZY-1+ | 20-512 | 43 | +45.7 | +47.0 | 8.6 | +54 | 26 | 7.3 | 1995 | 1895 |
| LZY-2+ | 500-1000 | 46 | +45.0 | +45.8 | 8.0 | +54 | 28 | 8.0 | 1995 | 1895 |
| ZHL-5W-1 | 5-500 | 44 | +39.5 | +40.5 | 4.0 | +49 | 25 | 3.3 | 995 | 970 |
| ZHL-5W-2G+ | 800-2000 | 45 | +37.0 | +38.0 | 8.0 | +44 | 24 | 2.0 | 995 | 945 |
| ZHL-10W-2G | 800-2000 | 43 | +40.0 | +41.0 | 7.0 | +50 | 24 | 5.0 | 1295 | 1220 |
| ZHL-16W-43+ | 1800-4000 | 45 | +41.0 | +42.0 | 6.0 | +47 | 28 | 4.3 | 1595 | 1545 |
| • ZHL-20W-13+ | 20-1000 | 50 | +41.0 | +43.0 | 3.5 | +50 | 24 | 2.8 | 1395 | 1320 |
| ZHL-30W-252+ | 700-2500 | 50 | +44.0 | +46.0 | 5.5 | +52 | 28 | 6.3 | 2995 | 2920 |
| ZHL-30W-262+ | 2300-2550 | 50 | +43.0 | +45.0 | 7.0 | +50 | 28 | 4.3 | 1995 | 1920 |
| • ZHL-50W-52 | 50-500 | 50 | +46.0 | +48.0 | 6.0 | +55 | 24 | 9.3 | 1395 | 1320 |
| • ZHL-100W-52 | 50-500 | 50 | +47.0 | +48.5 | 6.5 | +57 | 24 | 10.5 | 1995 | 1920 |
| • ZHL-100W-GAN+ | 20-500 | 42 | +49.0 | +50.0 | 7.0 | +60 | 30 | 9.5 | 2395 | 2320 |
| ZVE-3W-183+ | 5900-18000 | 35 | +34.0 | +35.0 | 5.5 | +44 | 15 | 2.2 | 1295 | 1220 |
| ZVE-3W-83+ | 2000-8000 | 36 | +33.0 | +35.0 | 5.8 | +42 | 15 | 1.5 | 1295 | 1220 |

• ***Protected under U.S. Patent 7,348,854***

*For models without heat sink, add **X suffix** to model No.(Example: LZY-1+, LZY-1X+)*

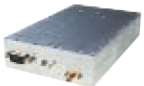

ZHL-16W-43X+
ZHL-30W-252X+
ZHL-30W-262X+

ZHL-5W-1X
ZHL-5W-2GX+

LZY-1X+
LZY-2X+
LZY-22X+
ZHL-10W-2GX
ZHL-50W-52X
ZHL-100W-52X
ZHL-100W-GANX+

ZHL-20W-13X+

ZVE-3W-83X+
ZVE-3W-183X+

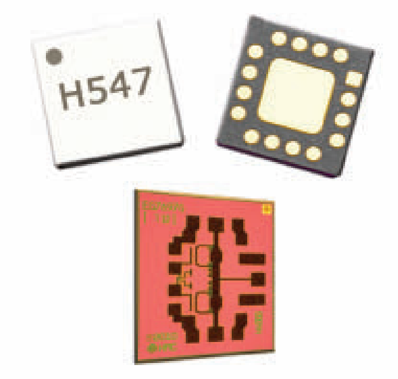


# DC to 28 GHz GaAs MMIC SPDT Switch

Hittite Microwave's HMC986 and HMC547LC3 are wideband single pole double throw (SPDT) MMIC switches that are ideal for demanding applications that require low insertion loss, fast switching speed and wide bandwidth. The HMC986 GaAs PHEMT SPDT switch die is rated from 100 MHz to 50 GHz and is controlled with two complementary inputs of 0/–3 V. The switch occupies less than 0.8 $mm^2$ of board area and employs a reflective topology. With an input signal at 40 GHz, the HMC986 exhibits 20 dB return loss, 31 dB isolation and 1.9 dB insertion loss.

The HMC547LC3 is a GaAs MESFET SPDT switch in a ceramic 3×3 mm leadless surface-mount package that covers DC to 28 GHz. This high isolation, non-reflective switch offers over 40 dB isolation and less than 2 dB insertion loss at mid-band. This versatile switch operates using complementary negative control voltage logic lines of 0/–5 V and requires no bias supply.

**Features include:**

- Wide bandwidth to 50 GHz
- Fast switching speed to 6 ns
- High isolation to 40 dB
- Low insertion loss to 1.9 dB
- High input IP3 to +46 dBm

Applications include: wideband switching matrices, high-speed data infrastructure, military communications and sensors, test and measurement equipment, jamming and EW subsystems. The HMC986 and the HMC547LC3 complement Hittite's extensive line of single, double and multi-throw MMIC switches with frequency coverage from DC to 86 GHz.

VENDORVIEW

**Hittite Microwave Corp., Chelmsford, MA, www.hittite.com, sales@hittite.com.**

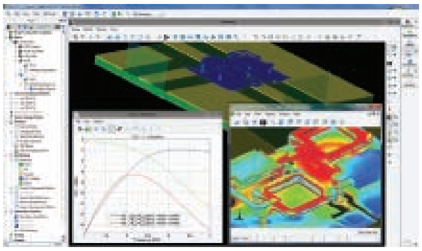

## 3D EM SIMULATION PLATFORM

VENDORVIEW

Agilent Technologies Inc. announced shipment of the latest release of its Electromagnetic Professional software, EMPro 2011.11. The updated 3D modeling and simulation platform features enhancements to further speed and improve RF design and verification. Tightly integrated with Agilent's Advanced Design System, EMPro is used to create 3D models and analyze electrical performance of packages, connectors, antennas and other RF components. The EMPro 2011.11 release builds on advances made available in the 2011.07 release, introducing key improvements to the finite-element method simulator.

***Agilent Technologies Inc.,***
***Santa Clara, CA (800) 829-4444, www.agilent.com.***

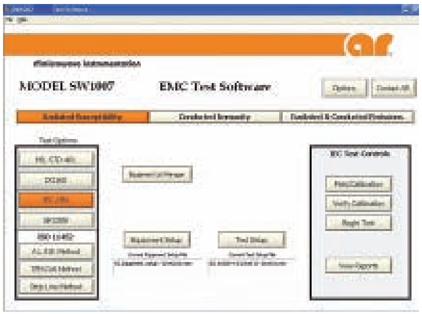


## EMC TEST SOFTWARE

VENDORVIEW

AR's SW1007 EMC test software combines radiated susceptibility, conducted immunity and emissions testing into one package to offer more control and a more intuitive interface. Built-in standards include IEC, MIL-STD, DO160, automotive standards and the ability to create personal test standards. The software has the ability to control more equipment and the report generating feature has been enhanced to offer more control and customization.

***AR RF/Microwave Instrumentation,***
***Souderton, PA (215) 723-8181, www.ar-worldwide.com.***

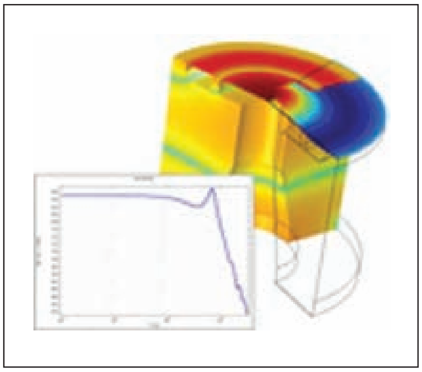

## ACOUSTICS MODULE UPGRADE

VENDORVIEW

COMSOL Inc. released a major upgrade of its add-on Acoustics Module for its flagship product COMSOL Multiphysics. This latest version of the Acoustics Module offers new capabilities and expanded multiphysics user interfaces for simulating thermoacoustic effects, poroelastic waves, acoustic-shell interactions and piezo-acoustic devices. Additional application areas for the Acoustics Module include speakers, microphones and sonar devices as well as noise control in areas such as muffler design, sound barriers and building acoustics. The module's physics interfaces provide easy-to-use tools to model acoustic pressure wave propagation in air, water and other fluids.

***COMSOL Inc.,***
***Burlington, MA (781) 273-3322, www.comsol.com.***


## DCR EVALUATION SOFTWARE

VENDORVIEW

The DCR evaluation development kit includes a full software suite that enables complete control and configuration of all sections of the receiver. This flexibility enables system designers to observe and understand the effects and implications of any parameter on its overall system design performance. Designers may test and fine tune their system design under realistic real-world signal input conditions and scenarios, make appropriate adjustments, and store data for further processing.

***Hittite Microwave Corp.,***
***Chelmsford, MA (978) 250-3343, www.hittite.com.***

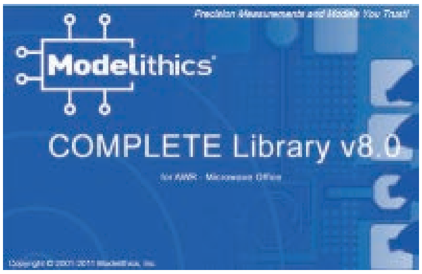


## MODEL LIBRARIES

Modelithics Inc. has released the latest version of its popular linear and nonlinear system level model libraries for RF, microwave and millimeter-wave device and components. The Modelithics COMPLETE Library version 8.0 for AWR's Microwave Office™ software introduces 46 new Global Models for passive RLCs, and 18 new nonlinear models for diodes, switches, amplifiers and transistors. Nearly all of the existing models for use with AWR's Microwave Office software have been updated with significant enhancements to enable full compatibility with AWR's APLAC® nonlinear circuit simulation technology. Version 8.0 also introduces a new measurement-derived substrate library. The enhanced APLAC compatibility as well as the new Substrate Library were added in response to designer requests to improve the convenience, accuracy and flexibility of its AWR simulations with Modelithics' models.

***Modelithics Inc.,***
***Tampa, FL (888) 359-6359, www.modelithics.com.***

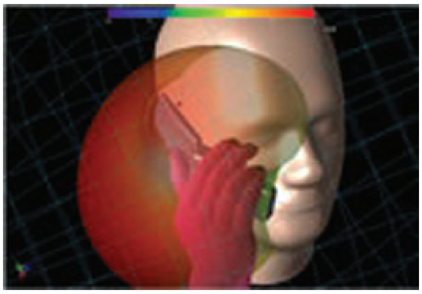

## EM SIMULATION SOFTWARE

VENDORVIEW

Remcom announces an update to its electromagnetic simulation software, XFdtd® Release 7 (XF7), with expanded import functionality and specialized options for biological EM applications. This update, Release 7.2.2, also features enhanced functionality for Remcom's unique CAD Merge capability, with support for printed circuit board (PCB) models now included. In addition to existing formats, the Virtual Population, ICRP, and NICT voxel models can now be imported for biological studies of radiation exposure to human voxel phantoms. In addition, import of all voxel types now automatically assigns correct biological materials, reducing the time to simulation. Significant SAR statistics have been added to XF7 as well, including mass, dissipated power and mean SAR over regions.

***Remcom Inc.,***
***State College, PA (814) 861-1299, www.remcom.com.***

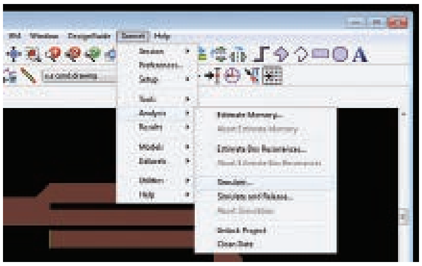

## 3D PLANAR EM SIMULATION

Sonnet Software announces the release of the Sonnet Suites Version 13.56. This new Sonnet release gives ADS 2011 users the ability to call Sonnet's high accuracy 3D planar EM simulation engine using ADS 2011 layout, drawing layer mapping and process stackup information. The Sonnet simulation creates layout look-alike schematic symbols and pushes EM-derived S-parameter extraction models back to ADS 2011 automatically. Sonnet Version 13.56 also provides improvements to interfaces to AWR Microwave Office and Cadence Virtuoso. New Stop-Via technology is also provided to support buried resistor and MIM capacitor layers in RFIC and MMIC processes.

***Sonnet Software,***
***North Syracuse, NY (877) 776-6638, www.sonnetsoftware.com.***


## IL CALC APP

The Teledyne Storm Products (TSP) microwave Insertion Loss Calculator (IL Calc) allows you to calculate insertion loss for the Teledyne Storm flexible cable lines, as well as various RG cables. You can specify connectors (straight or right angle), length, operating frequency and operating temperature. The calculator returns loss numbers for both bulk cable and assemblies. This application also contains specification sheets for flexible cable products. Lost your Internet connection? Once you have downloaded this application, the IL Calc and datasheets are available for use offline.

***Teledyne Storm Products,***
***Woodridge, IL (630) 754-3300, www.teledynestorm.com.***

## Resistive Power Divider/Combiner

Model 151270002 is a two-way, 50 Ω resistive power divider/combiner that has a DC to 6 GHz operating frequency range, 1.50:1 VSWR and SMA female connectors. This device exhibits

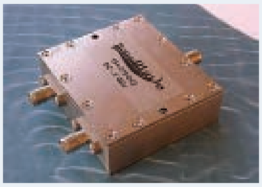

1 dB nominal insertion loss (above theoretical loss), ±0.5 dB amplitude tracking and is rated 2 W average power at the sum port. Applications for this unit include antenna sharing, intermodulation distortion measurements, diversity gain measurements and gain compression/isolation measurements. Model series 151270XXX* is available in two-, four-, six-, and eight-way configurations (*insert desired configuration, two-way = 002).

***BroadWave Technologies Inc., Greenwood, IN (317) 888-8316, www.broadwavetechnologies.com.***

## Multi Position Switch

The MM Series coaxial multi switch contains 4P3T electromechanical switches designed for cell sites with three antennas each receiving or transmitting over 120 degrees of one-third of the coverage area for cellular telephone carrier or wireless applications. The MM4 switch can replace three SDPT and SP3T switches or three transfer switches, creating space and cost savings. The switch has a VSWR of 1.20:1 maximum, insertion loss of 0.20 dB maximum, isolation of 80 dB minimum and operates at a frequency of DC to 18 GHz. Ducommun LaBarge Technologies has design engineers who can create custom versions for specific applications.

***Ducommun LaBarge Technologies, Carson, CA (310) 513-7214, www.ducommun.com.***

## Integrated Hybrid Combiner

VENDORVIEW

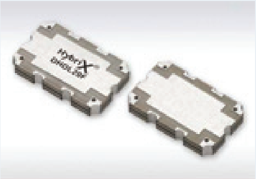

Florida RF Labs has introduced a solution for power combining and monitoring. The Doupler™ is a hybrid coupler and directional coupler integrated within a single SMT package. This approach brings together the benefits of reduced component count, lower insertion loss and minimized PCB footprint. Doupler allows for simplified PCB layout that eliminates impedance mismatch and interference, which are inherent with the conventional approach. This technologically advanced product is available in all 3G and 4G frequency bands. When Doupler is complemented by EMC Technology's Smart Detector power sensing terminations, a totally passive power combining and monitoring solution can be realized with the lowest loss and highest circuit reliability. Datasheets and evaluation boards are available upon request.

***EMC Technology & Florida RF Labs, Stuart, FL (772) 600-1632, www.emc-rflabs.com.***

## Beamforming Networks

KRYTAR Inc. announced the availability of custom designs and production of complete ultra-broadband beamforming networks for RF and microwave applications. KRYTAR beamforming networks are multifaceted assemblies for a wide range of applications, including multiple antenna and antenna arrays used in military electronic systems and commercial communications systems. KRYTAR's technological advances have extended the frequency range of ultra broadband components with frequencies ranging from DC to 67 GHz. Superior performance and functionality as well as unique form-fit-function designs bring unique solutions to those difficult engineering and manufacturing challenges. Many types of connectors can be designed into the integrated assembly including: SMA, Type-N, APC-7 and 3.5 mm.

***KRYTAR Inc., Sunnyvale, CA (408) 734-5999, www.krytar.com.***

## Digital Attenuators

VENDORVIEW


Two new SMT packaged MMIC 5-Bit digital attenuators are ideal for automotive, microwave radio, test equipment, military and space applications up to 33 GHz. The HMC939LP4E is a wideband SMT GaAs MMIC 5-Bit digital attenuator that is rated from 0.1 to 33 GHz. This wideband attenuator product exhibits insertion loss as low as 4 dB, and can be programmed to provide up to 31 dB attenuation in 1 dB steps. The HMC941LP4E is a wideband SMT GaAs MMIC 5-Bit digital attenuator that is rated from 0.1 to 33 GHz. This wideband attenuator product exhibits insertion loss as low as 4 dB, and can be programmed to provide up to 15.5 dB attenuation in 0.5 dB steps. Both feature excellent attenuation accuracy of ±0.3 dB and fast switching speed of 90 ns, and both accept positive control voltages of 0/+3 V or 0/+5 V. They exhibit high input IP3 performance of up to +45 dBm, allowing them to be used in various locations within a microwave or millimeter-wave transceiver. They are housed in RoHS-compliant, 4 × 4 mm QFN packages.

***Hittite Microwave Corp., Chelmsford, MA (978) 250-3343, www.hittite.com.***

## Temperature Variable Attenuators

The AV-Series 0805 are size temperature variable attenuators to 3 GHz. The AV-0805 is available in 1 to 10 dB attenuation with nine different temperature characteristics, N1 – N9. RoHS compliant terminals feature a nickel barrier layer for excellent solder leach resistance. These cost-effective temperature variable attenuators have a short lead time with a minimum order quantity of 25 pieces. Applications for the AV-0805 temperature variable attenuators include power amplifiers, LNAs, transceiver modules, synthesizers, WiMAX and WiFi equipment, fixed and mobile satellite radio and test and measurement instrumentation. Samples are available.

***International Manufacturing Services Inc., Portsmouth, RI (401) 683-9700, www.imsresistors.com.***

## Bi-Directional Coupler

VENDORVIEW

Mini-Circuits' new bi-directional coupler BDCN-20-13+ offers an industry-leading combination of operating bandwidth (360 to 1000 MHz) and size (3.2 × 1.6 mm). The low insertion loss (0.15 dB typical) makes this component a versatile building block for use in a variety of systems and subsystem designs.

***Mini-Circuits, Brooklyn, NY (718) 934-4500, www.minicircuits.com.***

## SP5T Absorptive Switch

VENDORVIEW

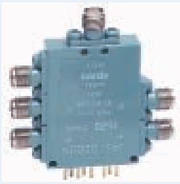

Narda, an L-3 Communications company, introduced the model SP153DHTS, a high-performance SP2T absorptive switch that is an excellent choice for broadband applications in all types of defense systems. The model SP153DHTS operates from 2 to 18 GHz with a switching speed of 25 ns, insertion loss of less than 3.8 dB and isolation as high as 60 dB. It has maximum VSWR of 2:1, operates from a power supply voltage of -12 to -15 V DC at 90 mA and + 5 V DC at 220 mA, and employs SMA female connectors.

***Narda Microwave, Hauppauge, NY (631) 231-1700, www.nardamicrowave.com/east.***

## 6550 MHz Ceramic Filter

VENDORVIEW

NIC's 6550 MHz is a high frequency filter built for use in C-Band applications. The features


include low insertion loss of < 2.5 dB at center frequency, rejection of > 50 dB at 6000 MHz and > 40 dB at 7200 MHz, built in a small package size of 0.83" × 0.51" × 0.19." Custom designs are available up to C-Band.

***Networks International Corp., Overland Park, KS (913) 685-3400, www.nickc.com.***

### Solid-state Switch

VENDORVIEW

PMI model P2T-18G40G-65-R-292FF is a single pole, two throw, solid-state switch that operates over the 18 to 40 GHz frequency range. This model provides 55 dB of isolation over the entire frequency range of operation and offers low insertion loss performance (3.5 dB maximum for 18 to 26.5 GHz and 4.5 dB maximum for 26.5 to 40 GHz) with 100 nsec maximum switching speed. It measures 1.2" × 0.95" × 0.46."

***Planar Monolithics Industries Inc., Frederick, MD (301) 662-5019, www.pmi-rf.com.***



### Millimeter-Wave Transport

VENDORVIEW

Approved by the FCC in the U.S., Industry Canada and ETSI in the European Union, Renaissance/HXI LightSpeed links can be custom configured for the most demanding commercial and military applications. LightSpeed series 6451/6651 and 7451/7651 radio links are just some of the numerous communication solutions from Renaissance/HXI, a time-tested supplier of millimeter-wave radios. Available in multiple configurations in either the unlicensed 60 GHz band or the light licensed 70/80 GHz band, with antenna configurations offering ranges of over 5 km, these radios have convincingly demonstrated their reliability in many demanding deployments worldwide.

***Renaissance/HXI, Harvard, MA (978) 772-7774, www.hxi.com.***

### Temperature-Compensating Attenuators


RFMD's new RFSA4013 and RFSA4023 are fully monolithic analog temperature-compensating attenuators (TCA) featuring exceptional linearity over their entire gain control range. These TCAs are designed to offset the gain reduction of an RF component over temperature without the need for closed loop feedback. Three customer selectable temperature coefficients make these TCAs a flexible solution for RF lineups. Each attenuator incorporates a new circuit architecture that solves a longstanding industry problem with regards to attenuator architecture: high IP3, low DC current and broad bandwidth. The RFSA4013 and RFSA4023 only require a single supply voltage and two logic bits to set the control attenuation slope versus temperature. Each TCA draws a low 1 mA current and is packaged in a small 3 × 3 mm QFN. These attenuators are internally matched to 50 Ω over their rated control range and frequency.

***RF Micro Devices, Greensboro, NC (336) 664-1233, www.rfmd.com.***

### 45° RF Connectors

SRI Connector Gage has two new 45° connectors for the RF/microwave industry. One is a SMA plug to SMA jack 20-921-2300-00 with performance up to 27 GHz and a VSWR 1.2:1. It is made of SST, corrosion resistant, non magnetic 303, per ASTM A484 and A582. The other is a TNC jack to SMA jack bulkhead 41-921-2300-00 with performance up to 18 GHz and a VSWR 1.2 to 18 GHz. It is made from SST, corrosion resistant, non magnetic 303, per ASTM A484 and A582.

***SRI Connector Gage, Melbourne, FL (800) 881-9689, www.sriconnectorgage.com.***

### Digital Step Attenuator

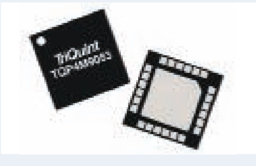

TriQuint Semiconductor's new TQP4M9083, seven-bit, digital step attenuator (DSA) offers up to 31.75 dB of attenuation in 0.25 dB increments. A serial periphery interface (SPI) controls attenuation changes. A wide frequency range of 0.4 to 3.5 GHz allows for use in test equipment, sensors, mobile infrastructure and general-purpose wireless applications. The TQP4M9083 is pin compatible with the TQP4M9072 allowing design flexibility and the ability to upgrade for higher resolution requirements. 1.5 dB insertion loss and 55 dBm IIP3 performance places the TQP4M9083 as best in class among available DSAs.

***TriQuint stocking distributor RFMW Ltd., San Jose, CA (408) 414-1450, www.rfmw.com.***

### Lowpass Filters

RLC Electronics now offers fourth order tubular Bessel lowpass filters with 3 dB cutoffs from 1 to 22 GHz. Computer design and tubular construction allow for excellent group delay characteristics with reasonable rejection while extending 3 dB cutoff approaching 30 Giga bits. These filters should be regarded as compromise designs for pulsed systems where truthful reproduction of the pulse shape is important. Primarily used on lightwave receivers to reduce the impact of higher order distortion and noise. It operates from -55° to +85°C and measures 1.8" × 1.54" × 1.25."

***RLC Electronics Inc., Mt. Kisco, NY (914) 241-1334, www.rlcelectronics.com.***

### 20 dB Bi-Directional Coupler

VENDORVIEW

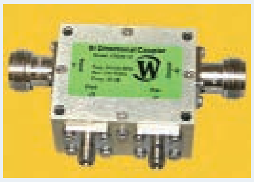

Model C8356 is a high power, low loss coupler for the 20 to 550 MHz band and is rated at 100 W CW. Ideal for high power applications, requiring tight coupling, while preserving a tight loss budget. Designed for military and commercial environmental conditions.

***Werlatone Inc., Patterson, NY (845) 278-2220, www.werlatone.com.***

## Amplifiers

### 600 W RF Amplifier

VENDORVIEW

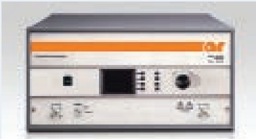

Model 600A225 is a 600 W RF power amplifier that covers the 10 kHz to 225 MHz frequency range. It is equipped with a digital control panel that provides both local and remote control using IEEE, RS-232, USB and Ethernet interfaces.

***AR RF/Microwave Instrumentation, Souderton, PA (215) 723-8181, www.ar-worldwide.com.***

### X-Band AGC Amplifier

AMLSW3011 is a GaAs X-Band switched gain selectable amplifier with excellent state-to-state gain and phase tracking. The amplifier offers

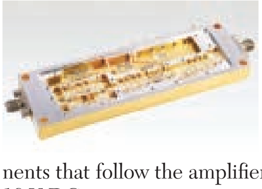

selectable gain steps of 0/10/20 and 30 dB. A minimum OIP3 of +35 dBm is provided in any of the gain states. This amplifier is also available with an input detector option that limits the output power to +30 dBm maximum under conditions of high input drive. This feature protects components that follow the amplifier in the system cascade. DC voltage is 12 to 18 V DC.
***Microsemi,***
***Camarillo, CA (805) 388-1345,***
***www.amlj.com.***

## Medium Power Amplifier

VENDORVIEW

Model AMF-4D-02002650-90-20P is a new addition to MITEQ's family of rugged, single bias ultra-broadband coaxial amplifiers. This amplifier has over 25 dB of gain from 2 to 26.5 GHz, in a housing that is only 1" × 0.83" without the field replaceable 2.92 mm connectors. Gain flatness is a maximum of ±2.5 dB, though typical is ±2.0 dB. The AMF-4D-02002650-90-20P has a maximum noise figure of 9 dB in the full band, though the typical value is near 6 dB. This amplifier operates from -40° to +75°C of base temperature, has a P1dB minimum of +20 dBm, IP3 is typically +26 dBm, and a current draw of maximum 450 mA from a single +15 V DC supply. Port VSWR is typically less than 2:1 for both input and output. Frequency options from as low as 100 MHz to as high as 40 GHz are available.

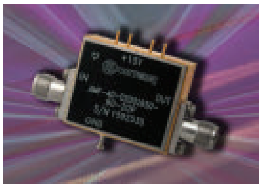

***MITEQ,***
***Hauppauge, NY***
***(631) 436-7400,***
***www.miteq.com.***



## Low Noise Amplifiers

The NXP BGU700x family offers the best reception for weak GPS signals, delivering an improvement of 10 dB or better IP3 under -40 to -20 dBm jamming conditions, while the noise figure remains below 1 dB. Requiring only two external components, the BGU700x LNAs save up to 50 percent in PCB size and 10 percent in component cost. The NXP BGU700x/BGU8007 series uses adaptive biasing to immediately detect any output power from jammers, and compensate by temporarily increasing the current. As a result, optimal GPS signal reception is maintained for as long as possible. Each device in the BGU700x/BGU8007 series requires only one input matching inductor and one supply decoupling capacitor to complete the design.
***NXP Semiconductors N.V.,***
***Eindhoven, Netherlands +31 40 27 29960,***
***www.nxp.com.***

# Semiconductors/ICs

## RF Power Transistors


The MRFE6VP8600H and MRFE6VP8600HS are push-pull power transistors that provide enhanced efficiency and operate over the 470 to 860 MHz frequency band. These two 50 V LDMOS RF power transistors are capable of transmitting highly linear, 125 W average DVB-T output power, with a peak envelope power output capability of over 600 W. Moreover, these devices are fully capable of withstanding a nearly 100 percent mismatched load, specified as greater than 65:1 VSWR at all phase angles, with no damage to the transistor. Ultimately, the MRFE6VP8600H and MRFE6VP8600HS provide a unique combination of linear power amplification, high efficiency and enhanced ruggedness for the UHF broadcast industry.
***Freescale Semiconductor distributor***
***Richardson RFPD,***
***LaFox, IL (630) 208-2700,***
***www.richardsonrfpd.com.***

## PIN Diode

VENDORVIEW

Skyworks Solutions has introduced a high power series PIN diode for transmit and receive switching applications. The SMP1325-087LF is a discrete solution available in a high thermal dissipative package – making it ideal for large signal switching and attenuation applications. It combines low insertion (0.04 dB) loss, high linearity (90 dBm), good isolation, excellent power handling (35 W) and low distortion in a small package. Target markets include handsets, infrastructure, military and others that may require high power switching.
***Skyworks Solutions Inc.,***
***Woburn, MA (781) 376-3000,***
***www.skyworksinc.com.***

# Sources

## Voltage-Controlled Oscillator

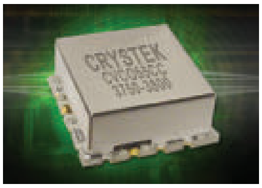

Crystek's CVCO55CC-3750-3800 VCO operates from 3750 to 3800 MHz with a control voltage range of 0.5 to 16 V. This VCO features a typical phase noise of -105 dBc/Hz at 10 KHz offset and has excellent linearity. Output power is typically +2 dBm. Engineered and manufactured in the USA, the model CVCO55CC-3750-3800 is packaged in the industry-standard 0.5" × 0.5" SMD package. Input voltage is 5 V, with a maximum current consumption of 30 mA. Pulling and pushing are

# High Voltage 8V Ku-Band
# 0.25µm Power pHEMT

- Stepper based 0.25µm gate length
- 8V operation / 70 GHz Ft
- 1 W/mm saturated power density
- BCB encapsulation for repeatable packaged performance

## PP25-21 Power Performance

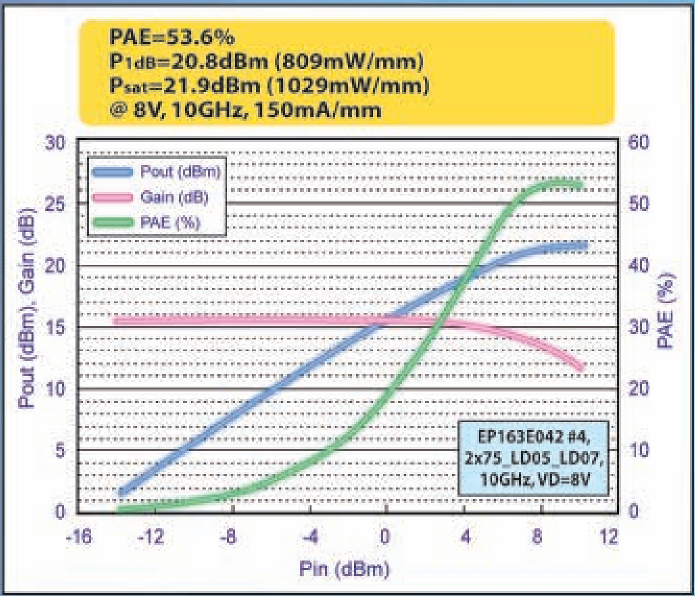


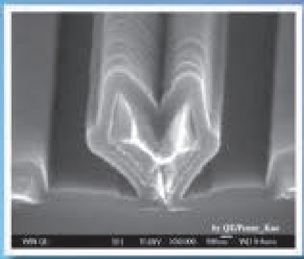

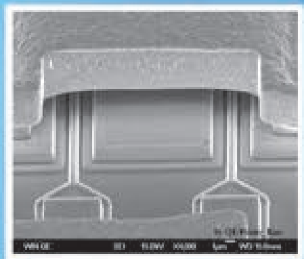

## Comparison Table for 0.1µm, 0.15µm, 0.25µm and 0.5µm pHEMT

| | PP10 | PP15 | PP25-21 | PP50-11 |
|---|---|---|---|---|
| Vto (V) | -0.9 | -1.2 | -1.2 | -1.4 |
| Idss (mA/mm) | 450 | 500 | 345 | 350 |
| Idmax (mA/mm) | 720 | 650 | 460 | 480 |
| GM (mS/mm) | 750 | 495 | 380 | 310 |
| VDG (V) | 9 | 10 | 19.2 | 20 |
| ft (GHz) | 130 | 85 | 65~72 | 32 |
| Fmax (GHz) | 175 | 180 | 160 | 85 |
| PldB (mW/mm) | 533.25 (3.5V) | 670 (5V) | 809 (8V) | 587 (8V) |
| Psat (mW/mm) | 764.3 (3.5V) | 820 (5V) | 1029 (8V) | 851 (8V) |
| Gain (dB) | 14.35 | 18.1 | 15.6 | 15.5 |
| PAE (%) | 53.57 | 55 | 53.6 | 53.5 |
| Frequency | 29 GHz | 10 GHz | 10 GHz | 10 GHz |

WIN SEMICONDUCTORS

Tel:+886-3-397-5999
E-mail:sales@winfoundry.com
Fax: +886-3-397-5069
http://www.winfoundry.com

minimized to 1 MHz and 2.5 MHz/V, respectively. Second harmonic suppression is -15 dBc typical.
***Crystek Corp.,***
***Ft. Myers, FL (800) 237-3061,***
***www.crystek.com.***

## Phase-Locked Oscillator


The ESP-2400 phase-locked oscillator operates at 2400 MHz and features exceptionally low phase noise (<-116 dBc/Hz at 10 KHz) and low power consumption. The unit is supplied with an internal frequency reference, and offers +15 dBm output power and low spurs (<-70 dBc). Designed for ruggedized ground mobile or airborne operation, the ESP-2400 also features an extended operating temperature range (-40° to +85°C), high vibration tolerance and low power consumption. The ESP units are custom-designed as DRO replacements in Hi-Rel applications, such as SATCOM, electronic warfare and telemetry. Custom units are available in fixed frequencies from 50 MHz to 26 GHz in a connectorized DRO standard package of 2.25" × 2.25" × 0.6". The package can be optionally hermetically sealed.
***EM Research Inc.,***
***Reno, NV (775) 345-2411,***
***www.emresearch.com.***

## Radar Reference Oscillator

ULN-8R is an eight-frequency, 80 to 120 MHz frequency reference for radar applications. ULN-8R has up to eight different low-g sensitivity crystal frequencies built-in that can be selected via a 3-pin TTL interface for in-situ channel selection. ULN-8R is designed to work as a selectable low phase-noise frequency reference for radar applications, SATCOM, broadcast, and test and measurement equipment. At only 3" × 2.5" × 0.7", ULN-8R is tested against shock to MIL-STD-202G, M213 Condition C, and against vibration to MIL-STD-202G, M204 Condition C, and ages at less than 1 ppm per year. ULN-8R has an extended temperature range operation, and can operate from +9 to +18 V at less than 0.7 W power consumption. Customers can order the ULN-8R with eight custom frequencies, or select from off-the-shelf frequency ranges, such as 106 to 109 MHz.
***Jackson Labs Technology,***
***Los Gatos, CA (408) 354-7888,***
***www.jackson-labs.com.***

## Micrometer-Tuned Gunn Oscillator

Spacek Labs model GW-920PM is a cost-effective, high power Gunn oscillator. The center frequency is 92 GHz with ±1 GHz of mechanical tuning with other frequencies available. Tuning is accomplished with a finely graduated micrometer with locking screw. The output power is 25 mW minimum. This model incorporates an InP Gunn diode with an input bias of +10 V DC at 0.3A typical. Heat is dissipated with an integrated heatsink.

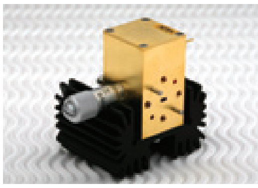

***Spacek Labs Inc.,***
***Santa Barbara, CA (805) 564-4404,***
***www.spaceklabs.com.***

## DRO Oscillators

The DRO series of high frequency oscillators use high-Q dielectric resonators and are available at 8 to 12 GHz. The electrical tuning option for the DRO operating at 10 GHz has a control range of 0 to 12 V DC. The electrical tuning provides ±3 MHz of frequency control. They provide a low phase noise and an exceptional spectral purity as good as -110 dBc/Hz, typically, at 10 kHz from the carrier. DROs minimize power consumption by operating off a 5 V DC bias while drawing only 20 mA, typically, and are available in surface-mount packages measuring 0.91" × 0.91" × 0.40." DROs are available in a connectorized metal enclosure measuring 1.25" × 1.25" × 0.85." The oscillators deliver 0±3 dBm of output power into a 50 Ω load. DROs are designed to operate over the industrial temperature range of -40° to 85°C.
***Z-Communications Inc.,***
***Poway, CA (858) 621-2700,***
***www.zcomm.com.***

SYNERGY®
MICROWAVE CORPORATION

# ULTRA WIDE BANDWIDTH VCO'S

| Model | Frequency ( MHz ) | Tuning Voltage ( VDC ) | DC Bias ( VDC ) | Typical Phase Noise @ 10 kHz ( dBc/Hz ) |
|---|---|---|---|---|
| **DCMO & DCFO Series** | | | | |
| DCMO25-5 | 20 - 50 | 0.5 - 24 | +5 @ 30 mA | -114 |
| DCMO514-5 | 50 - 140 | 0.5 - 24 | +5 @ 28 mA | -105 |
| DCMO616-5 | 65 - 160 | 0.5 - 24 | +5 @ 28 mA | -108 |
| DCMO1027 | 100 - 270 | 0.5 - 24 | +5 to +12 @ 20 mA | -112 |
| DCMO1129 | 110 - 330 | 0.5 - 24 | +5 to +12 @ 22 mA | -112 |
| DCMO1545 | 150 - 450 | 0.5 - 24 | +5 to +12 @ 22 mA | -108 |
| DCMO1857 | 180 - 570 | 0.5 - 24 | +5 to +12 @ 26 mA | -108 |
| DCMO2260-5 | 220 - 600 | 0.5 - 24 | +5 @ 28 mA | -108 |
| DCMO2476 | 240 - 760 | 0.5 - 24 | +5 to +12 @ 26 mA | -108 |
| DCMO3288-5 | 320 - 880 | 0.5 - 24 | +5 @ 21 mA | -109 |
| DCMO3288-12 | 320 - 880 | 0.5 - 24 | +12 @ 25 mA | -80 |
| DCFO35105-5 | 350 - 1050 | 0.5 - 25 | +5 @ 51 mA | -112 |
| DCMO40110-5 | 400 - 1100 | 0.5 - 24 | +5 @ 37 mA | -103 |
| DCMO40110-8 | 400 - 1100 | 0.5 - 24 | +8 @ 39 mA | -104 |
| DCMO40110-12 | 400 - 1100 | 0.5 - 24 | +12 @ 38 mA | -105 |
| DCMO50120-5 | 500 - 1200 | 0.5 - 24 | +5 @ 37 mA | -102 |
| DCMO50120-12 | 500 - 1200 | 0.5 - 24 | +12 @ 28 mA | -103 |
| DCMO60170-5 | 600 - 1700 | 0.5 - 25 | +5 @ 35 mA | -100 |
| DCMO60170-12 | 600 - 1700 | 0.5 - 25 | +12 @ 29 mA | -100 |
| DCMO80210-5 | 800 - 2100 | 0.5 - 24 | +5 @ 28 mA | -96 |
| DCMO80210-10 | 800 - 2100 | 0.5 - 24 | +10 @ 25 mA | -100 |
| DCMO80220-5 | 800 - 2200 | 0.5 - 24 | +5 @ 28 mA | -98 |
| DCMO90220-12 | 900 - 2200 | 0.5 - 24 | +12 @ 29 mA | -99 |
| DCMO92200-12 | 925 - 2000 | 0.5 - 18 | +12 @ 35 mA | -101 |
| DCMO100230-5 | 1000 -2300 | 0.5 - 24 | +5 @ 35 mA | -98 |
| DCMO100230-12 | 1000 - 2300 | 0.5 - 24 | +12 @ 33 mA | -101 |
| DCMO110250-5 | 1100 - 2500 | 0.5 - 28 | +5 @ 25 mA | -100 |
| DCMO110250-8 | 1100 - 2500 | 0.5 - 28 | +8 @ 30 mA | -102 |
| DCMO130275-5 | 1300 - 2750 | 0.5 - 24 | +5 @ 20 mA | -93 |
| DCMO135270-8 | 1350 - 2700 | 0.5 - 20 | +8 @ 36 mA | -93 |
| DCMO150310-10 | 1500 - 3100 | 0.5 - 22 | +10 @ 32 mA | -96 |
| DCMO150318-5 | 1500 - 3200 | 0.5 - 20 | +5 @ 24 mA | -93 |
| DCMO150320-5 | 1500 - 3200 | 0.5 - 18 | +5 @ 33 mA | -92 |
| DCMO170340-3 | 1700 - 3400 | 0.5 - 20 | +3.5 @ 18 mA | -85 |
| DCMO170345-5 | 1700 - 3450 | 0.5 - 16 | +5 @ 43 mA | -88 |
| DCMO172332-5 | 1720 - 3320 | 0.5 - 24 | +5 @ 22 mA | -94 |
| DCMO190410-5 | 1900 - 4100 | 0.5 - 18 | +5 @ 45 mA | -90 |
| DCMO200430-5 | 2000-4300 | 0.5 - 17 | +5 @ 50 mA | -89 |
| DCMO250512-5 | 2500 - 5125 | 0.5 - 14 | +5 @ 51 mA | -76 |
| **DCYR & DCYS Series** | | | | |
| DCYR2060-5 | 200 - 600 | 0.5 - 28 | +5 @ 60 mA | -119 |
| DCYR3097-5 | 300 - 970 | 0.5 - 28 | +5 @ 38 mA | -112 |
| DCYR50125-10 | 500 - 1250 | 0.5 - 24 | +10 @ 43 mA | -110 |
| DCYS100200-12 | 1000 - 2000 | 0.5 - 28 | +12 @ 33 mA | -105 |
| DCYS160360-5 | 1600 - 3600 | 0.5 - 20 | +5 @ 47 mA | -90 |
| DCYS200400-5 | 2000 - 4000 | 0.5 - 16 | +5 @ 45 mA | -90 |
| DCYS200400P-5 | 2000 - 4000 | 0.5 - 22 | +5 @ 45 mA | -95 |
| DCYS250500-5 | 2500 - 5000 | 0.5 - 14 | +5 @ 45 mA | -75 |
| DCYS275550-5 | 2750 - 5550 | 0.5 - 22 | +5 @ 43 mA | -77 |
| DCYS300600-5 | 3000 - 6000 | 0.3 - 17 | +5 @ 43 mA | -77 |

*Patented Technology*

## Features

- -- Octave & Higher Than Octave Bandwidth
- -- Exceptional Phase Noise Performance
- -- Very Low Post Thermal Drift
- -- Simplifies Design... Better Value
- -- Power Efficient
- -- Compact Size: 0.5" x 0.5" & 0.91" x 0.91"
- -- REL-PRO® Patented Technology

ULTRA
WIDE
BANDWIDTH


For additional information, contact Synergy's sales and application team.
Phone: (973) 881-8800 Fax: (973) 881-8361 E-mail: sales@synergymwave.com
201 McLean Boulevard, Paterson, NJ 07504


RoHS COMPLIANT

***Visit Our Website At WWW.SYNERGYMWAVE.COM***

## *Test Equipment*

### In-Line Peak Power Sensor

VENDORVIEW

Anritsu introduces the MA24105A, a standalone, compact and highly accurate in-line peak power sensor that provides a wide range of power measurement capability over a frequency range of 350 MHz to 4 GHz. Featuring a widest-in-class 2 mW to 150 W measurement range, and a combination of forward and reverse measurement functionality, the MA24105A can be used by both manufacturing and field engineers in a variety of commercial cellular, land mobile radio (LMR) and general-purpose military/defense RF applications.

***Anritsu Co.,***
***Morgan Hill, CA (800) 267-4878,***
***www.anritsu.com.***

### Network Analyzer

This latest generation network analyzer comes with four test ports and a second internal generator. Users who need to characterize multiport DUTs, mixers and amplifiers will benefit from the wide dynamic range, short measurement times and easy operation. The new four-port R&S ZNB models cover the frequency ranges from 9 kHz to 4.5 GHz or 8.5 GHz. Rohde & Schwarz has designed powerful instruments for demanding applications in the production and development of RF components with multiple ports. Two internal signal sources and a frequency-converting mode enable comprehensive measurements on mixers or amplifiers.

***Rohde & Schwarz,***
***Munich, Germany +49 89 4129 12345,***
***www.rohde-schwarz.com.***

# Phase Adjusters

| Part Number | Con-nec-tors | Fre-quency Range (GHz) | VSWR max. | Inser-tion Loss max. (dB) | Phase Shift min. (°) | No. of Turns | Phase Shift Deg/ GHz/ Turn | Time Delay min. (psec.) | Time Delay max. (psec.) | Tem-perature (°C) | Weight max. (g) |
|---|---|---|---|---|---|---|---|---|---|---|---|
| LS-0002-YYYY[1] | div. | DC - 2 | 1.2:1 | 0.3 | 85 | 37 | | 393 | 516 | | 98-220[2] |
| LS-0103-6161 | Nf | DC - 3 | 1.15 | 0.4 | 540 | cont. | 1.15 | 1826 | 2328 | -65 to +125 | 700 |
| LS-0203-6161 | | | | 0.8 | 1080 | | | 3693 | 4694 | | 1200 |
| LS-0012-YYYY[1] | div. | DC - 12 | 1.3:1 | 0.8 | 520 | 37 | | 406 | 530 | | 114-234[2] |
| LS-0112-XXXX[3] | SMA | DC-12.0 | 1.25:1 | 0.4 | 230 | 16.5 | 1.2 | 238 | 293 | -65 to +125 | 70 |
| LS-A112-XXXX[3] | | | | | | | | | | | 47 |
| LS-0212-1121 | | | | | | | | | | | 70 |
| LS-A212-1121 | | | | | | | | | | | 47 |
| LS-0118-XXXX[3] | | DC-18.0 | | 0.6 | 350 | | | | | | 70 |
| LS-A118-XXXX[3] | | | | | | | | | | | 47 |
| LS-0218-1121 | | | | | | | | | | | 70 |
| LS-A218-1121 | | | | | | | | | | | 47 |
| LS-0118-5161 | N | | | | | | | 300 | 355 | -65/+70 | 105 |
| LS-U118-5161 | | | | | | | | | | -65/+165 | |
| LS-0018-YYYY[1] | div. | DC - 18 | 1.5:1 | 1.0 | 770 | 37 | 1.15 | 406 | 530 | | 114 |
| LS-0121-XXXX[3] | SMA | DC-26.0 | 1.30:1 | 0.8 | 500 | 16.5 | 1.2 | 238 | 293 | -65 to +125 | 70 |
| LS-A121-XXXX[3] | | | | | | | | | | | 47 |
| LS-0221-1121 | | | | | | | | | | | 70 |
| LS-A221-1121 | | | | | | | | | | | 47 |
| LS-0321-1121 | | | 1.31:1 | | 500 | 35 | 0.6 | 236.7 | 290.5 | | 30 |
| LS-0170-1121 | | | 1.26:1 | 0.26 | 127 | 13.5 | 0.36 | 109.2 | 122.8 | | 9 |
| LS-S008-1121 | | | 1.50:1 | 0.4 | 155 | 10 | 0.6 | 118.6 | 135.1 | | 20 |
| LS-P140-KFKM | 2.92 mm | DC-40.0 | 1.2:1 | 0.6 | 590 | 12 | | 168 | 208 | | 51 |
| LS-0140-KFKM | | | 1.4:1 | | | | | | | | 49 |
| LS-P150-HFHM | 2.40 mm | DC-50.0 | 1.3 | 0.8 | 400 | 7 | 1.2 | 172 | 195 | -65 to +65 | 55 |
| LS-0150-HFHM | | | 1.5 | | | | | | | | 53 |
| LS-P165-VFVM | 1.85 mm | DC-63.0 | 1.4 | 0.8 | 600 | 8 | | 167 | 195 | | 55 |
| LS-0165-VFVM | | | 1.5 | | | | | | | | 53 |

1) div.: Connector Configuration available: SMA, male and female; N, male and female; TNC male and female
2) Weight depends on connector configuration
3) SMA Connector Configuration available: male/female; male/male; female/female; female/male

**Spectrum** Elektrotechnik GmbH **when Quality is needed**

**80905 Munich, Germany** **P.O. Box 450533**
**Telephone: +49-89-3548-040** **Facsimile: +49-89-3548-0490**
**www.spectrum-et.com** * **Email: sales@spectrum-et.com**

## Satellite Communications Network Design and Analysis

**Kenneth Y. Jo**

*Satellite Communications Network Design and Analysis* provides a thorough presentation of the fundamental concepts of satellite communications (SATCOM) network design and performance assessments. It contains discussions on a wide class of SATCOM networks using satellites as core components, as well as coverage of key applications in the field. It presents a broad range of critical topics, from geosynchronous Earth orbiting (GEO) satellites and direct broadcast satellite systems, to low Earth orbiting (LEO) satellites, radio standards and protocols. For the RF engineer, it also focuses on the numerous technologies employing high frequency band satellites, small mobile terminals, RF multiband terminals, multichannel services and IP modems.

The book explains the many specific uses of satellite networks, including small-terminal wireless and mobile communications systems as well as advanced topics such as satellite RF link analyses, optimum transponder loading, on-board processing, antenna characteristics, protected systems, information assurance and spread spectrums. It also covers current and future SATCOM systems and details their performance supportabilities plus trends in multimedia satellite applications and IP services over satellites.

The book is intended to introduce systems engineering approaches for modern satellite networks that provide advanced wideband communications services through satellites, Earth stations, terminals and terrestrial networks. The book assumes fundamental knowledge in information systems and architectures, telecommunications networks and telecommunications standards and protocols in addition to some advanced math knowledge. It is essential to have secure, worldwide, reliable, network-centric data services for the future and this book is a good tool for learning about this subject.

***To order this book, contact:***

Artech House
685 Canton Street
Norwood, MA 02062
(800) 225-9977
or
16 Sussex Street
London, SW1V 4RW, UK
+44 (0) 20 7596 8750
505 pages; $149, £99
ISBN: 978-1-60807-194-4

# Advertising Index



## Coming in March

Test and Measurement

- **Addressing Test System Obsolescence in Aerospace and Defense**
- **Tackling MIMO Design and Test Challenges for Next Gen 802.11ac WLAN**
- **Compact Transistor Models, The Roadmap to First Pass Amplifier Design Success**

## Sales Representatives

Microwave Journal — Frequency Matters.


**Carl Sheffres**, Publisher

**Ed Kiessling**, Traffic Manager

**Eastern and Central Time Zones**
Chuck Boyd
*Northeast Reg. Sales Mgr.*
(New England, New York, Eastern Canada)
685 Canton Street
Norwood, MA 02062
Tel: (781) 769-9750
FAX: (781) 769-5037
cboyd@mwjournal.com

Michael Hallman
*Eastern Reg. Sales Mgr.*
(Mid-Atlantic, Southeast, Midwest)
4 Valley View Court
Middletown, MD 21769
Tel: (301) 371-8830
FAX: (301) 371-8832
mhallman@mwjournal.com

**Pacific and Mountain Time Zones**
Wynn Cook
*Western Reg. Sales Mgr.*
208 Colibri Court
San Jose, CA 95119
Tel: (408) 224-9060
FAX: (408) 224-6106
wcook@mwjournal.com

**International Sales**
Richard Vaughan
*International Sales Manager*
16 Sussex Street
London SW1V 4RW, England
Tel: +44 207 596 8742
FAX: +44 207 596 8749
rvaughan@horizonhouse.co.uk

**Germany, Austria, and Switzerland (German-speaking)**
WMS.Werbe- und Media Service
Brigitte Beranek
Gerhart-Hauptmann-Street 33,
D-72574 Bad Urach
Germany
Tel: +49 7125 407 31 18
FAX: +49 7125 407 31 08
bberanek@horizonhouse.com

**Israel**
Oreet Ben Yaacov
Oreet International Media
15 Kineret Street
51201 Bene-Berak, Israel
Tel: +972 3 570 6527
FAX: +972 3 570 6526
obenyaacov@horizonhouse.com

**Korea**
Young-Seoh Chinn
JES Media International
2nd Floor, ANA Bldg.
257-1, Myungil-Dong
Kangdong-Gu
Seoul, 134-070 Korea
Tel: +82 2 481-3411
FAX: +82 2 481-3414
yschinn@horizonhouse.com

**Japan**
Katsuhiro Ishii
Ace Media Service Inc.
12-6, 4-Chome,
Nishiiko, Adachi-Ku
Tokyo 121-0824, Japan
Tel: +81 3 5691 3335
FAX: +81 3 5691 3336
amskatsu@dream.com

**China**
Michael Tsui
ACT International
Tel: 86-755-25988571
Tel: 86-21-62511200
FAX: 86-10-58607751
michaelT@actintl.com.hk

**Hong Kong**
Mark Mak
ACT International
Tel: 852-28386298
markm@actintl.com.hk

MWJ Puzzler

## Components, Boards and Systems

(Courtesy of Andrea Gilbert, www.clickmazes.com)

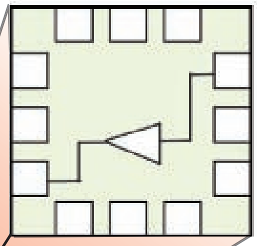

### Connect the amplifier to the antenna switch.

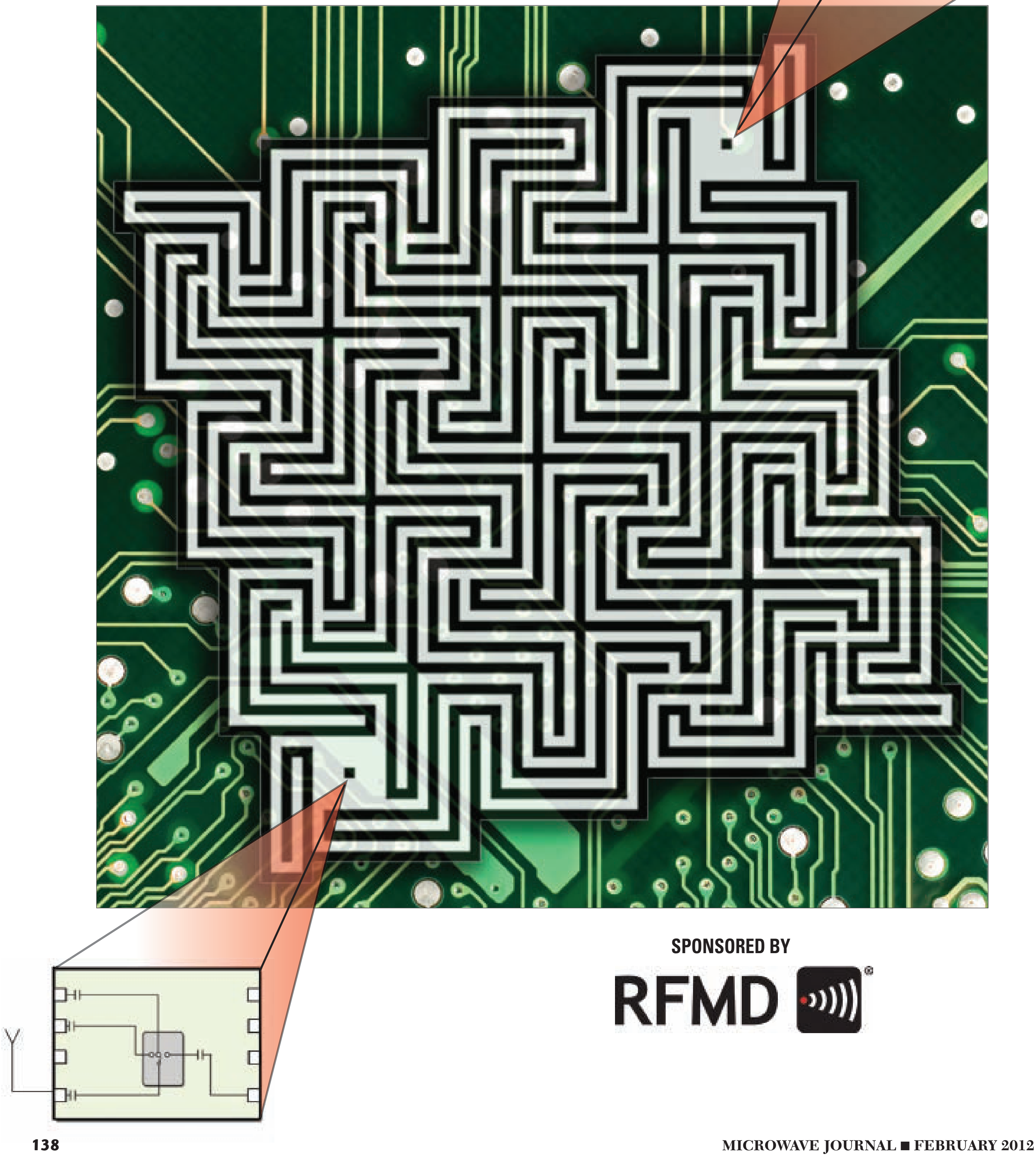

WERLATONE

# Mismatch Tolerant®

## HIGH POWER, MULTI-OCTAVE PERFORMANCE

# 20-1000 MHz

## IN-PHASE COMBINERS & DIRECTIONAL COUPLERS

- **Tolerate Severe Power Unbalances**
- **Lowest Loss**
- **Excellent Port-to-Port Isolation**
- **Small Package Sizes**
- **Conservative Power Ratings**

- POWER COMBINERS/DIVIDERS
- DIRECTIONAL COUPLERS
- 90° HYBRID COUPLERS
- 0°/180° HYBRID JUNCTIONS

Werlatone, Inc.
17 Jon Barrett Road
Patterson, New York 12563
T 845.278.2220
F 845.278.3440
www.werlatone.com

### In-Phase Combiners/Dividers

| Model | Type | Frequency (MHz) | Power (WCW) | Size (Inches) | Insertion Loss (dB) | VSWR | Isolation (dB) |
|---|---|---|---|---|---|---|---|
| D6233 | 2-Way | 10-1000 | 25 | 3.25 x 2 x 1.1 | 0.75 | 1.35:1 | 20 |
| D8632 | 2-Way | 20-1000 | 50 | 2.2 x 2.02 x 1.5 | 0.7 | 1.40:1 | 20 |
| D8300 | 2-Way | 20-1000 | 100 | 2.45 x 2 x 0.91 | 0.5 | 1.35:1 | 20 |
| D8544W* | 2-Way | 20-1000 | 100 | 2.85 x 2.5 x 1 | 0.5 | 1.35:1 | 18 |
| D8682 | 2-Way | 20-1000 | 500 | 5.2 x 2.65 x 1.8 | 0.6 | 1.35:1 | 15 |
| D8851W* | 2-Way | 20-1000 | 500 | 5.6 x 3.05 x 1.8 | 0.6 | 1.35:1 | 15 |
| D7365 | 4-Way | 20-1000 | 100 | 5 x 2 x 1 | 0.75 | 1.35:1 | 20 |
| D7439 | 4-Way | 20-1000 | 250 | 5 x 5 x 1.5 | 0.75 | 1.35:1 | 18 |
| D8746 | 4-Way | 20-1000 | 500 | 7.2 x 3.5 x 1.4 | 0.7 | 1.35:1 | 15 |
| D9048 | 4-Way | 20-1000 | 500 | 5 x 4.7 x 1.4 | 0.6 | 1.35:1 | 17 |

* "W" references a Watertight Design

### Dual Directional Couplers

| Model | Coupling (dB) | Frequency (MHz) | Power (WCW) | Size (Inches) | Insertion Loss (dB) | VSWR | Directivity (dB) |
|---|---|---|---|---|---|---|---|
| C8858 | 40 | 10-1000 | 250 | 2.09 x 1.16 x 0.57 | 0.4 | 1.30:1 | 20 |
| C8631* | 40 | 20-1000 | 150 | 1.5 x 0.95 x 0.5 | 0.35 | 1.25:1 | 20 |
| C8696 | 40 | 20-1000 | 150 | 1.76 x 1.16 x 0.57 | 0.35 | 1.25:1 | 20 |
| C8686 | 40 | 20-1000 | 500 | 5.2 x 2.7 x 1.7 | 0.35 | 1.25:1 | 20 |

* Non-Connectorized / Tabs

Our Patented, Low Loss designs tolerate high unbalanced input powers, while operating into severe Load Mismatch conditions.